Supplementary Information for Are All Charge-Transfer Parameters Created Equally? A Study of Functional Dependence and Excited-State Charge-Transfer Quantification Across Two Dye Families

Richard Drew Marshburn,[†] Daniel C. Ashley,[†] Gregory M. Curtin,[†] Nadia Sultana,[‡] Chang Liu,[†] Nelson R. Vinueza,[‡] Elon A. Ison,[†] Elena Jakubikova[†]*

[†]Department of Chemistry, North Carolina State University, Raleigh, North Carolina 27695, United States

[‡]Department of Textile Engineering, Chemistry, and Science, North Carolina State University, 1020 Main Campus Drive, Raleigh, NC 27606, United States

Table of Contents

Note for all figures: All data for B3LYP is referred to as "B3LYP+D2", which is the method used for the geometry optimization. The D2 does not affect calculated orbitals or TDDFT results beyond the indirect manner in which it influenced the original optimization.

Azo Ground State Orbitals

All ground state orbital images were obtained at the B3LYP+D2/6-311G* level of theory in solvent (acetonitrile, PCM) and rendered with an isovalue of 0.03 (e/Å^3).

Table S1. Frontier orbitals for dye **A1**.

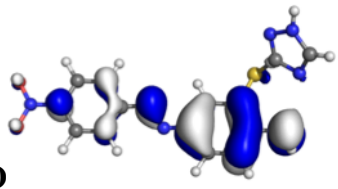 **HOMO**	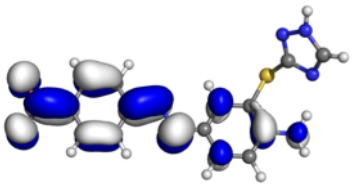 **LUMO**
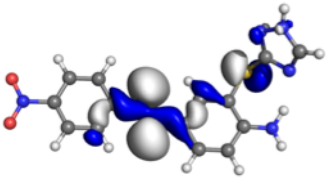 **HOMO-1**	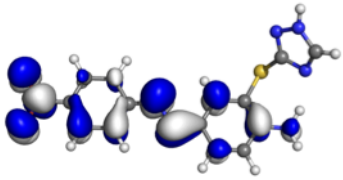 **LUMO+1**
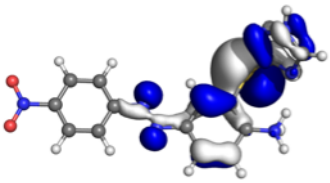 **HOMO-2**	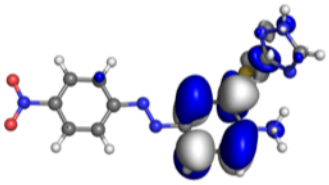 **LUMO+2**
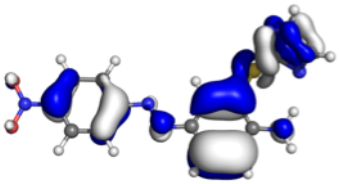 **HOMO-3**	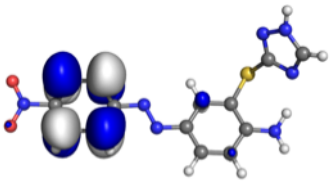 **LUMO+3**

Table S2. Frontier orbitals for dye **A2**.

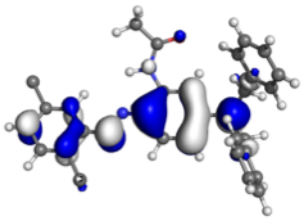 **HOMO**	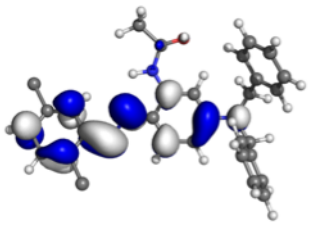 **LUMO**

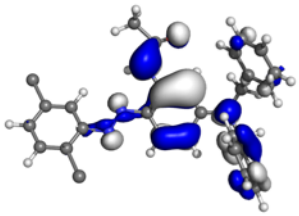 HOMO-1	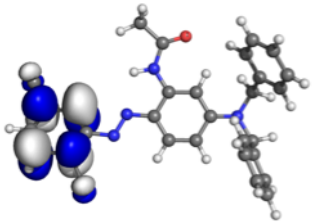 LUMO+1
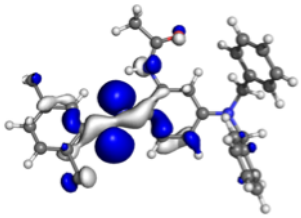 HOMO-2	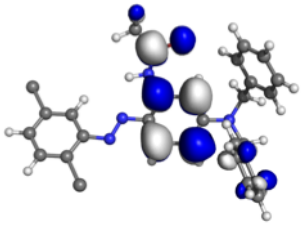 LUMO+2
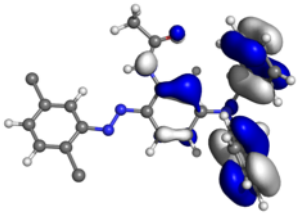 HOMO-3	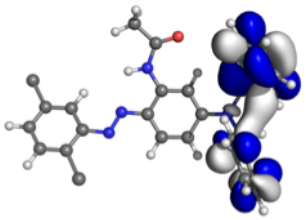 LUMO+3

Table S3. Frontier orbitals for dye **A3**.

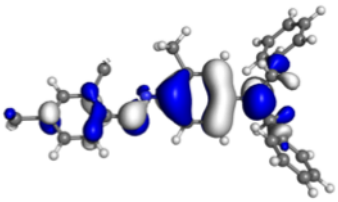 HOMO	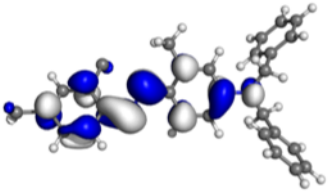 LUMO
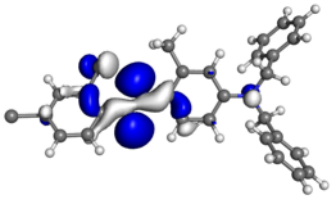 HOMO-1	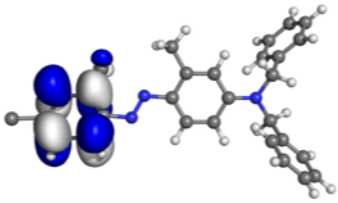 LUMO+1
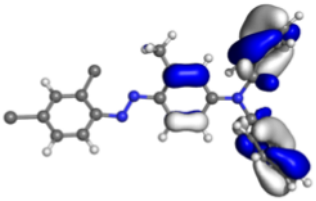 HOMO-2	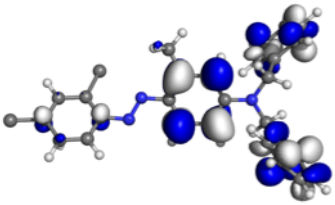 LUMO+2
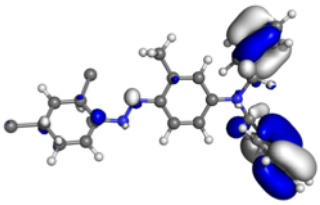 HOMO-3	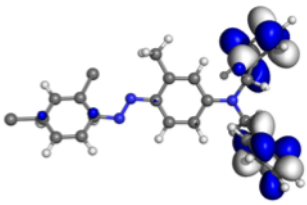 LUMO+3

Table S4. Frontier orbitals for dye **A4**.

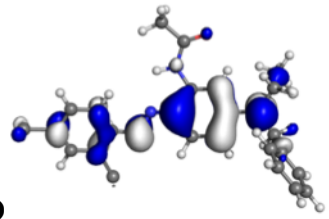 **HOMO**	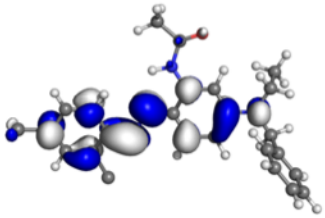 **LUMO**
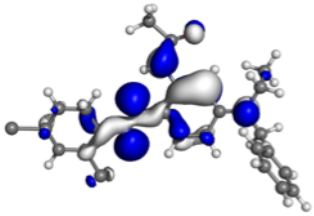 **HOMO-1**	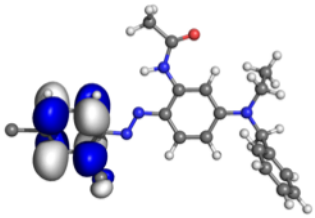 **LUMO+1**
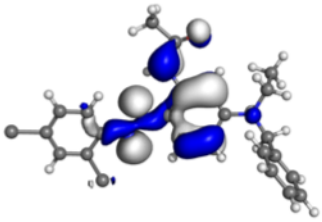 **HOMO-2**	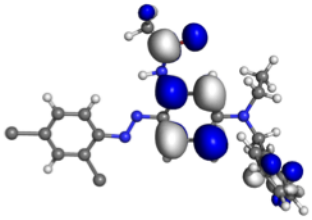 **LUMO+2**
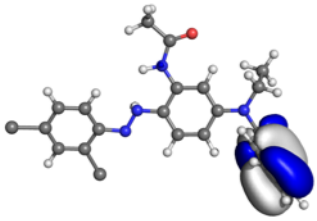 **HOMO-3**	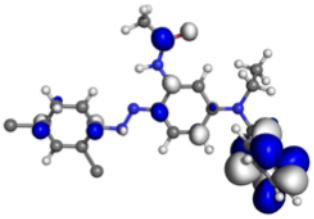 **LUMO+3**

Table S5. Frontier orbitals for dye **A5**.

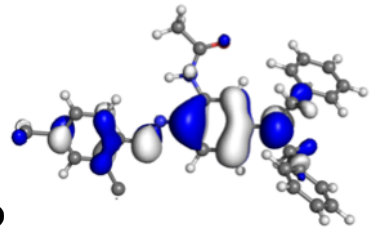 **HOMO**	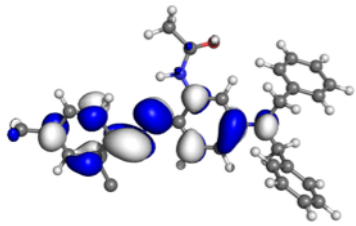 **LUMO**
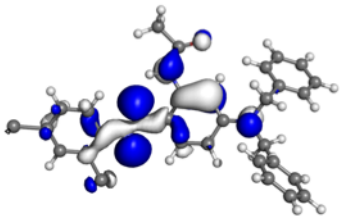 **HOMO-1**	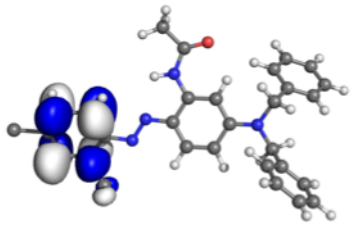 **LUMO+1**

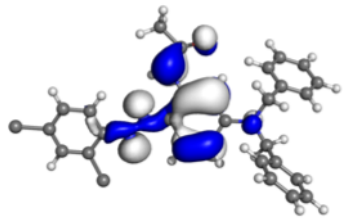 HOMO-2	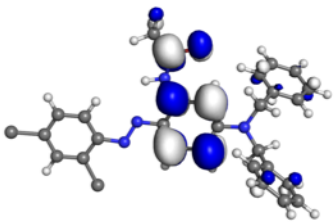 LUMO+2
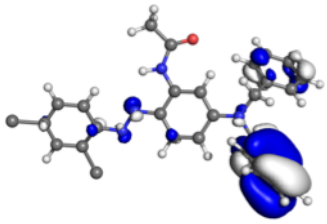 HOMO-3	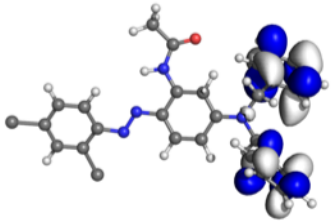 LUMO+3

Table S6. Frontier orbitals for dye **A6**.

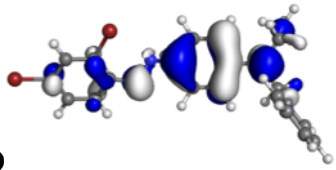 HOMO	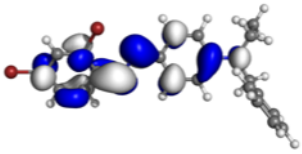 LUMO
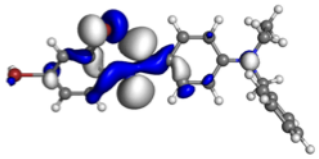 HOMO-1	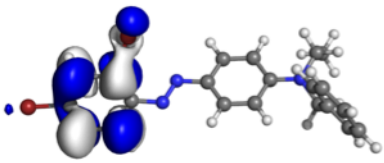 LUMO+1
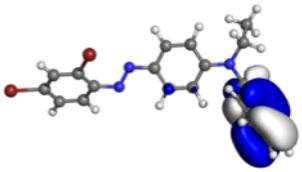 HOMO-2	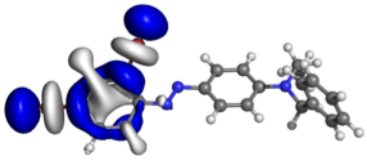 LUMO+2
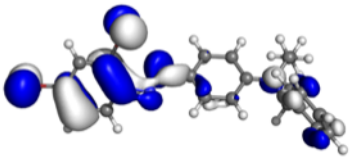 HOMO-3	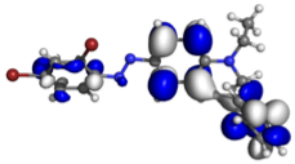 LUMO+3

Table S7. Frontier orbitals for dye **A7**.

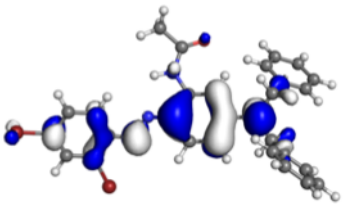 HOMO	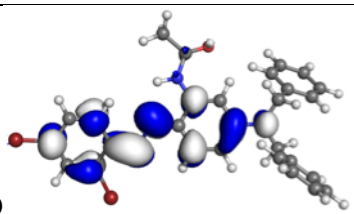 LUMO

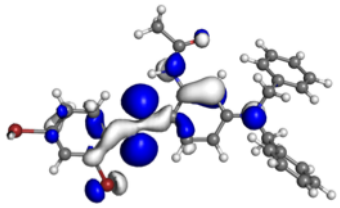 **HOMO-1**	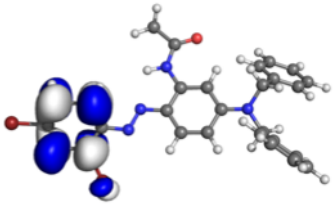 **LUMO+1**
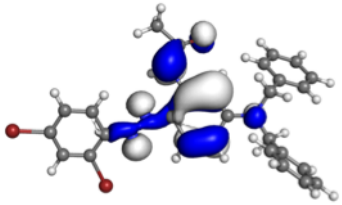 **HOMO-2**	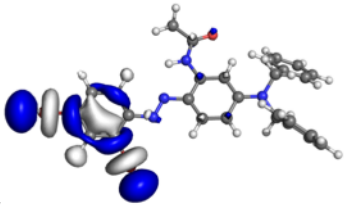 **LUMO+2**
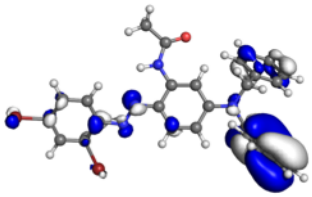 **HOMO-3**	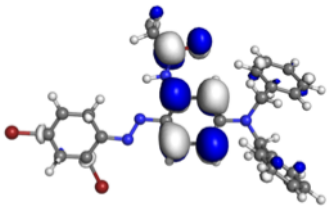 **LUMO+3**

Table S8. Frontier orbitals for dye **A8**.

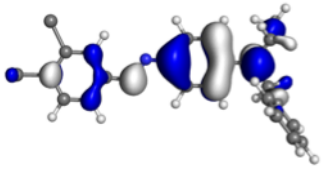 **HOMO**	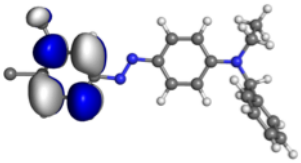 **LUMO**
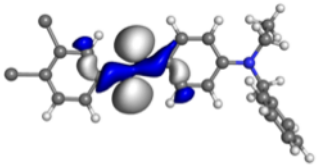 **HOMO-1**	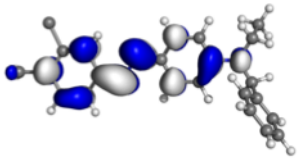 **LUMO+1**
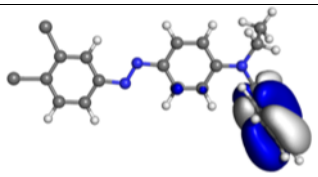 **HOMO-2**	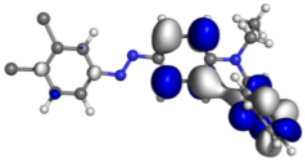 **LUMO+2**
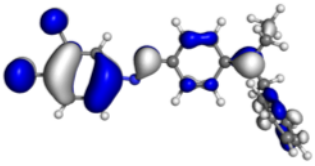 **HOMO-3**	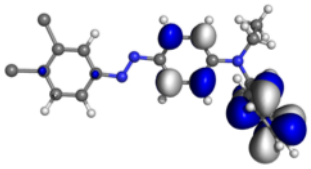 **LUMO+3**

Table S9. Frontier orbitals for dye **A9**.

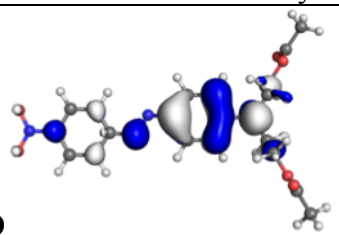 **HOMO**	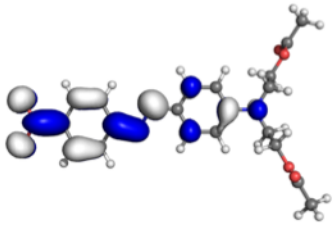 **LUMO**
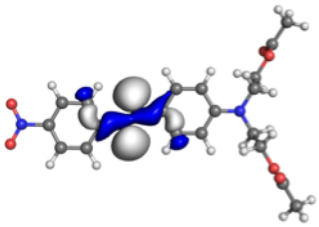 **HOMO-1**	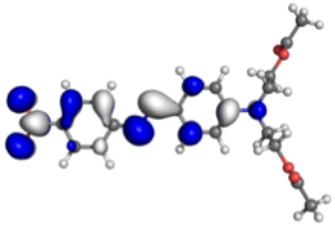 **LUMO+1**
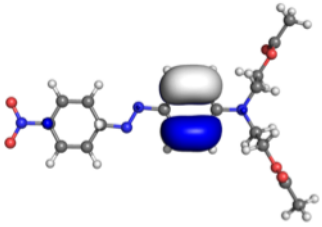 **HOMO-2**	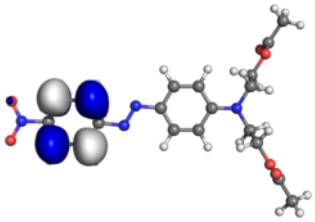 **LUMO+2**
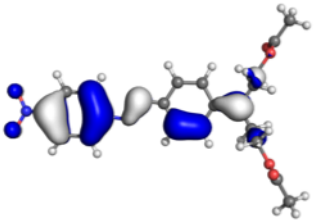 **HOMO-3**	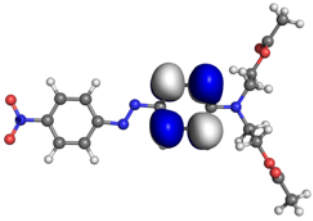 **LUMO+3**

Table S10. Frontier orbitals for dye **A10**.

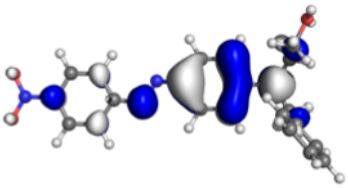 **HOMO**	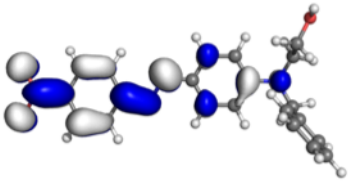 **LUMO**
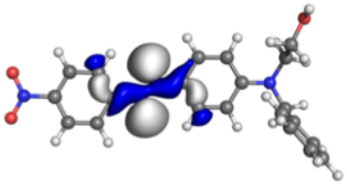 **HOMO-1**	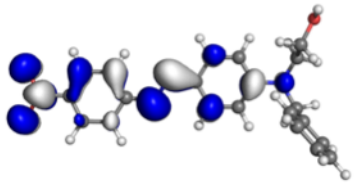 **LUMO+1**
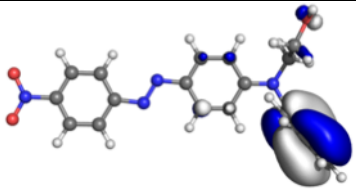 **HOMO-2**	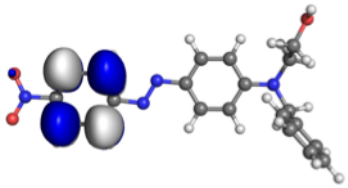 **LUMO+2**

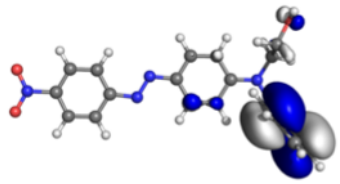 **HOMO-3**	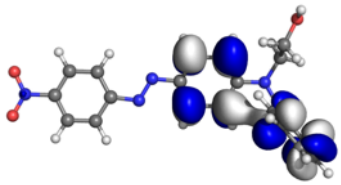 **LUMO+3**

Cyano Ground State Orbitals

All ground state orbital images were obtained at the B3LYP+D2/6-311G* level of theory in solvent (acetonitrile, PCM) and rendered with an isovalue of 0.03 (e/Å^3).

Table S11. Frontier orbitals for dye **C1**.

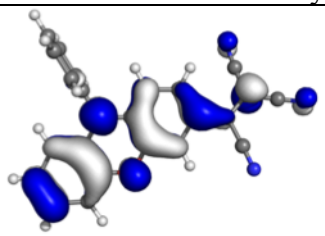 **HOMO**	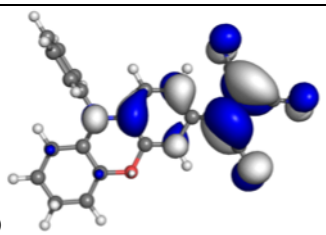 **LUMO**
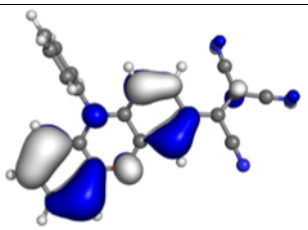 **HOMO-1**	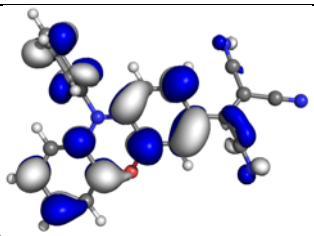 **LUMO+1**
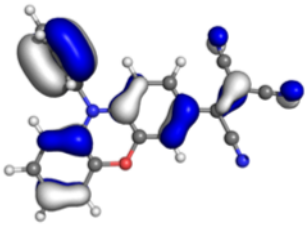 **HOMO-2**	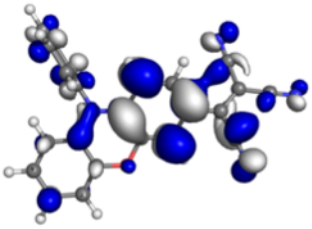 **LUMO+2**
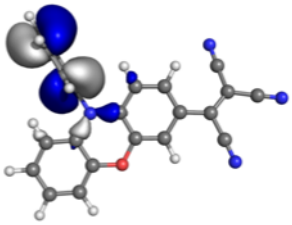 **HOMO-3**	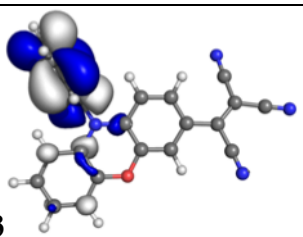 **LUMO+3**

Table S12. Frontier orbitals for dye **C2**.

 **HOMO**	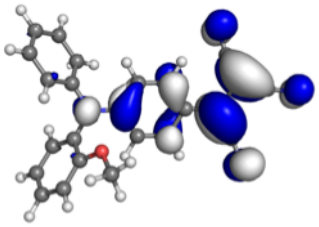 **LUMO**
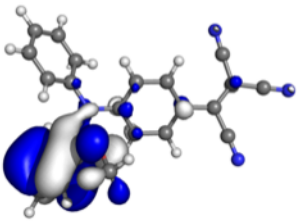 **HOMO-1**	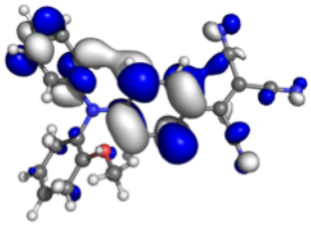 **LUMO+1**

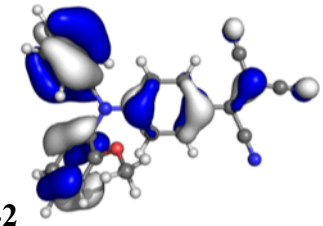 HOMO-2	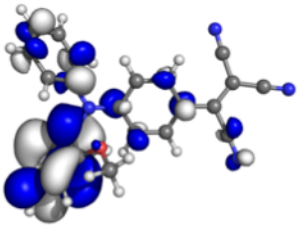 LUMO+2
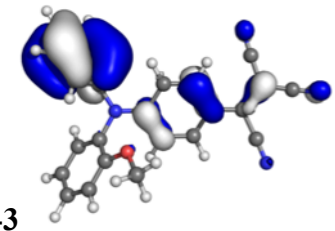 HOMO-3	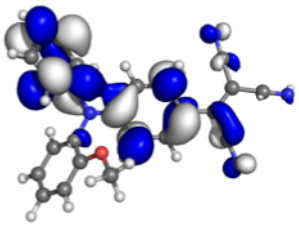 LUMO+3

Table S13. Frontier orbitals for dye **C3**.

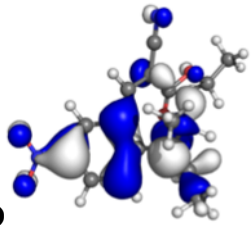 HOMO	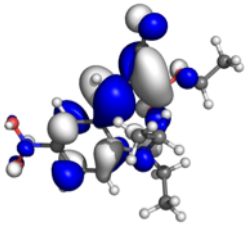 LUMO
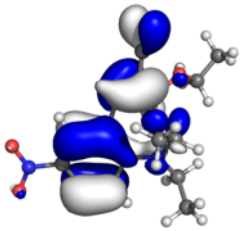 HOMO-1	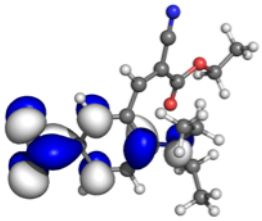 LUMO+1
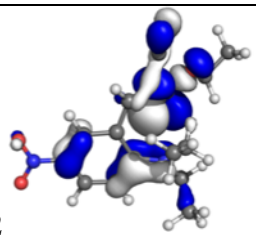 HOMO-2	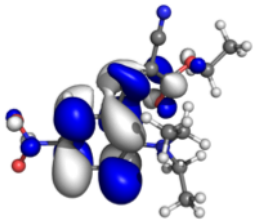 LUMO+2
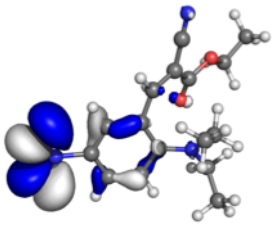 HOMO-3	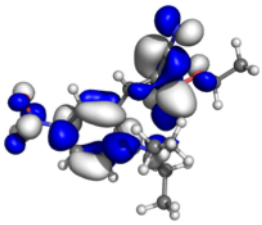 LUMO+3

Table S14. Frontier orbitals for dye **C4**.

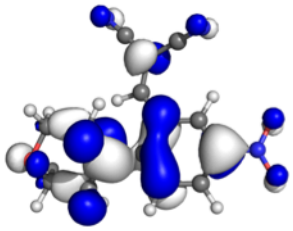 **HOMO**	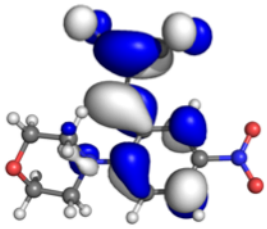 **LUMO**
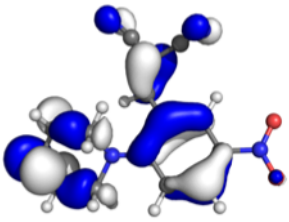 **HOMO-1**	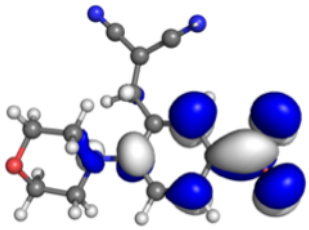 **LUMO+1**
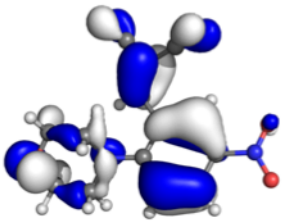 **HOMO-2**	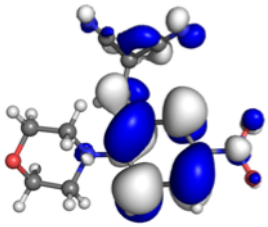 **LUMO+2**
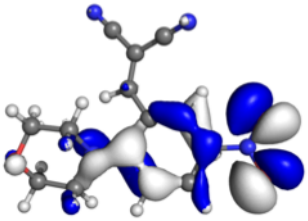 **HOMO-3**	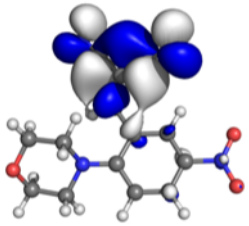 **LUMO+3**

Table S15. Frontier orbitals for dye **C5**.

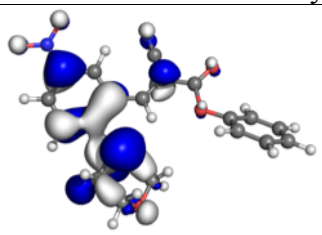 **HOMO**	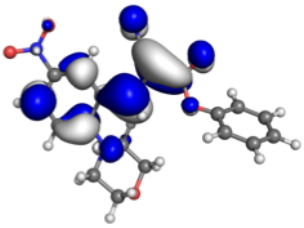 **LUMO**
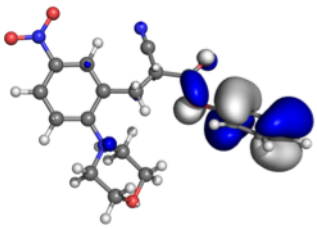 **HOMO-1**	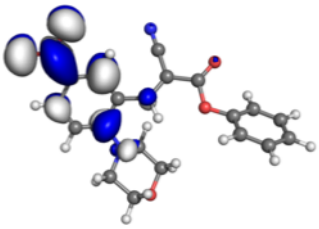 **LUMO+1**

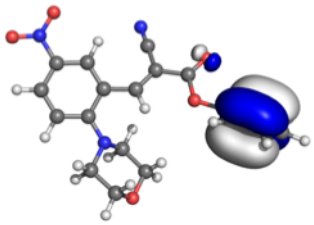 HOMO-2	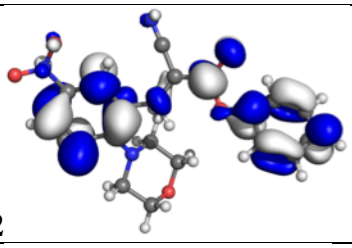 LUMO+2
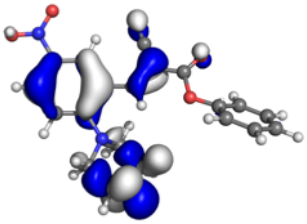 HOMO-3	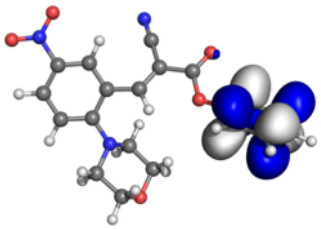 LUMO+3

Table S16. Frontier orbitals for dye **C6**.

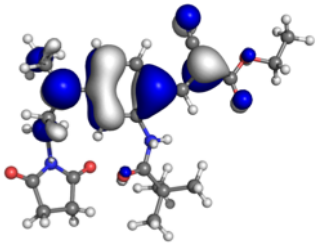 HOMO	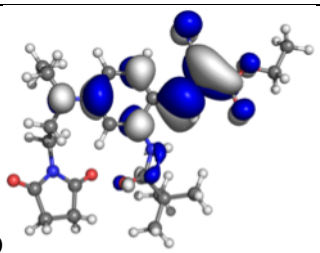 LUMO
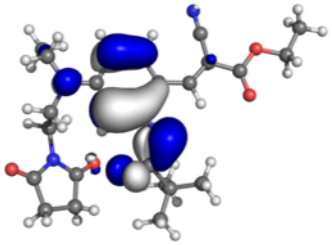 HOMO-1	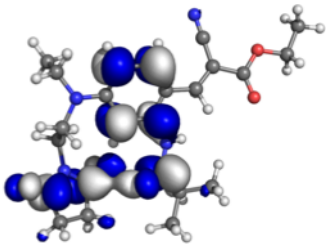 LUMO+1
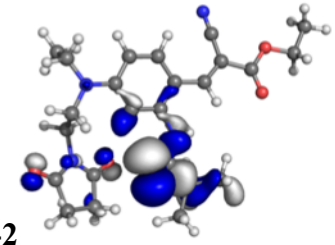 HOMO-2	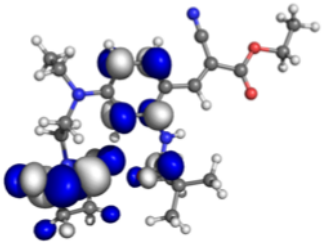 LUMO+2
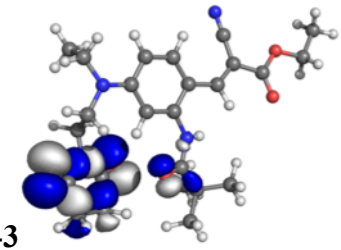 HOMO-3	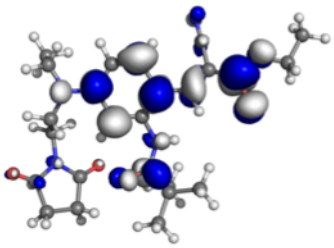 LUMO+3

Table S17. Frontier orbitals for dye **C7**.

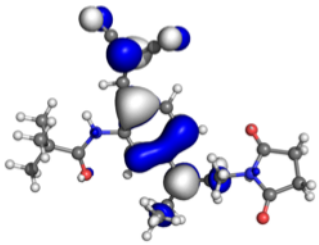 **HOMO**	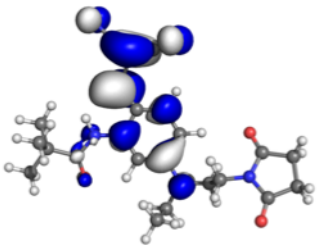 **LUMO**
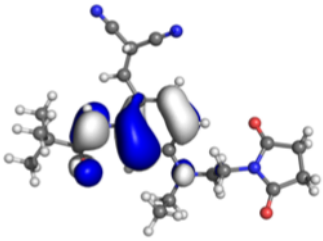 **HOMO-1**	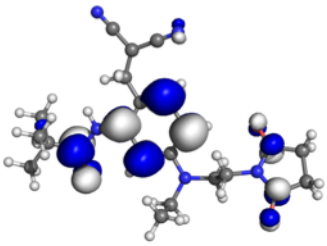 **LUMO+1**
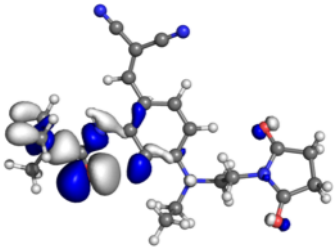 **HOMO-2**	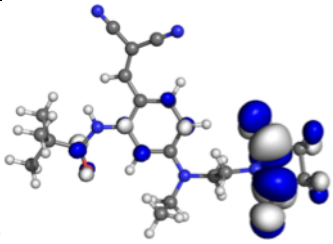 **LUMO+2**
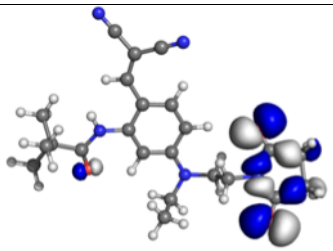 **HOMO-3**	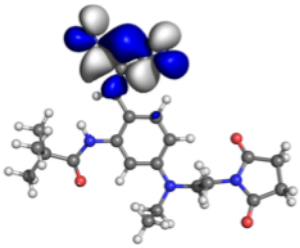 **LUMO+3**

Table S18. Frontier orbitals for dye **C8**.

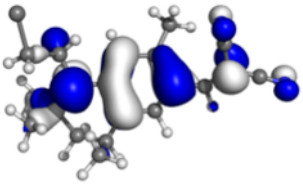 **HOMO**	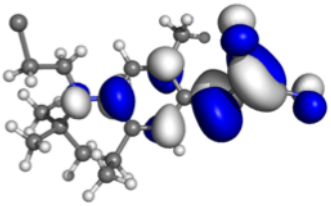 **LUMO**
 **HOMO-1**	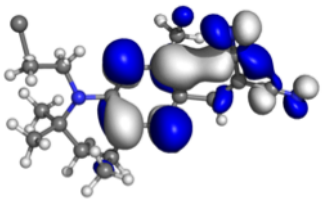 **LUMO+1**

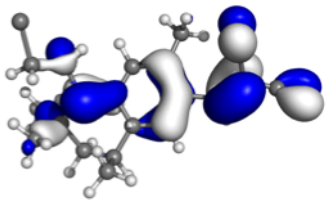 **HOMO-2**	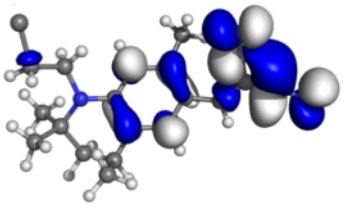 **LUMO+2**
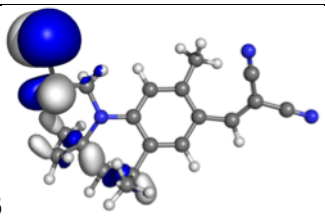 **HOMO-3**	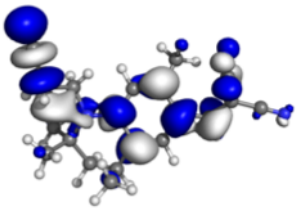 **LUMO+3**

Table S19. Frontier orbitals for dye **C9**.

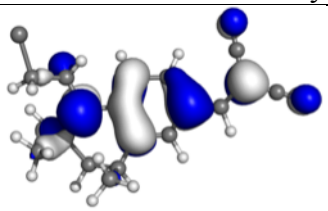 **HOMO**	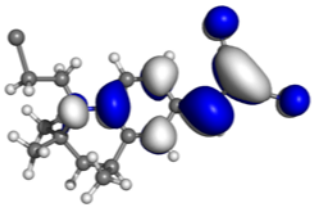 **LUMO**
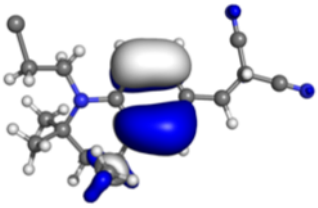 **HOMO-1**	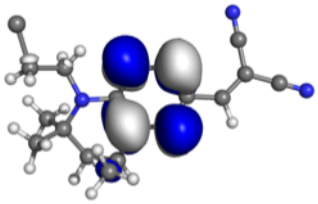 **LUMO+1**
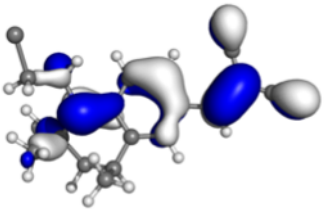 **HOMO-2**	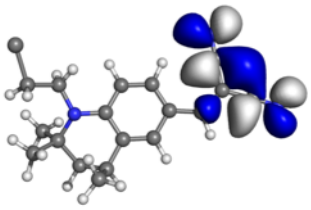 **LUMO+2**
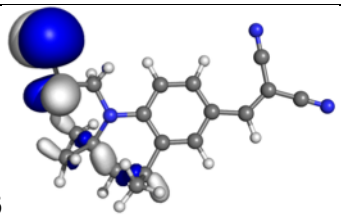 **HOMO-3**	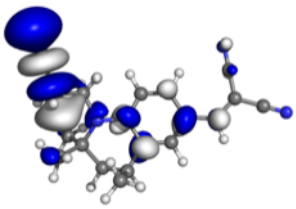 **LUMO+3**

Table S20. Frontier orbitals for dye **C10**.

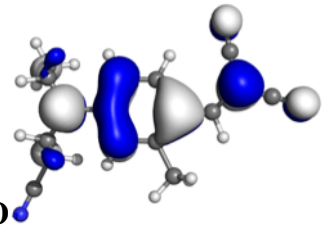 **HOMO**	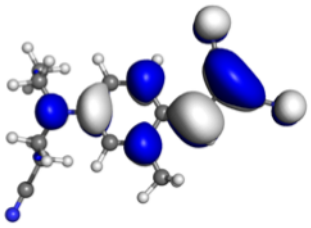 **LUMO**
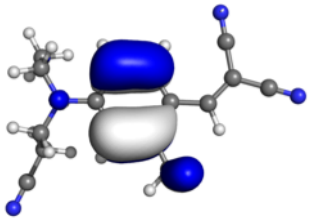 **HOMO-1**	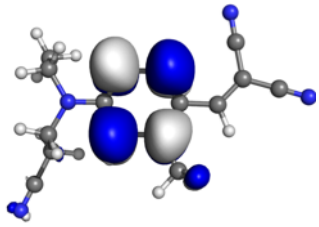 **LUMO+1**
 **HOMO-2**	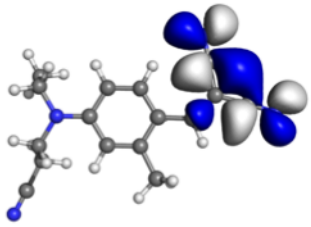 **LUMO+2**
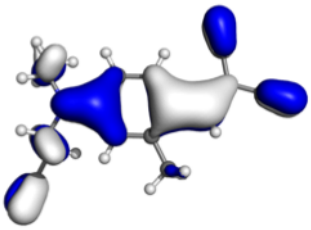 **HOMO-3**	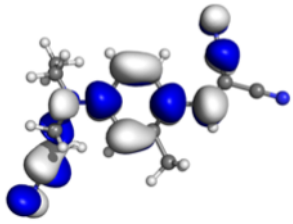 **LUMO+3**

Calculated and experimental spectra: Azo dyes

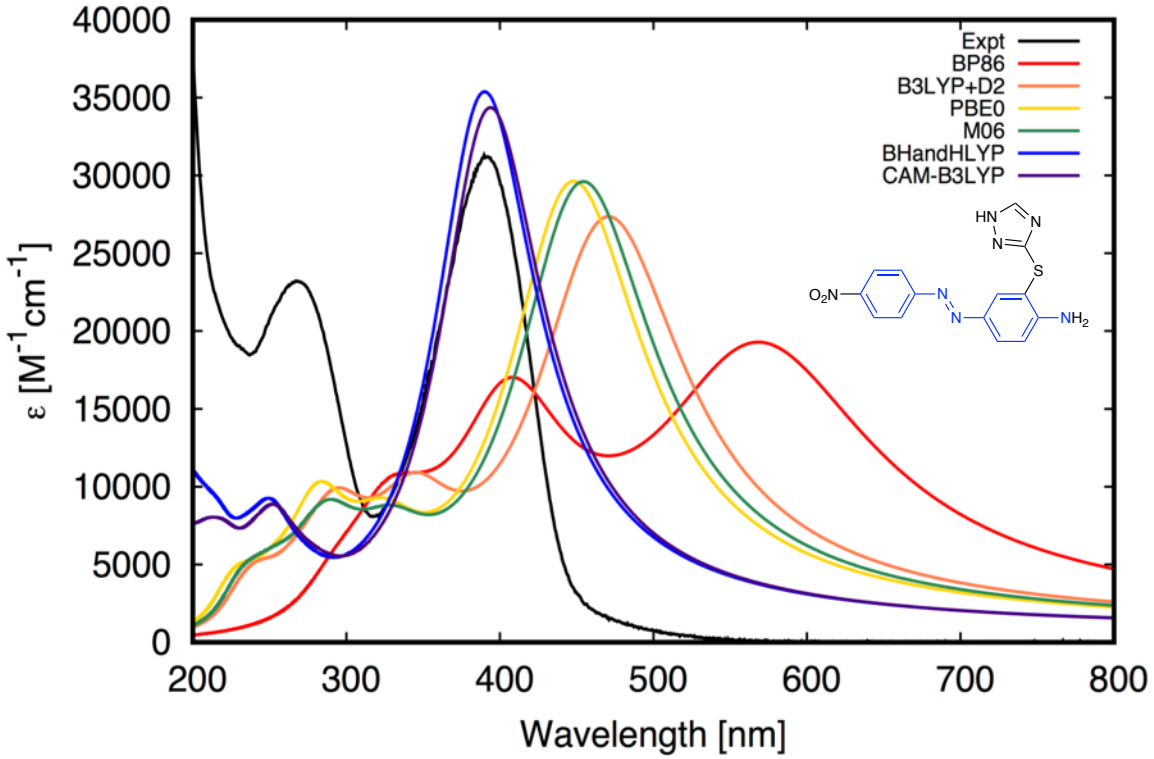

Figure S1. Experimentally measured and calculated TD-DFT spectra of dye **A1**.

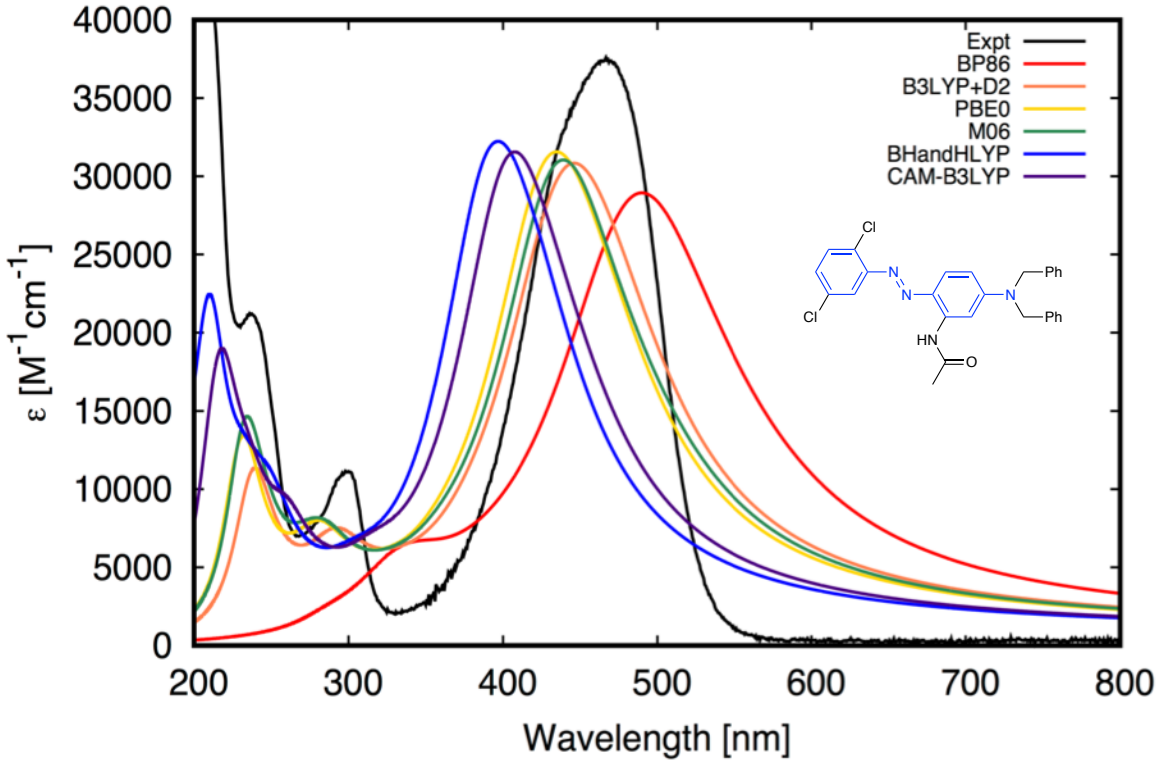

Figure S2. Experimentally measured and calculated TD-DFT spectra of dye **A2**.

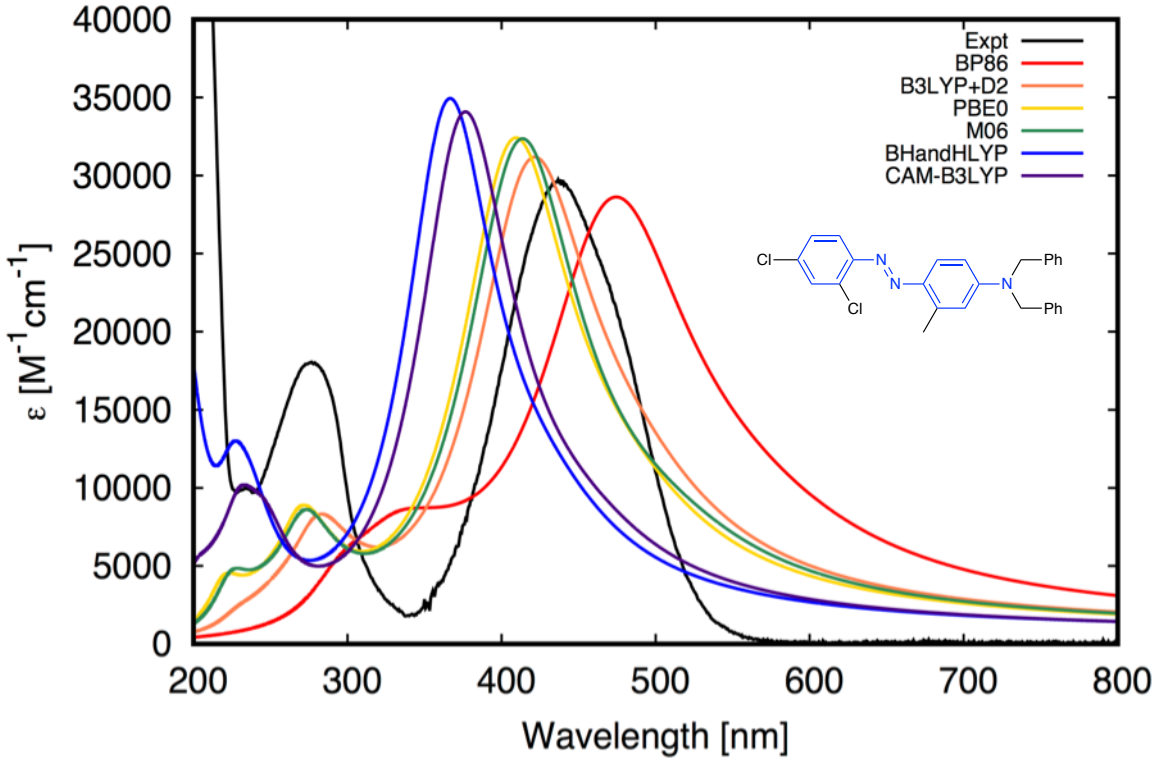

Figure S3. Experimentally measured and calculated TD-DFT spectra of dye **A3**.

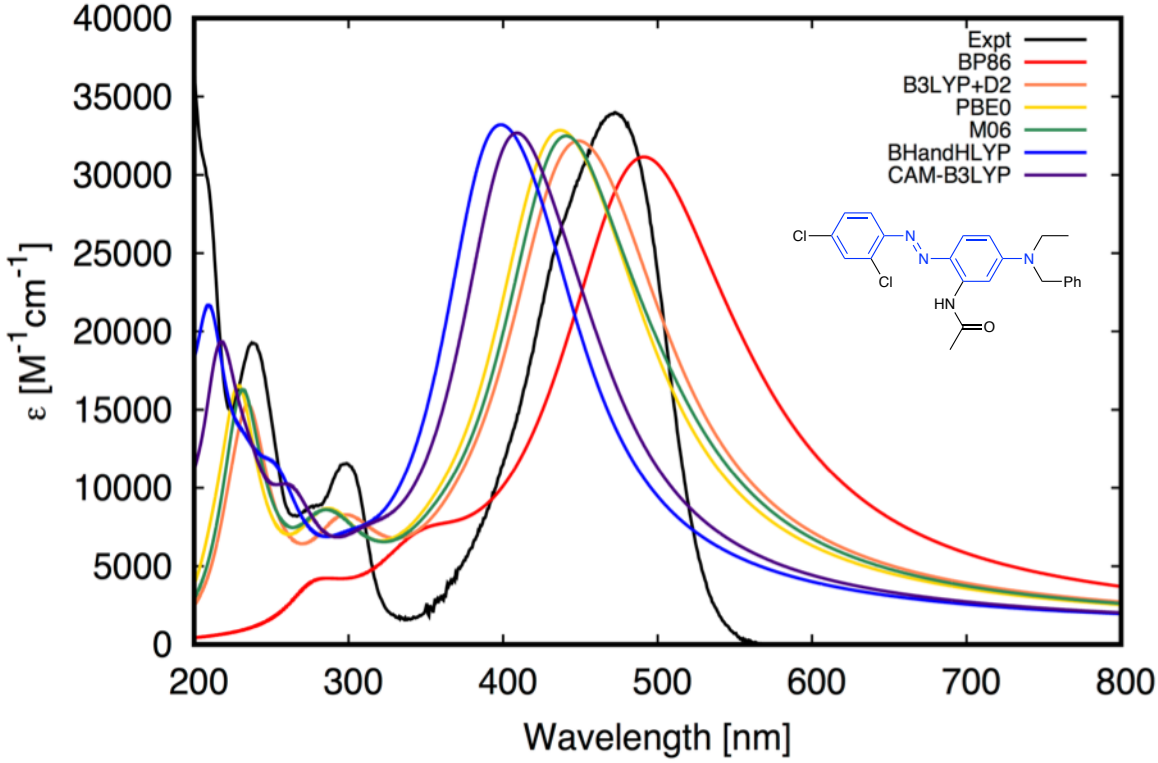

Figure S4. Experimentally measured and calculated TD-DFT spectra of dye **A4**.

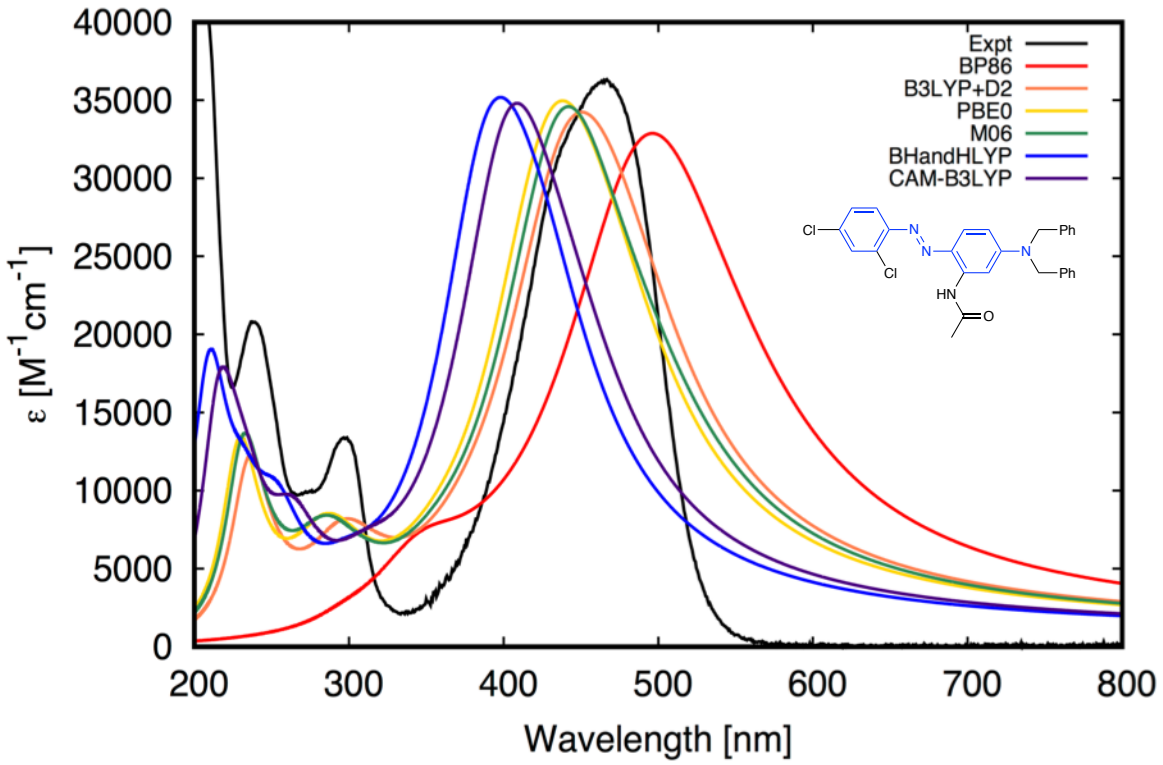

Figure S5. Experimentally measured and calculated TD-DFT spectra of dye **A5**.

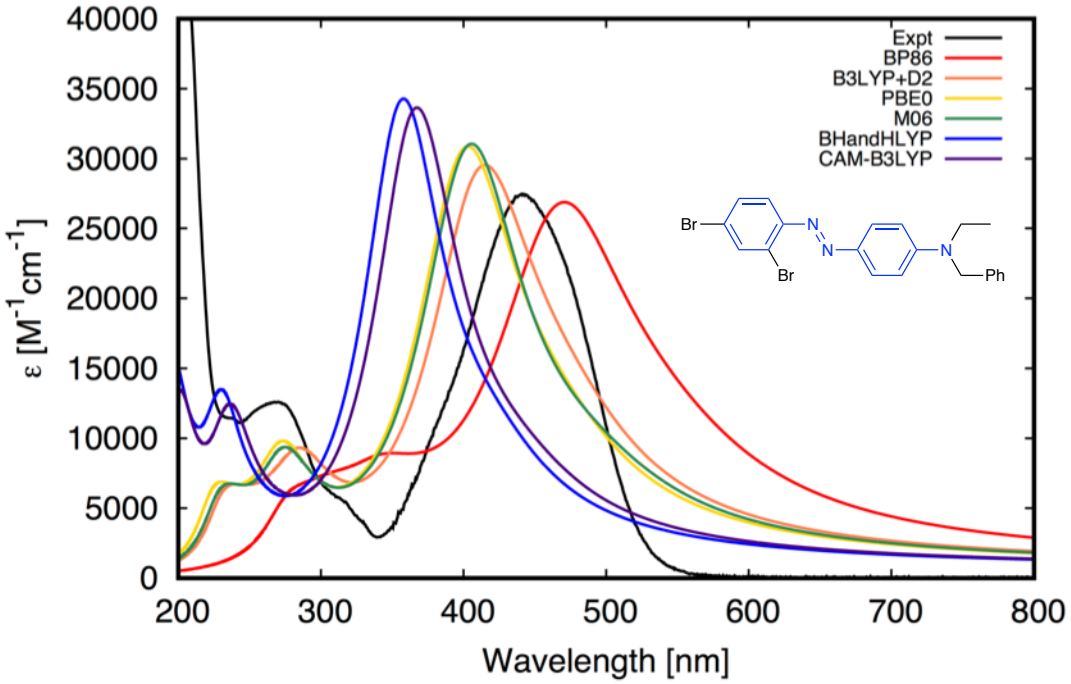

Figure S6. Experimentally measured and calculated TD-DFT spectra of dye **A6**.

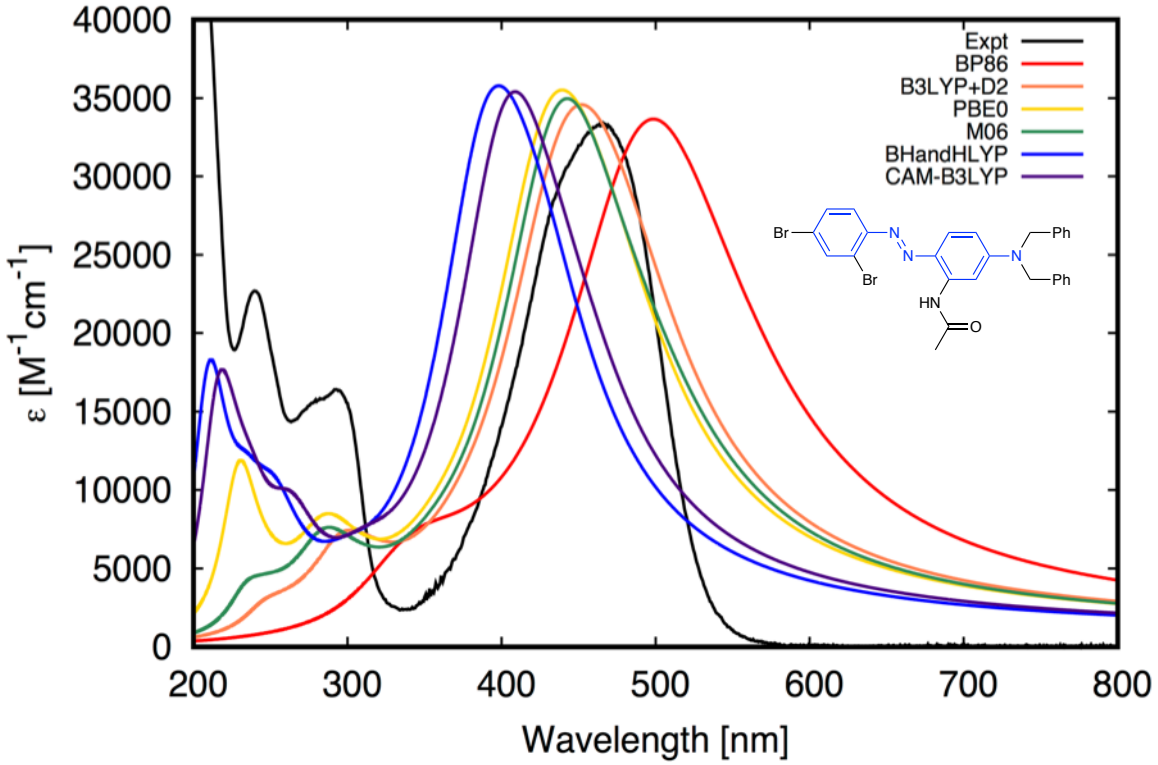

Figure S7. Experimentally measured and calculated TD-DFT spectra of dye **A7**.

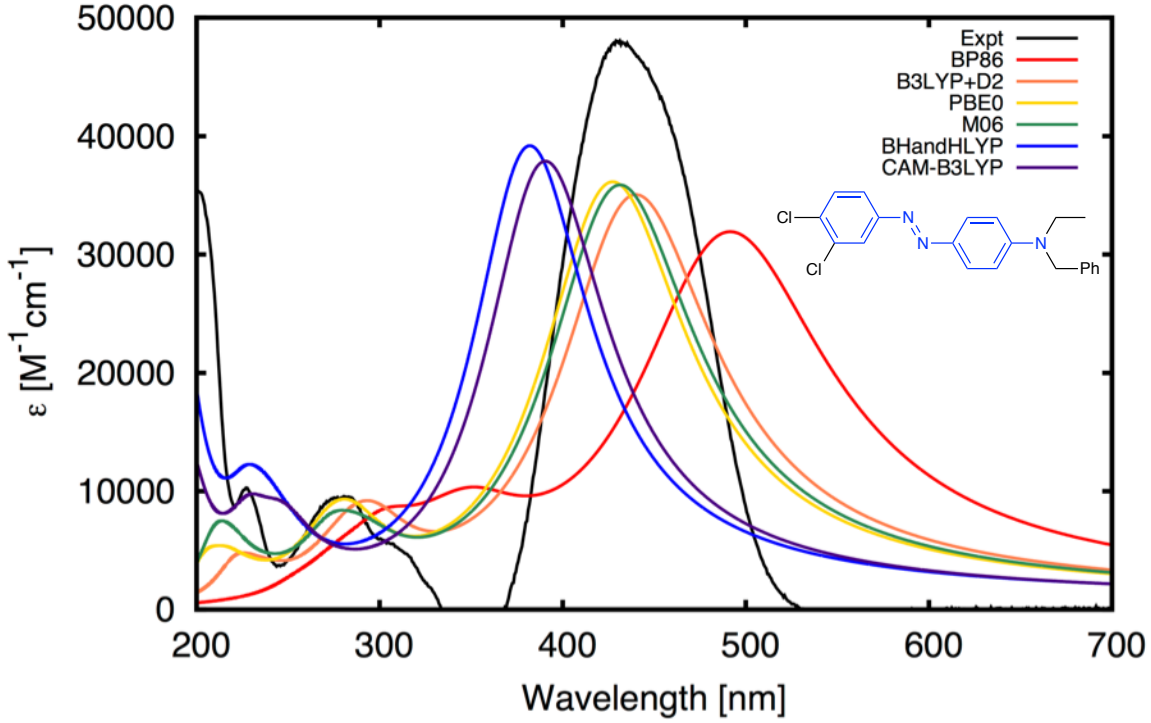

Figure S8. Experimentally measured and calculated TD-DFT spectra of dye **A8**.

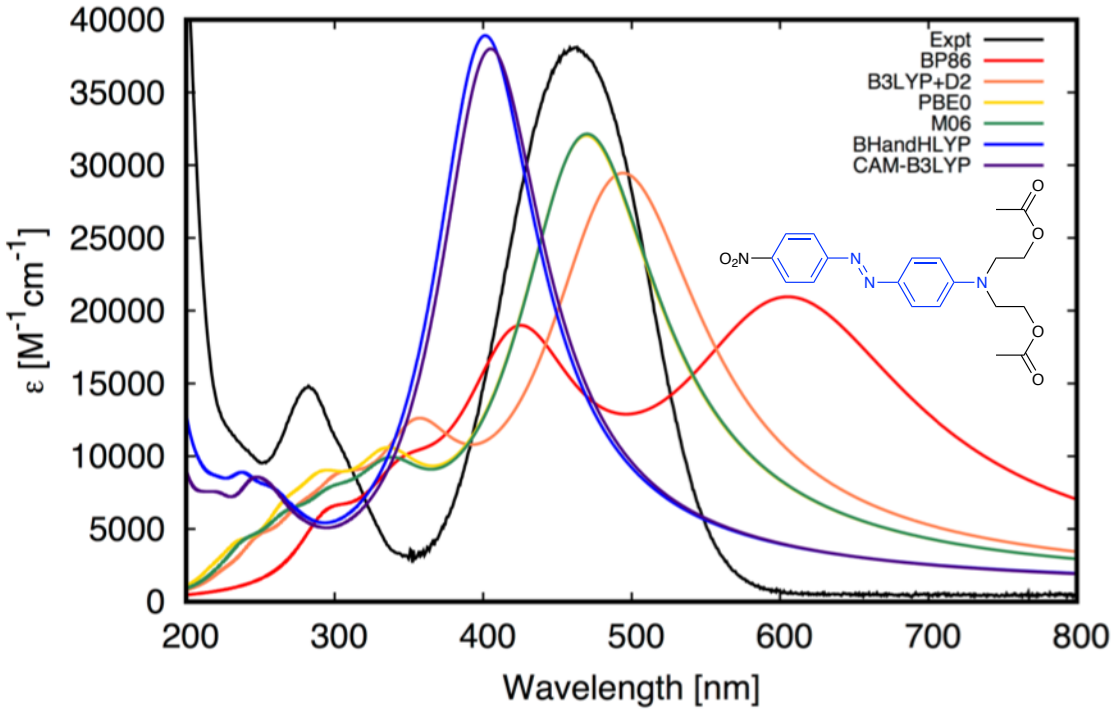

Figure S9. Experimentally measured and calculated TD-DFT spectra of dye **A9**.

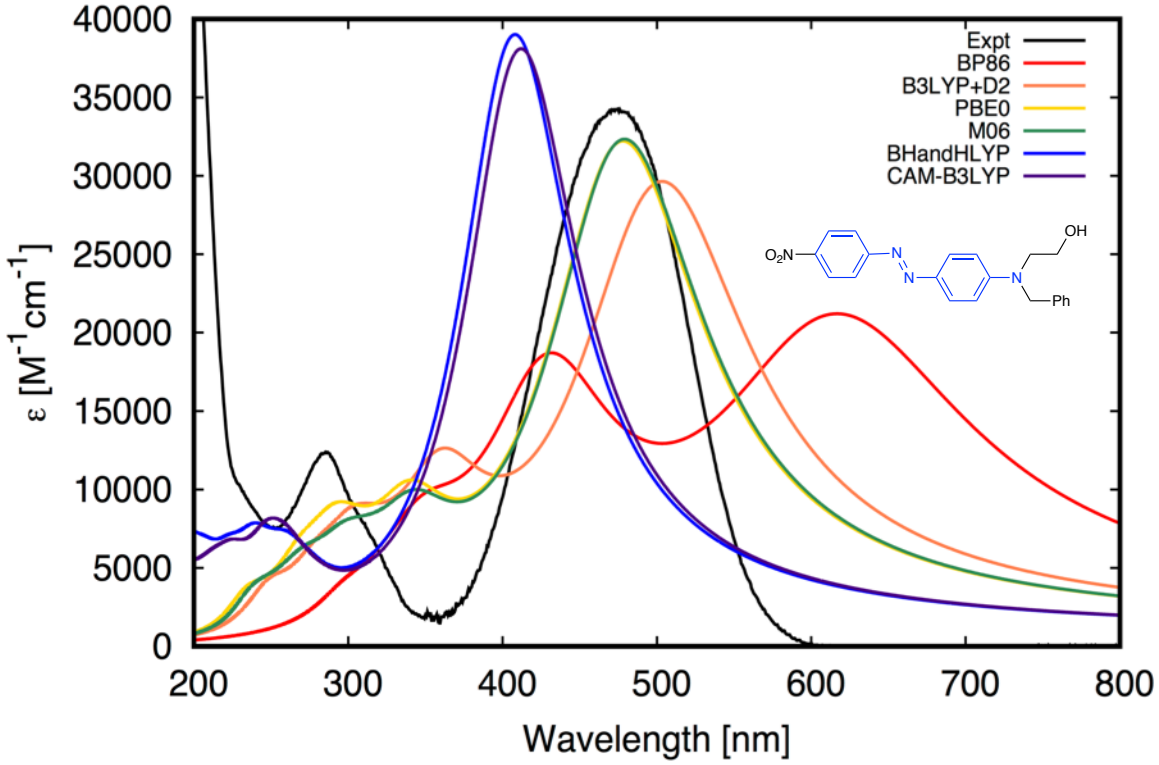

Figure S10. Experimentally measured and calculated TD-DFT spectra of dye **A10**.

Calculated and experimental spectra: Cyano dyes

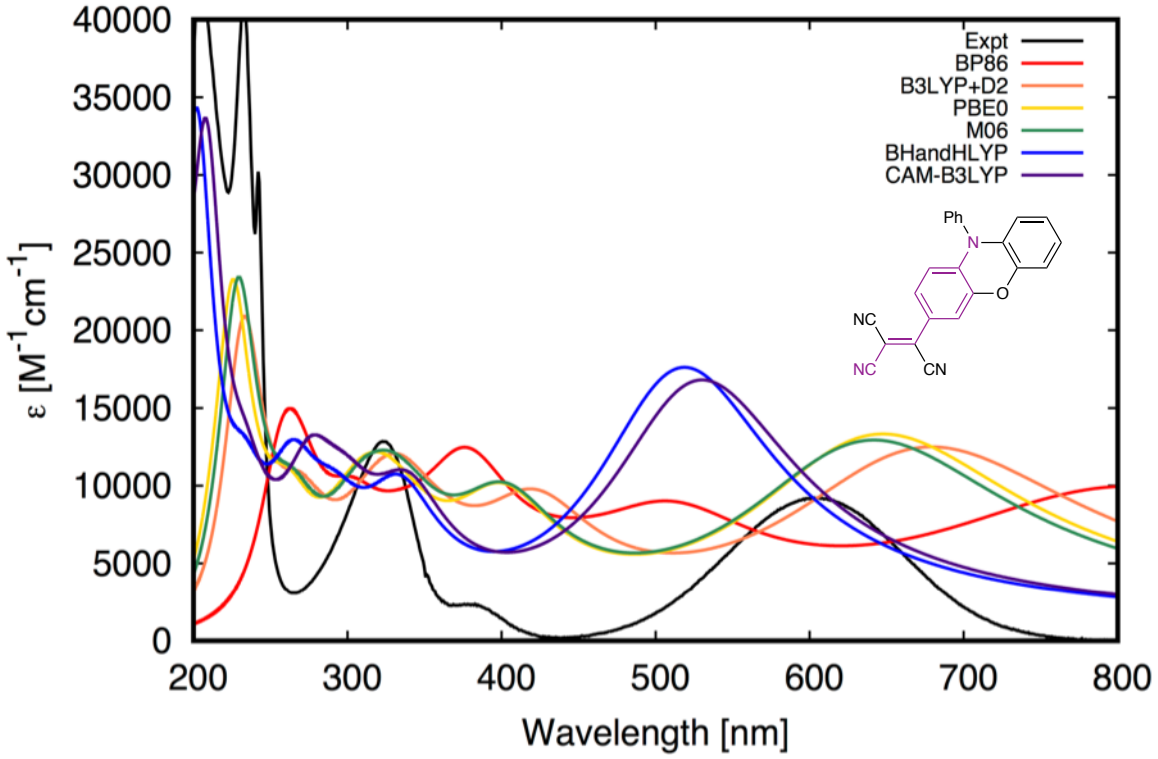

Figure S11. Experimentally measured and calculated TD-DFT spectra of dye **C1**.

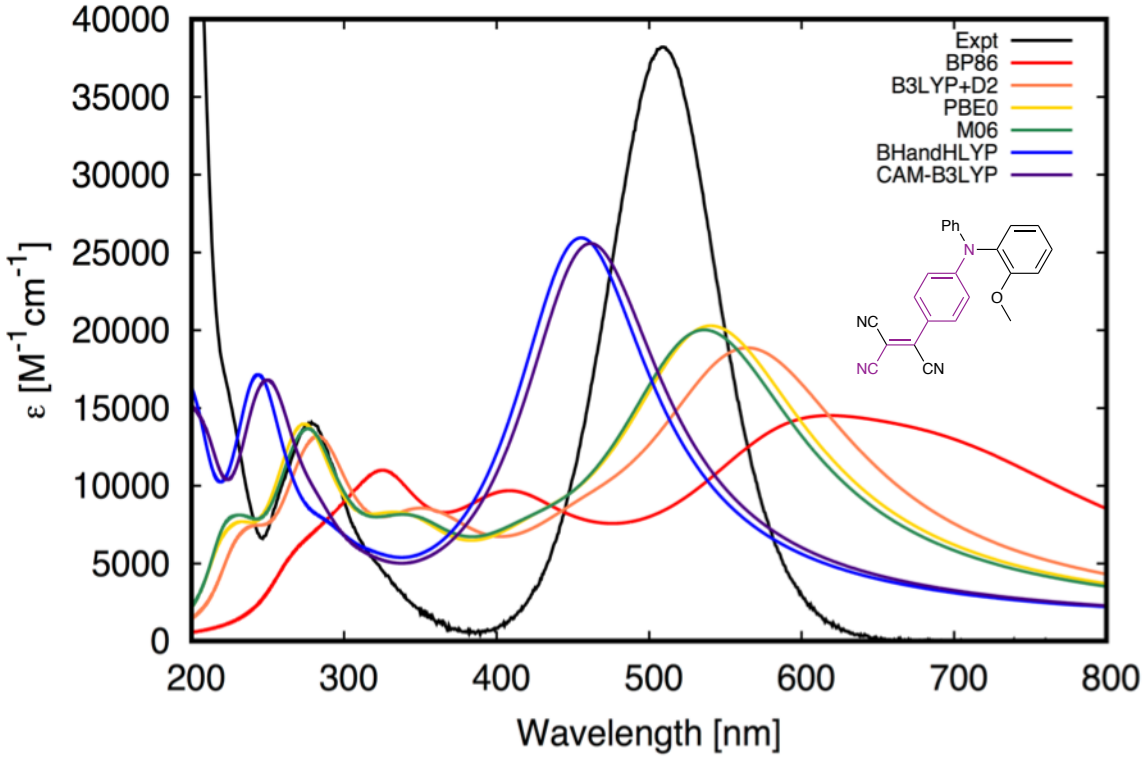

Figure S12. Experimentally measured and calculated TD-DFT spectra of dye **C2**.

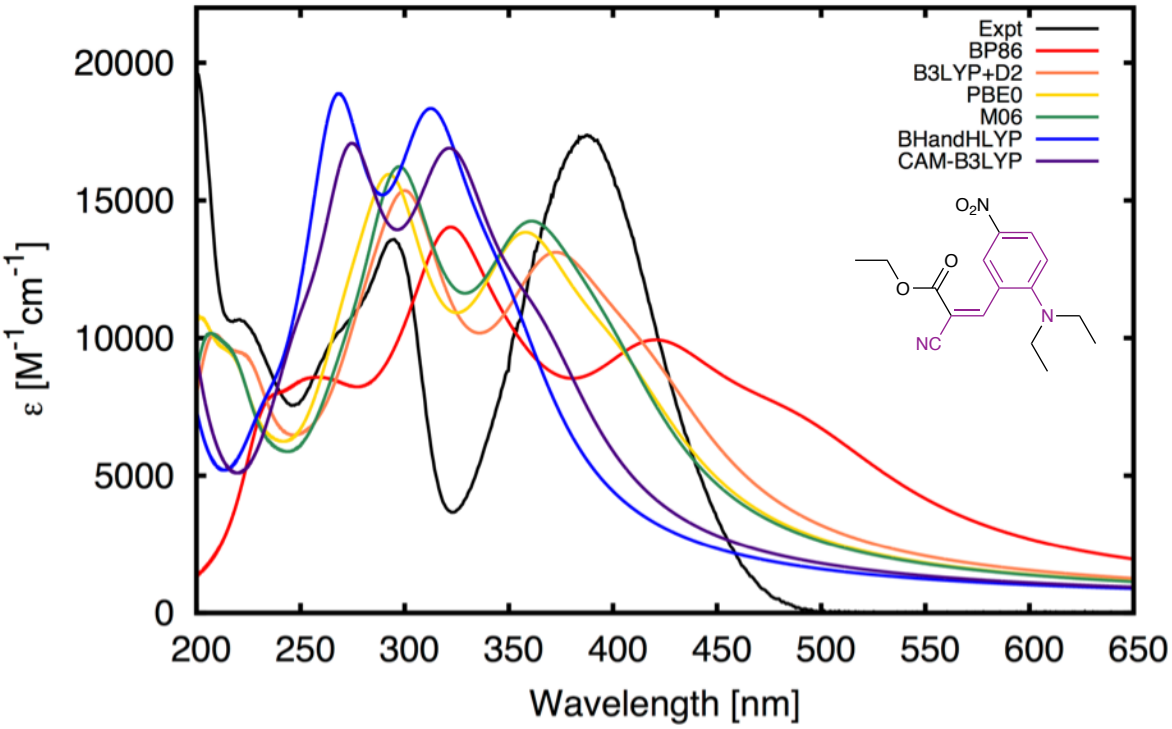

Figure S13. Experimentally measured and calculated TD-DFT spectra of dye **C3**.

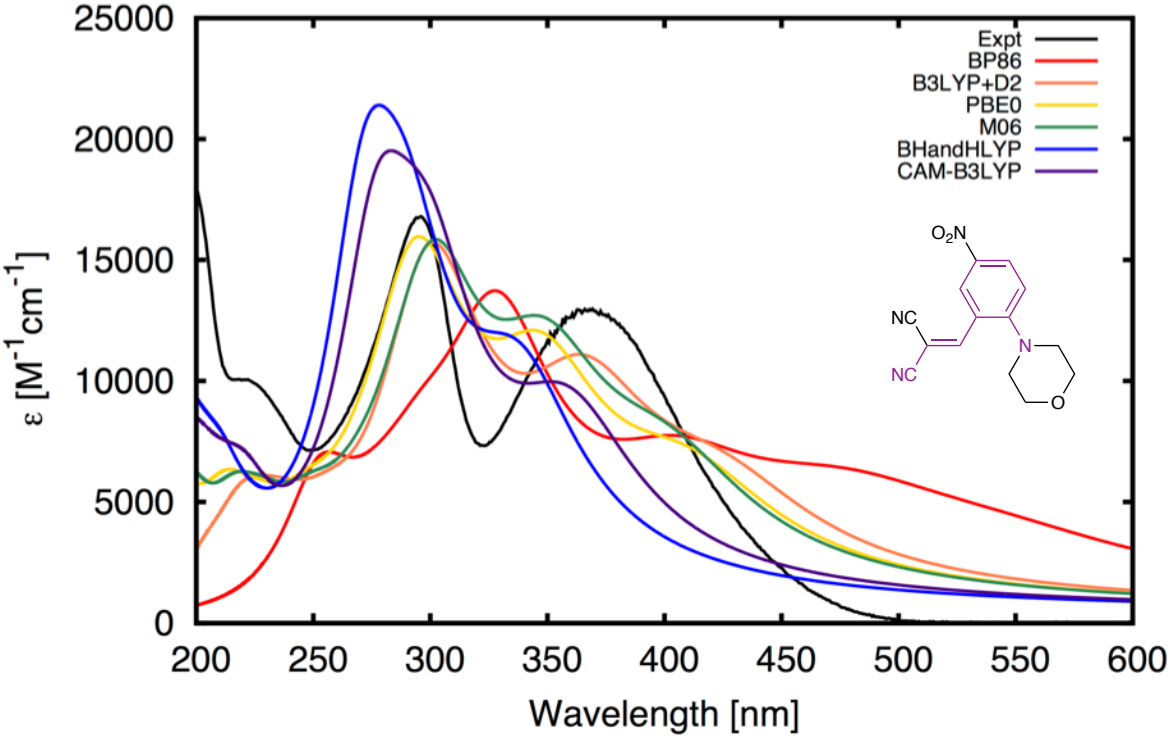

Figure S14. Experimentally measured and calculated TD-DFT spectra of dye **C4**.

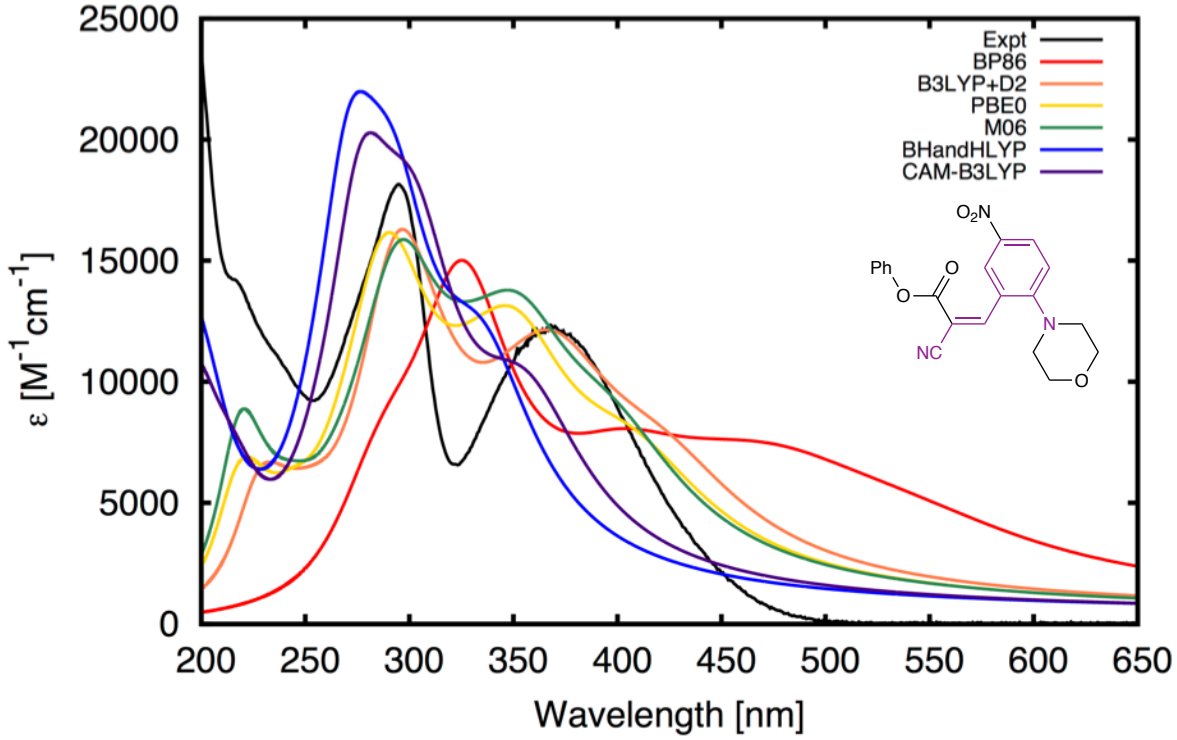

Figure S15. Experimentally measured and calculated TD-DFT spectra of dye **C5**.

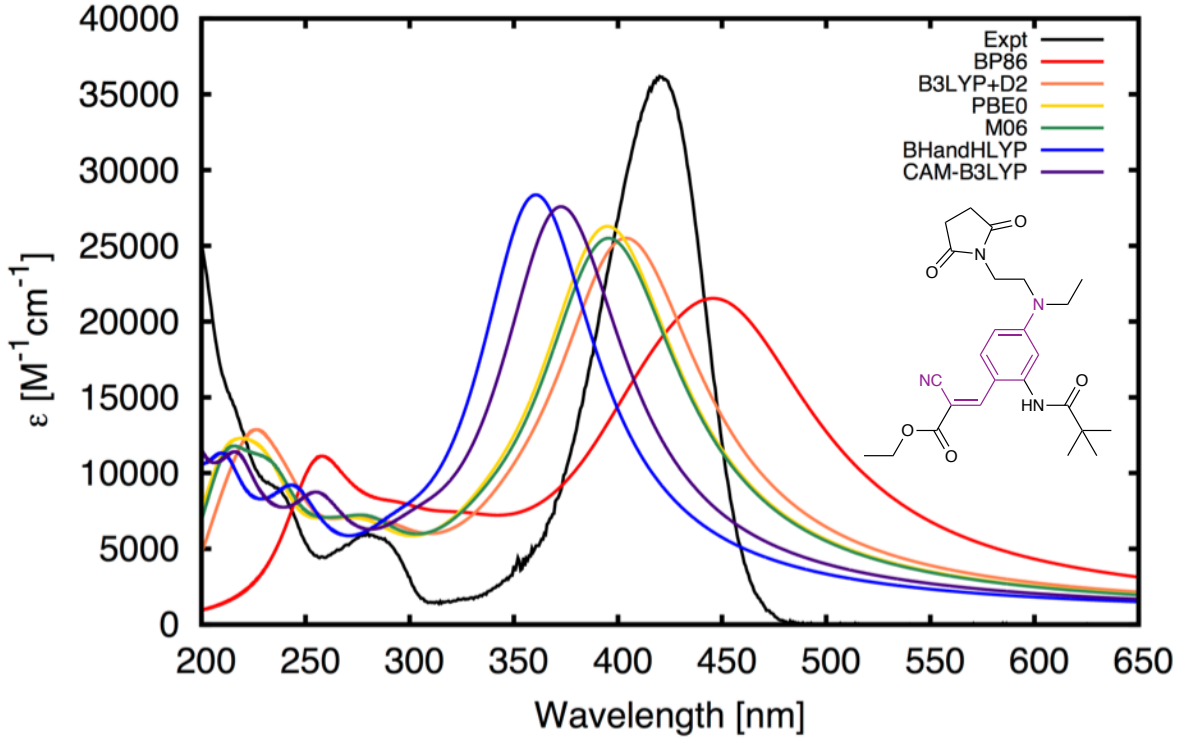

Figure S16. Experimentally measured and calculated TD-DFT spectra of dye **C6**.

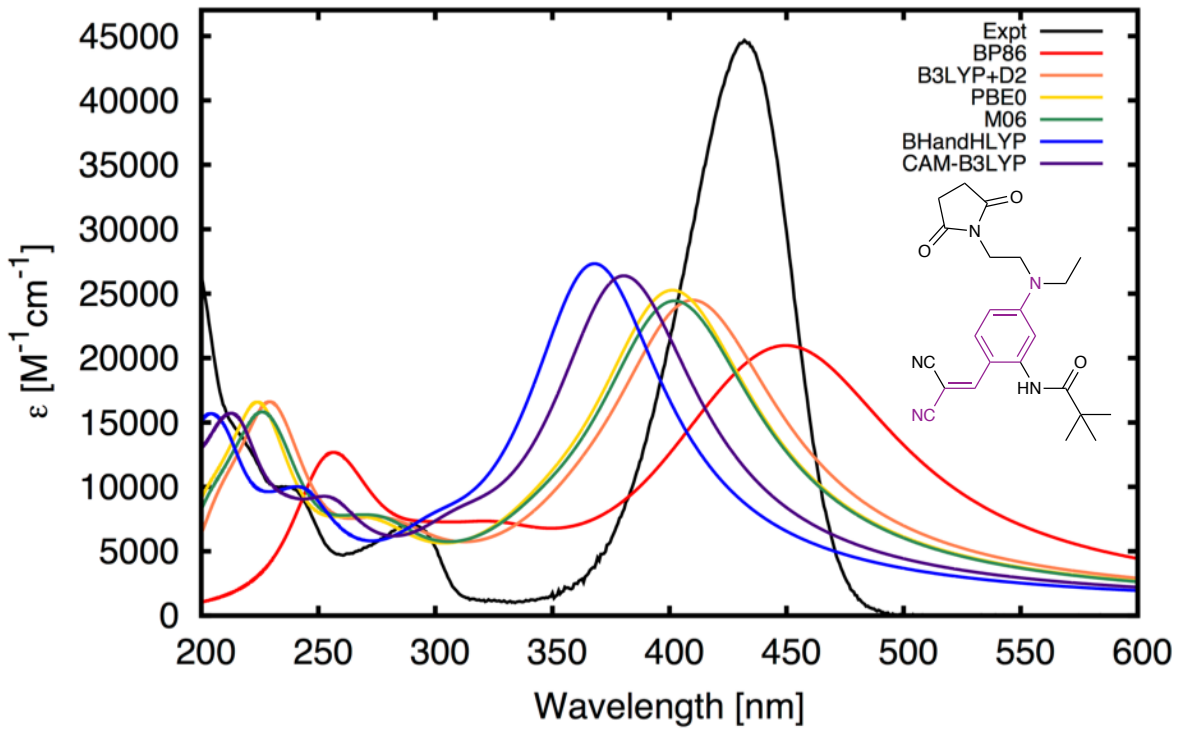

Figure S17. Experimentally measured and calculated TD-DFT spectra of dye **C7**.

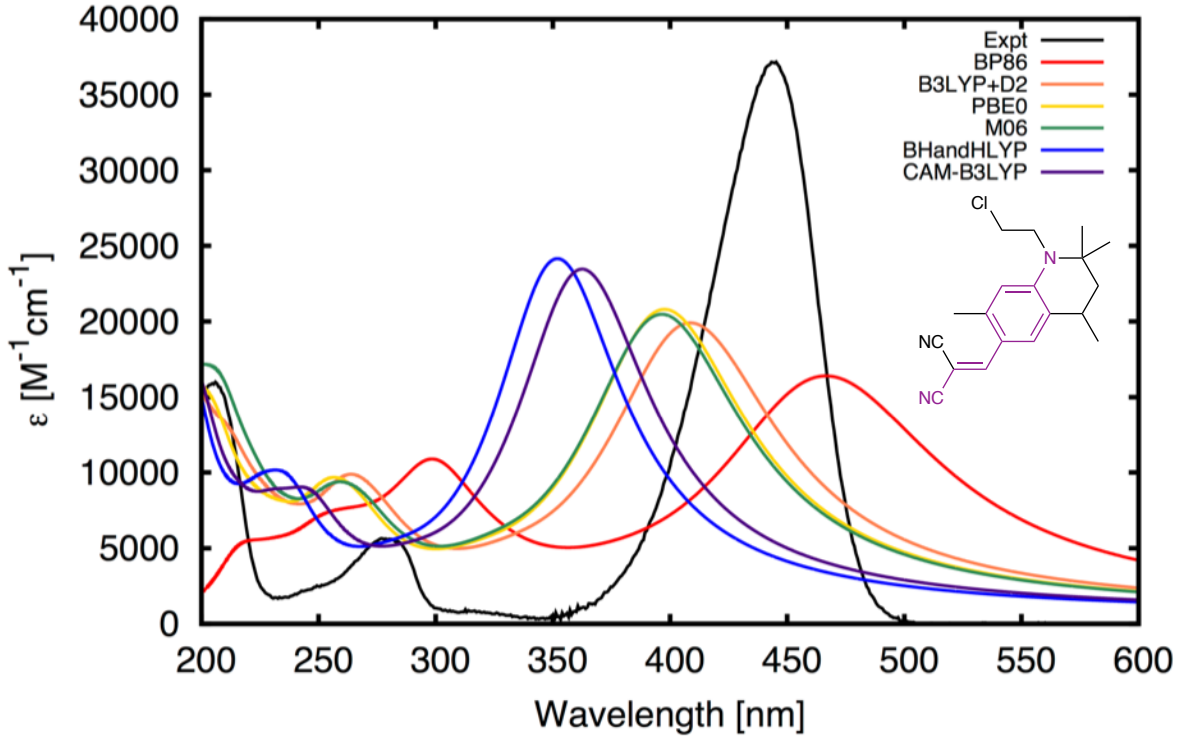

Figure S18. Experimentally measured and calculated TD-DFT spectra of dye **C8**.

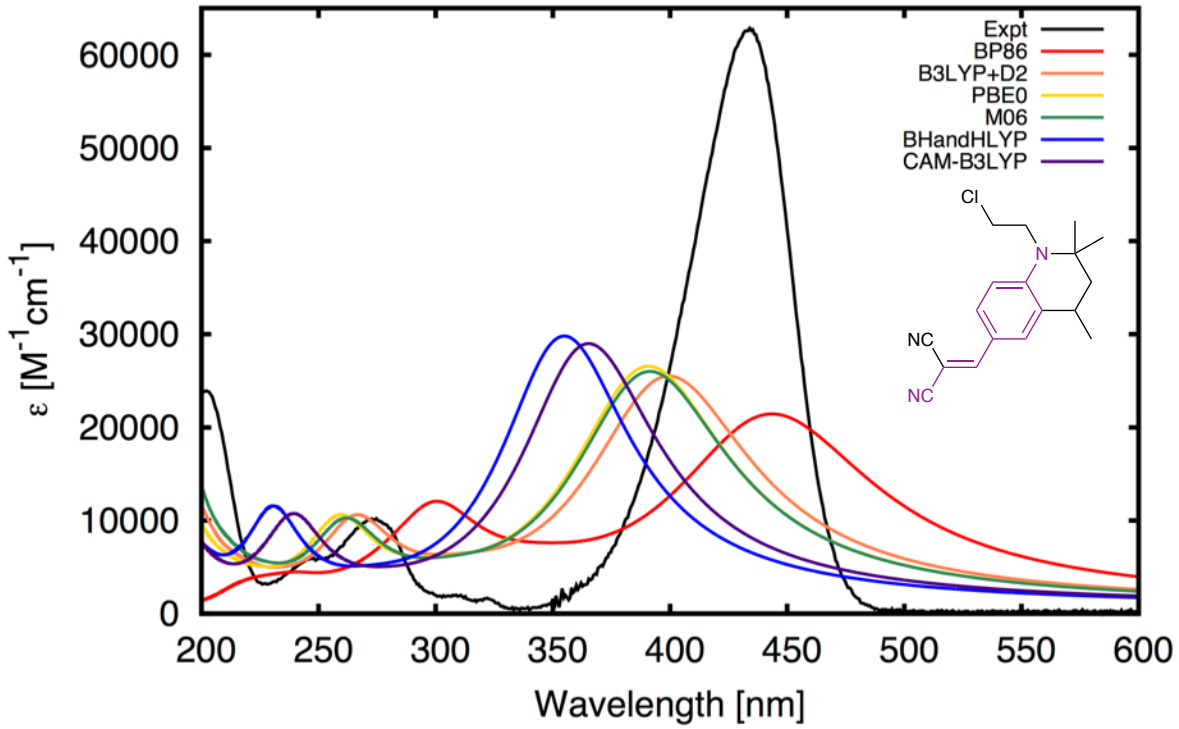

Figure S19. Experimentally measured and calculated TD-DFT spectra of dye **C9**.

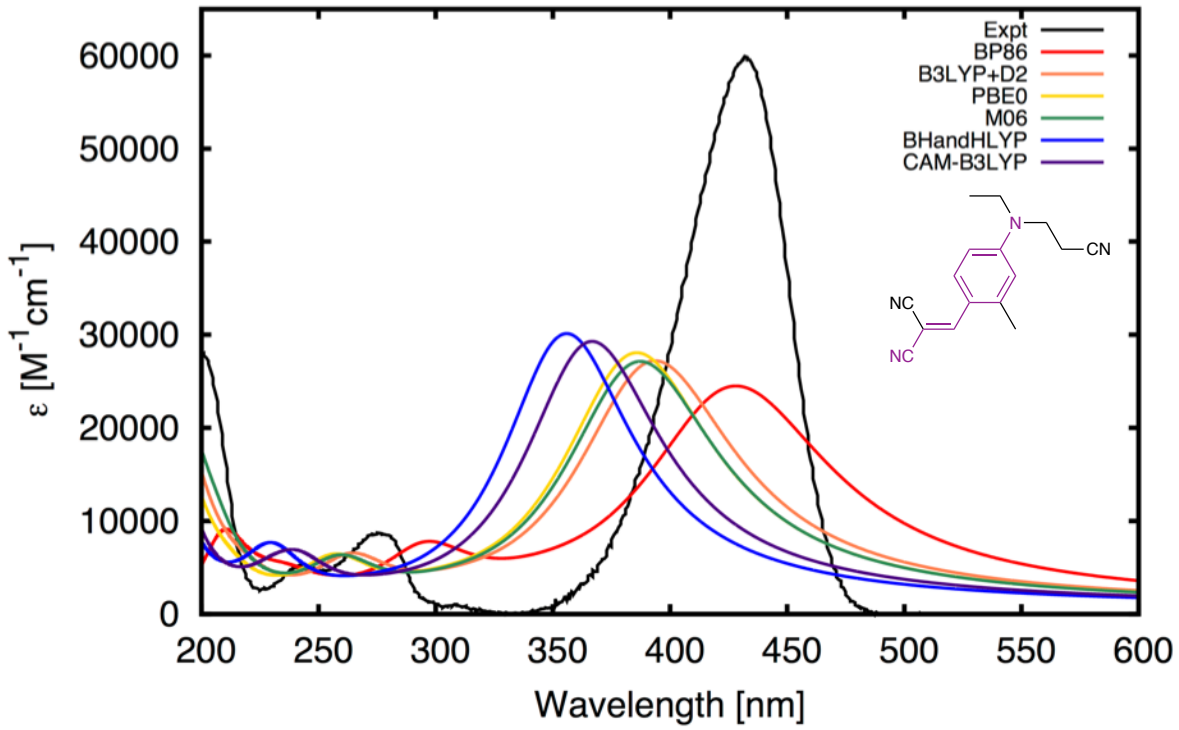

Figure S20. Experimentally measured and calculated TD-DFT spectra of dye **C10**.

HOMO-LUMO gap vs. calculated energies

Note that all plots below were made only for the high oscillator strength selection paradigm.

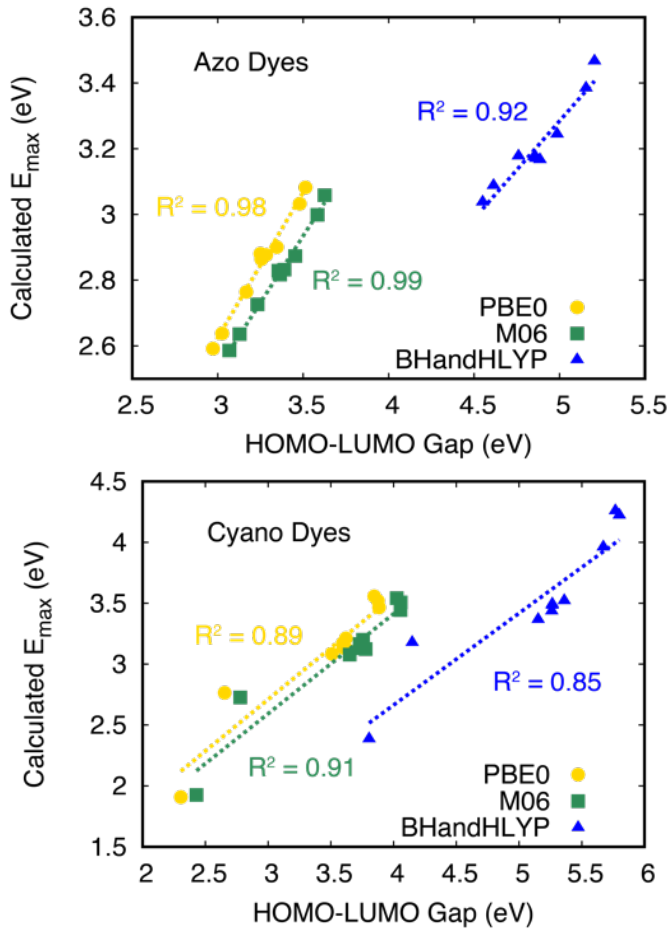

Figure S21: Relationship between HOMO-LUMO gap and calculated E_{max} for PBE0, M06, and BHandHLYP.

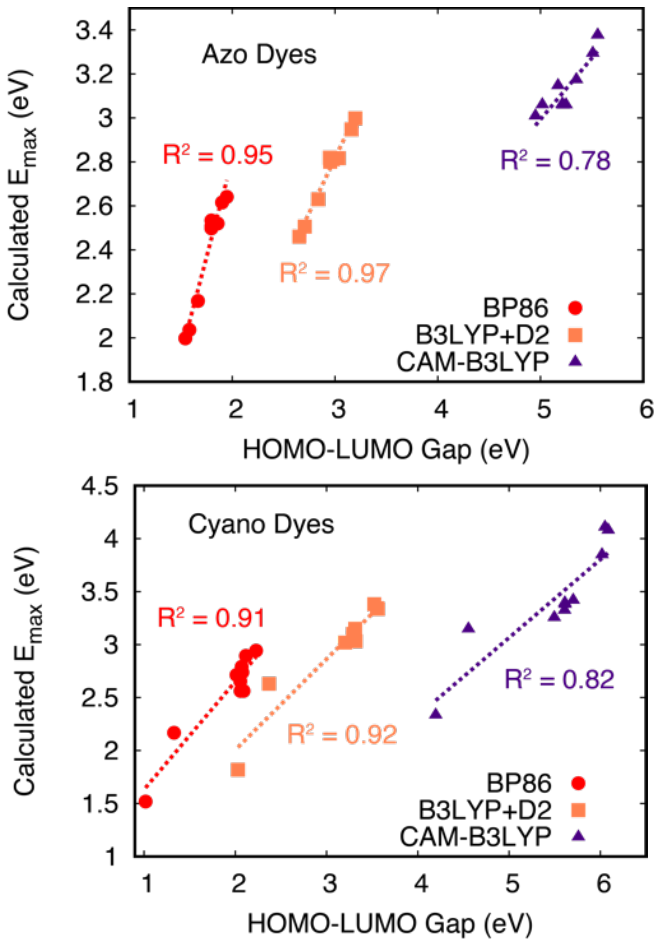

Figure S22: Relationship between HOMO-LUMO gap and calculated E_{max} for BP86, B3LYP+D2, and CAM-B3LYP.

Azo excitation data: High oscillator strength selection paradigm

Number	Library Code	Experimental E_{max} (eV)	Functional	H-L Gap (eV)	Calculated E_{max} (eV)	Osc. Strength	Transition Number	Λ	Δr (Å)	D_{CT} (Å)	S_C	$\Delta\mu$ (D)
A1	X-12516-134	3.18	B3LYP+D2	2.837	2.63	0.96	2	0.579	4.995	5.072	0.751	15.83
			M06	3.233	2.73	1.05	2	0.575	4.924	4.593	0.784	14.02
			CAM-B3LYP	5.170	3.15	1.24	2	0.563	4.903	3.806	0.821	10.71
			BP86	1.666	2.17	0.62	2	0.609	4.567	5.468	0.716	16.96
			PBE0	3.168	2.76	1.05	2	0.582	4.870	4.934	0.759	14.83
			BHandHLYP	4.760	3.18	1.27	2	0.572	4.795	3.791	0.829	11.25
A2	X-12683-21C	2.65	B3LYP+D2	2.979	2.81	0.87	2	0.665	1.617	1.844	0.939	4.10
			M06	3.390	2.83	1.04	2	0.680	1.886	1.869	0.931	4.25
			CAM-B3LYP	5.249	3.06	1.00	2	0.653	2.241	1.930	0.923	4.95
			BP86	1.821	2.53	0.89	2	0.671	1.680	2.851	0.889	5.49
			PBE0	3.283	2.88	0.95	2	0.667	1.775	1.983	0.929	4.45
			BHandHLYP	4.886	3.17	0.89	2	0.680	1.700	1.520	0.948	4.11
A3	X-12683-22A	2.84	B3LYP+D2	3.161	2.95	1.07	2	0.654	2.235	2.992	0.873	7.44
			M06	3.584	3.00	1.15	2	0.660	2.174	2.622	0.893	6.81
			CAM-B3LYP	5.509	3.29	1.21	2	0.640	2.676	2.629	0.889	7.49
			BP86	1.900	2.62	0.98	2	0.674	1.171	3.483	0.841	7.27
			PBE0	3.480	3.03	1.13	2	0.653	2.352	2.999	0.871	7.66
			BHandHLYP	5.155	3.38	1.22	2	0.651	2.600	2.492	0.900	7.36
A4	X-12683-22B	2.62	B3LYP+D2	2.949	2.82	0.80	2	0.666	1.847	1.548	0.950	3.53
			M06	3.356	2.83	1.04	2	0.677	1.769	1.700	0.944	3.85
			CAM-B3LYP	5.211	3.06	0.98	2	0.641	2.249	1.750	0.934	4.47
			BP86	1.797	2.53	0.98	2	0.674	1.401	2.386	0.926	4.18
			PBE0	3.250	2.88	0.89	2	0.665	1.654	1.715	0.942	3.90
			BHandHLYP	4.851	3.18	0.84	2	0.652	1.717	1.301	0.955	3.55
A5	X-12683-22C	2.65	B3LYP+D2	2.952	2.81	0.85	2	0.667	1.788	1.655	0.942	3.86
			M06	3.361	2.82	1.12	2	0.679	1.781	1.798	0.932	4.15
			CAM-B3LYP	5.218	3.06	1.06	2	0.632	2.513	1.829	0.924	4.73
			BP86	1.797	2.51	1.03	2	0.675	1.435	2.711	0.893	5.03
			PBE0	3.256	2.87	0.96	2	0.670	1.921	1.831	0.931	4.24
			BHandHLYP	4.860	3.17	0.92	2	0.660	1.625	1.394	0.948	3.83
A6	X-12683-23A	2.81	B3LYP+D2	3.198	3.00	0.98	2	0.650	2.362	3.049	0.875	7.89
			M06	3.626	3.06	1.09	2	0.652	2.336	2.762	0.891	7.51
			CAM-B3LYP	5.557	3.38	1.18	2	0.631	2.821	2.769	0.886	8.19
			BP86	1.947	2.64	0.89	2	0.672	1.197	3.435	0.858	7.40
			PBE0	3.514	3.08	1.06	2	0.646	2.491	3.102	0.870	8.25
			BHandHLYP	5.205	3.47	1.20	2	0.641	2.726	2.636	0.895	8.10
A7	X-12683-23C	2.66	B3LYP+D2	2.953	2.80	0.87	2	0.669	1.597	1.604	0.945	3.74
			M06	3.365	2.82	1.14	2	0.679	1.747	1.729	0.937	4.02
			CAM-B3LYP	5.221	3.06	1.09	2	0.624	2.525	1.830	0.928	4.74
			BP86	1.796	2.50	1.05	2	0.686	1.557	2.482	0.906	4.61
			PBE0	3.256	2.86	0.99	2	0.672	1.931	1.792	0.935	4.16
			BHandHLYP	4.862	3.17	0.95	2	0.655	1.781	1.415	0.950	3.89
A8	X-12683-24A	2.86	B3LYP+D2	3.037	2.82	1.26	2	0.653	2.938	3.197	0.865	7.66
			M06	3.453	2.87	1.29	2	0.653	2.840	2.832	0.886	7.21
			CAM-B3LYP	5.349	3.17	1.37	2	0.633	3.085	2.864	0.879	8.16
			BP86	1.857	2.52	1.13	2	0.669	2.782	3.285	0.865	6.39
			PBE0	3.346	2.90	1.30	2	0.650	2.982	3.213	0.862	7.99
			BHandHLYP	4.986	3.24	1.41	2	0.647	2.918	2.730	0.889	8.01
A9	X-12683-25	2.68	B3LYP+D2	2.706	2.51	1.03	2	0.558	5.498	5.246	0.779	17.44
			M06	3.128	2.64	1.15	2	0.556	5.366	4.777	0.802	15.56
			CAM-B3LYP	5.017	3.06	1.37	2	0.542	5.320	4.037	0.831	12.25
			BP86	1.583	2.04	0.68	2	0.591	5.443	5.553	0.757	17.41
			PBE0	3.026	2.64	1.14	2	0.559	5.389	5.138	0.782	16.58
			BHandHLYP	4.614	3.09	1.40	2	0.552	5.175	4.016	0.838	12.84
A10	X-12683-33A	2.63	B3LYP+D2	2.653	2.46	1.01	2	0.553	5.446	5.174	0.792	16.98
			M06	3.068	2.59	1.15	2	0.554	5.411	4.756	0.813	15.60
			CAM-B3LYP	4.951	3.01	1.38	2	0.537	5.390	4.028	0.837	12.33
			BP86	1.543	2.00	0.69	2	0.593	5.451	5.539	0.769	17.02
			PBE0	2.972	2.59	1.14	2	0.558	5.412	5.107	0.794	16.49
			BHandHLYP	4.550	3.04	1.41	2	0.548	5.248	3.999	0.845	12.92

Table S21. Measured and calculated values of azo dyes using the high oscillator paradigm.

Cyano excitation data: High oscillator strength selection paradigm

Number	Library Code	Experimental E_{max} (eV)	Functional	H-L Gap (eV)	Calculated E_{max} (eV)	Osc. Strength	Transition Number	Λ	Δr (Å)	D_{CT} (Å)	S_C	Δμ (D)
C1	X-12833-43-1	2.05	B3LYP+D2	2.030	1.82	0.42	1	0.607	4.084	3.719	0.721	10.16
			M06	2.429	1.93	0.43	1	0.578	4.226	3.804	0.716	11.64
			CAM-B3LYP	4.196	2.33	0.57	1	0.530	4.386	3.924	0.707	13.42
			BP86	1.017	1.52	0.31	1	0.658	3.585	2.829	0.804	6.53
			PBE0	2.305	1.91	0.45	1	0.595	4.141	3.838	0.710	10.96
			BHandHLYP	3.805	2.39	0.60	1	0.536	4.377	3.844	0.716	13.63
C2	X-12833-45-2	2.44	B3LYP+D2	2.371	2.19	0.63	1	0.587	4.088	4.227	0.699	12.62
			M06	2.778	2.31	0.69	1	0.561	4.206	4.041	0.718	12.90
			CAM-B3LYP	4.555	2.68	0.91	1	0.530	4.257	3.624	0.752	11.67
			BP86	1.330	1.75	0.27	1	0.534	4.590	4.360	0.643	16.19
			PBE0	2.654	2.29	0.70	1	0.577	4.124	4.191	0.702	12.60
			BHandHLYP	4.149	2.72	0.92	1	0.536	4.237	3.598	0.757	12.16
C3	X-12833-83-1	3.20	B3LYP+D2	3.562	3.34	0.32	2	0.546	3.274	2.677	0.762	7.36
			M06	4.055	3.44	0.34	2	0.535	3.128	2.607	0.769	7.85
			CAM-B3LYP	6.018	3.85	0.44	2	0.516	3.359	2.658	0.766	9.00
			BP86	2.228	2.94	0.23	2	0.615	2.897	2.286	0.822	4.60
			PBE0	3.884	3.47	0.35	2	0.532	3.342	2.766	0.750	8.12
			BHandHLYP	5.672	3.96	0.47	2	0.531	3.181	2.554	0.780	9.14
C4	X-12833-88-1	3.36	B3LYP+D2	3.523	3.38	0.26	2	0.464	3.936	3.280	0.714	12.21
			M06	4.025	3.54	0.28	2	0.469	3.832	3.055	0.737	11.44
			CAM-B3LYP	6.051	4.11	0.21	2	0.489	2.657	1.605	0.882	5.25
			BP86	2.057	2.56	0.09	2	0.401	4.720	4.19	0.675	18.62
			PBE0	3.847	3.56	0.28	2	0.464	3.960	3.234	0.719	12.10
			BHandHLYP	5.768	4.26	0.35	2	0.495	3.387	2.617	0.793	9.75
C5	X-12833-89-1	3.37	B3LYP+D2	3.552	3.34	0.25	2	0.467	3.885	3.304	0.706	12.28
			M06	4.057	3.51	0.28	2	0.472	3.722	3.069	0.731	11.55
			CAM-B3LYP	6.086	4.08	0.34	2	0.476	3.389	2.588	0.790	9.19
			BP86	2.090	2.56	0.11	2	0.409	4.704	4.221	0.639	17.65
			PBE0	3.876	3.52	0.28	2	0.467	3.909	3.242	0.711	12.16
			BHandHLYP	5.799	4.22	0.38	2	0.492	3.484	2.649	0.783	10.07
C6	X-13641-126	2.95	B3LYP+D2	3.289	3.07	0.89	**1**	0.653	2.201	2.512	0.857	5.84
			M06	3.739	3.13	0.90	**1**	0.648	2.144	2.264	0.873	5.63
			CAM-B3LYP	5.607	3.32	0.97	**1**	0.637	2.184	2.315	0.864	6.07
			BP86	2.078	2.74	0.61	**1**	0.649	2.327	3.010	0.826	6.96
			PBE0	3.599	3.14	0.92	**1**	0.651	2.206	2.509	0.855	5.94
			BHandHLYP	5.261	3.44	1.00	**1**	0.646	2.035	2.115	0.882	5.76
C7	X-13641-87	2.87	B3LYP+D2	3.204	3.02	0.85	**1**	0.656	2.110	2.389	0.848	5.22
			M06	3.650	3.08	0.85	**1**	0.650	2.069	2.157	0.864	5.11
			CAM-B3LYP	5.495	3.26	0.92	**1**	0.637	2.104	2.214	0.854	5.56
			BP86	2.013	2.71	0.58	**1**	0.641	2.266	2.573	0.825	5.72
			PBE0	3.510	3.08	0.88	**1**	0.654	2.121	2.392	0.846	5.34
			BHandHLYP	5.152	3.37	0.96	**1**	0.646	1.970	2.039	0.873	5.38
C8	X-13699-140	2.79	B3LYP+D2	3.318	3.03	0.70	**1**	0.604	2.981	3.034	0.852	8.61
			M06	3.777	3.12	0.72	**1**	0.601	2.911	2.854	0.863	8.54
			CAM-B3LYP	5.702	3.42	0.83	**1**	0.588	2.937	2.845	0.866	8.90
			BP86	2.056	2.65	0.57	**1**	0.619	3.083	3.098	0.846	7.43
			PBE0	3.634	3.12	0.73	**1**	0.602	2.984	3.051	0.851	8.83
			BHandHLYP	5.360	3.52	0.85	**1**	0.602	2.762	2.685	0.877	8.63
C9	X-13699-147	2.86	B3LYP+D2	3.290	3.10	0.91	**1**	0.654	2.392	2.786	0.864	6.75
			M06	3.730	3.17	0.92	**1**	0.650	2.340	2.567	0.879	6.62
			CAM-B3LYP	5.611	3.39	1.04	**1**	0.638	2.383	2.631	0.877	7.19
			BP86	2.071	2.79	0.75	**1**	0.666	2.406	2.862	0.854	5.98
			PBE0	3.595	3.17	0.95	**1**	0.652	2.403	2.809	0.863	6.94
			BHandHLYP	5.265	3.49	1.07	**1**	0.646	2.203	2.409	0.893	6.81
C10	X-9745-103A	2.87	B3LYP+D2	3.314	3.15	0.98	**1**	0.666	1.998	2.411	0.830	5.14
			M06	3.757	3.20	0.97	**1**	0.661	1.946	2.179	0.851	5.04
			CAM-B3LYP	5.613	3.38	1.05	**1**	0.649	2.014	2.332	0.834	5.77
			BP86	2.117	2.89	0.87	**1**	0.679	1.985	2.489	0.827	4.46
			PBE0	3.621	3.21	1.01	**1**	0.664	2.007	2.439	0.826	5.33
			BHandHLYP	5.265	3.48	1.08	**1**	0.658	1.853	2.094	0.859	5.41

Table S22. Measured and calculated values of cyano dyes using the high oscillator paradigm.

Azo excitation images: High oscillator strength selection paradigm

The following tables show the orbital pairs that contribute to each λ_{max} excitation for the azo dyes. In this section, λ_{max} excitations were selected based on the highest oscillator strength paradigm when there was potential conflict. Images of the orbital pairs with the highest contribution values are provided. All orbital images in the SI were rendered with an isovalue of 0.03 (e/Å^3). The percent contribution of each excitation is indicated.

Table S23. Dominant orbitals involved in excited state corresponding to λ_{max} for **A1**. High oscillator strength paradigm.

A1			
B3LYP+D2			
HOMO		LUMO	0.996
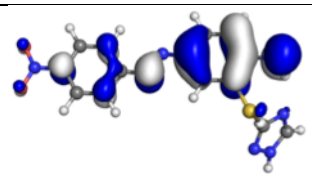	→	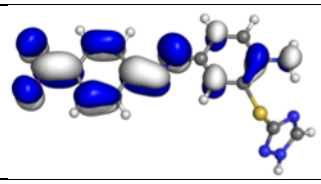	
M06			
HOMO		LUMO	0.988
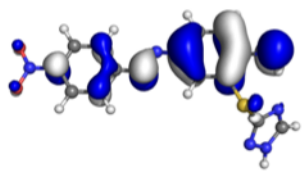	→	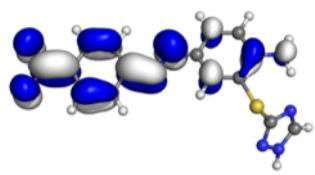	
CAM-B3LYP			
HOMO	→	LUMO+1	0.071
HOMO		LUMO	0.877
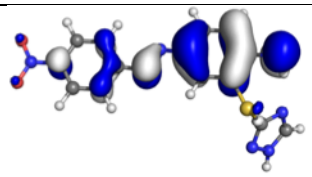	→	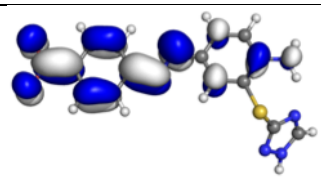	
BP86			
HOMO	→	LUMO	0.067
HOMO-1	→	LUMO+1	0.089
HOMO-1		LUMO	0.824
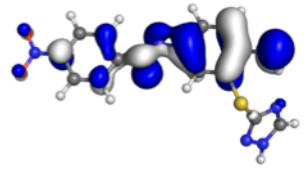	→	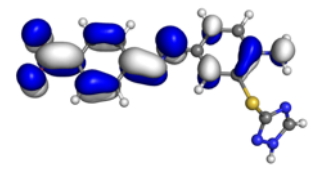	
PBE0			

HOMO		LUMO	0.995
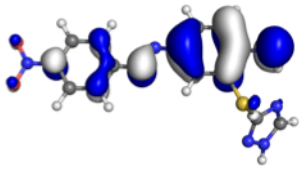	→	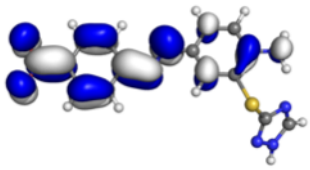	
BHandHLYP			
HOMO	→	LUMO+1	0.054
HOMO		LUMO	0.903
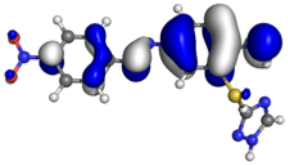	→	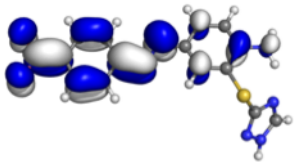	

Table S24. Dominant orbitals involved in excited state corresponding to λ_{max} for **A2**. High oscillator strength paradigm.

A2			
B3LYP+D2			
HOMO-5	→	LUMO	0.020
HOMO-2	→	LUMO	0.262
HOMO		LUMO	0.695
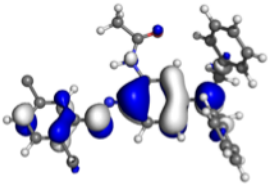	→	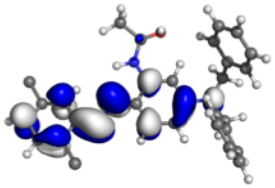	
M06			
HOMO-2	→	LUMO	0.115
HOMO		LUMO	0.838
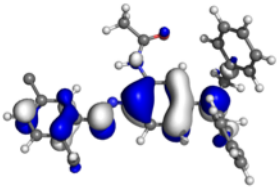	→	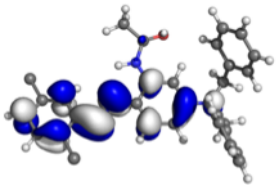	
CAM-B3LYP			
HOMO-5	→	LUMO	0.023
HOMO-3	→	LUMO	0.062
HOMO-6	→	LUMO	0.084
HOMO	→	LUMO	0.761

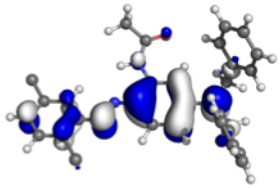		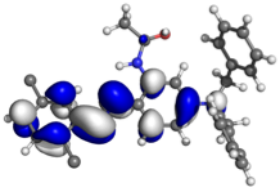	
BP86			
HOMO	←	LUMO	0.020
HOMO-2	→	LUMO	0.042
HOMO-1	→	LUMO	0.166
HOMO	→	LUMO	0.767
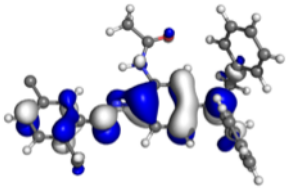		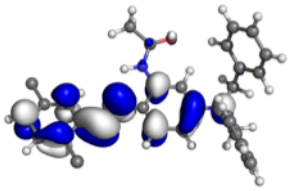	
PBE0			
HOMO-5	→	LUMO	0.026
HOMO-2	→	LUMO	0.214
HOMO	→	LUMO	0.745
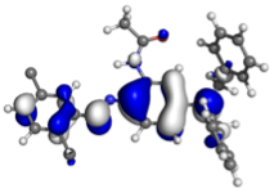		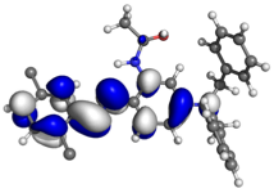	
BHandHLYP			
HOMO-8	→	LUMO	0.136
HOMO-7	→	LUMO	0.148
HOMO	→	LUMO	0.647
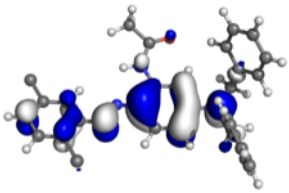		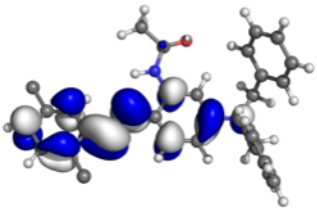	

Table S25. Dominant orbitals involved in excited state corresponding to λ_{max} for **A3**. High oscillator strength paradigm.

A3			
B3LYP+D2			
HOMO-1	→	LUMO	0.165
HOMO	→	LUMO	0.815

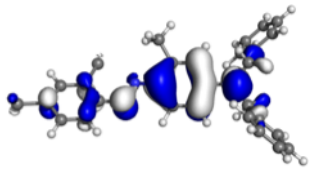		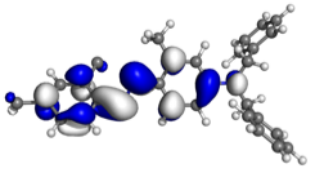	
M06			
HOMO-1	→	LUMO	0.124
HOMO	→	LUMO	0.843
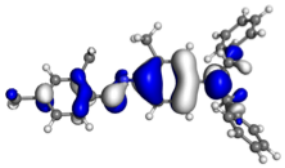		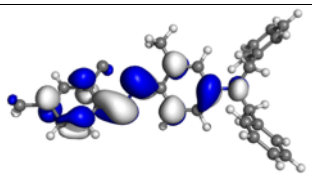	
CAM-B3LYP			
HOMO-1	→	LUMO	0.050
HOMO	→	LUMO	0.848
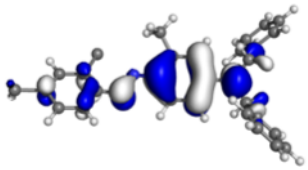		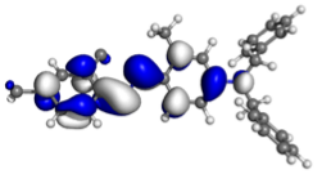	
BP86			
HOMO	→	LUMO	0.350
HOMO-1	→	LUMO	0.622
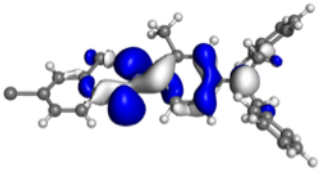		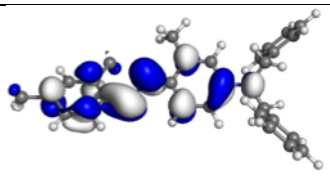	
PBE0			
HOMO-1	→	LUMO	0.132
HOMO	→	LUMO	0.842
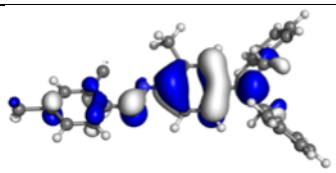		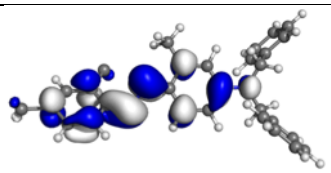	
BHandHLYP			
HOMO-8	→	LUMO	0.035
HOMO-7	→	LUMO	0.043
HOMO	→	LUMO	0.841

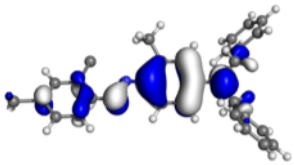		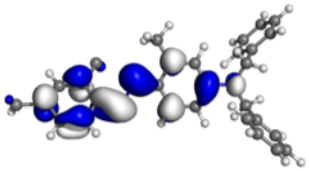	

Table S26. Dominant orbitals involved in excited state corresponding to λ_{max} for **A4**. High oscillator strength paradigm.

A4			
B3LYP+D2			
HOMO-1	→	LUMO	0.185
HOMO-2	→	LUMO	0.200
HOMO	→	LUMO	0.586
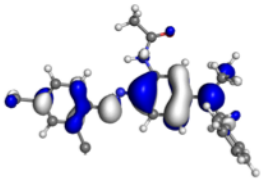		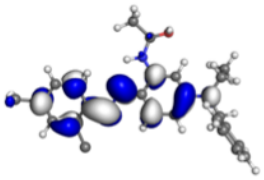	
M06			
HOMO-2	→	LUMO	0.053
HOMO-1	→	LUMO	0.144
HOMO	→	LUMO	0.770
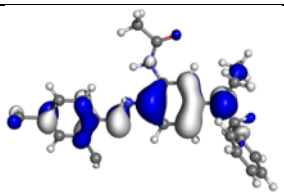		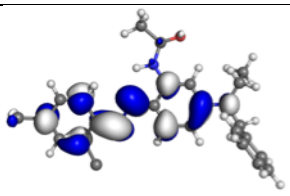	
CAM-B3LYP			
HOMO-4	→	LUMO	0.020
HOMO-3	→	LUMO	0.047
HOMO-5	→	LUMO	0.082
HOMO-2	→	LUMO	0.121
HOMO	→	LUMO	0.688
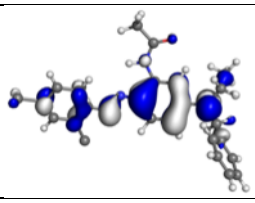		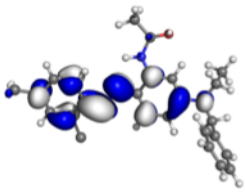	
BP86			
HOMO	←	LUMO	0.022
HOMO-1	→	LUMO	0.236

HOMO		LUMO	0.746
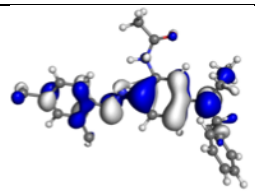	→	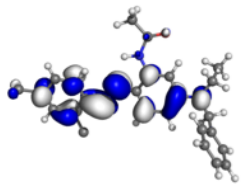	
PBE0			
HOMO-1	→	LUMO	0.039
HOMO-2	→	LUMO	0.277
HOMO		LUMO	0.647
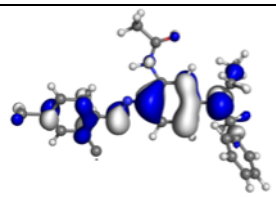	→	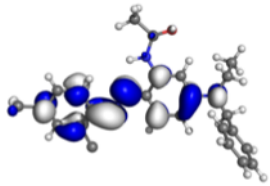	
BHandHLYP			
HOMO-3	→	LUMO	0.028
HOMO-4	→	LUMO	0.050
HOMO-6	→	LUMO	0.311
HOMO		LUMO	0.559
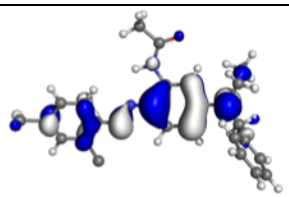	→	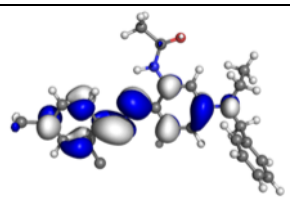	

Table S27. Dominant orbitals involved in excited state corresponding to λ_{max} for **A5**. High oscillator strength paradigm.

A5			
B3LYP+D2			
HOMO-2	→	LUMO	0.131
HOMO-1	→	LUMO	0.253
HOMO		LUMO	0.585
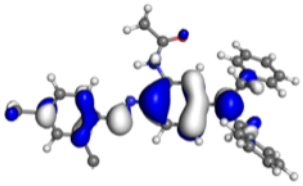	→	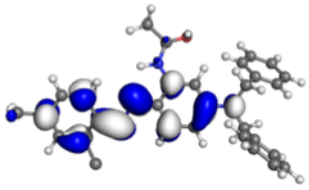	
M06			
HOMO-2	→	LUMO	0.043
HOMO-1	→	LUMO	0.147

HOMO		LUMO	0.774
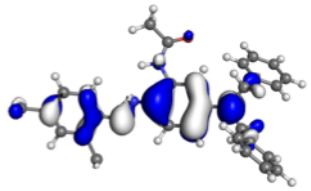	→	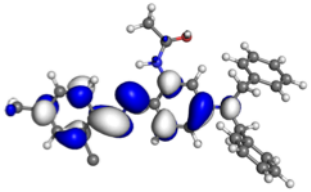	
CAM-B3LYP			
HOMO-4	→	LUMO	0.022
HOMO-7	→	LUMO	0.069
HOMO-2	→	LUMO	0.079
HOMO-3	→	LUMO	0.080
HOMO		LUMO	0.699
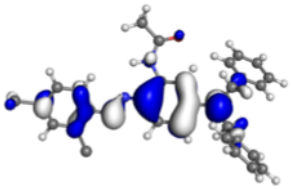	→	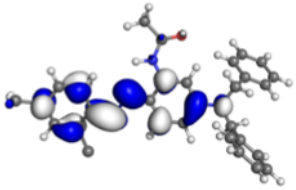	
BP86			
HOMO	←	LUMO	0.020
HOMO-1	→	LUMO	0.237
HOMO		LUMO	0.735
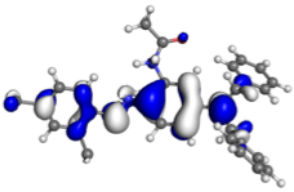	→	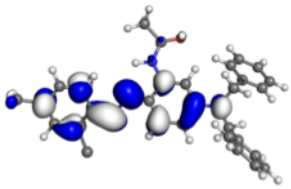	
PBE0			
HOMO-1	→	LUMO	0.094
HOMO-2	→	LUMO	0.210
HOMO		LUMO	0.654
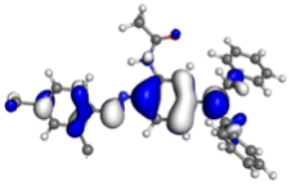	→	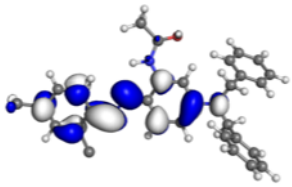	
BHandHLYP			
HOMO-6	→	LUMO	0.067
HOMO-8	→	LUMO	0.292
HOMO	→	LUMO	0.576

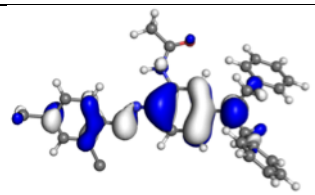		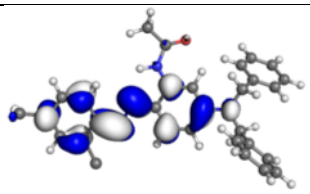	

Table S28. Dominant orbitals involved in excited state corresponding to λ_{max} for **A6**. High oscillator strength paradigm.

A6			
B3LYP+D2			
HOMO-1	→	LUMO	0.189
HOMO	→	LUMO	0.779
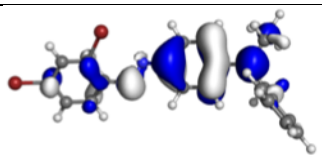		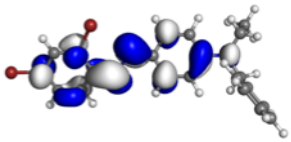	
M06			
HOMO-3	→	LUMO	0.023
HOMO-1	→	LUMO	0.131
HOMO	→	LUMO	0.825
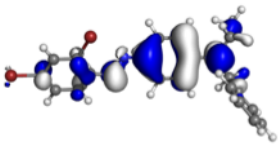		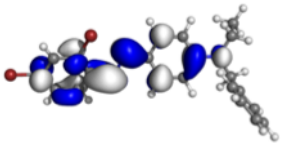	
CAM-B3LYP			
HOMO-4	→	LUMO	0.044
HOMO-1	→	LUMO	0.051
HOMO	→	LUMO	0.837
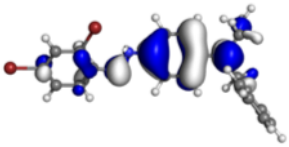		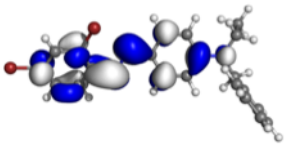	
BP86			
HOMO	→	LUMO	0.478
HOMO-1	→	LUMO	0.489
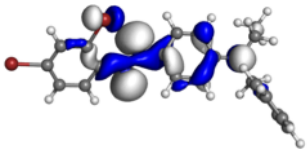		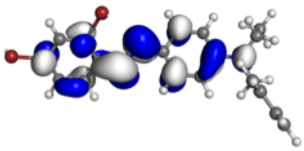	
PBE0			
HOMO-3	→	LUMO	0.021

HOMO-1	→	LUMO	0.147
HOMO	→	LUMO	0.816
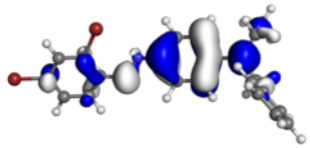		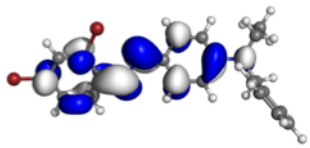	
BHandHLYP			
HOMO-1	→	LUMO	0.027
HOMO-6	→	LUMO	0.068
HOMO	→	LUMO	0.826
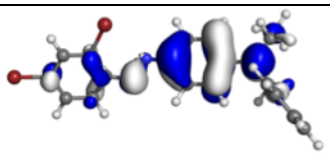		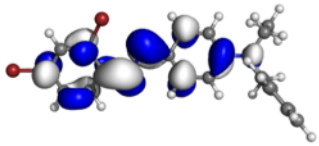	

Table S29. Dominant orbitals involved in excited state corresponding to λ_{max} for **A7**. High oscillator strength paradigm.

A7			
B3LYP+D2			
HOMO-2	→	LUMO	0.089
HOMO-1	→	LUMO	0.286
HOMO	→	LUMO	0.584
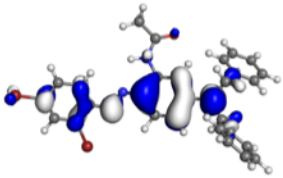		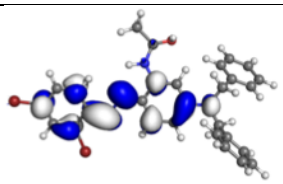	
M06			
HOMO-2	→	LUMO	0.036
HOMO-1	→	LUMO	0.153
HOMO	→	LUMO	0.770
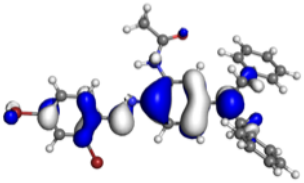		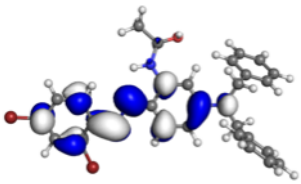	
CAM-B3LYP			
HOMO-4	→	LUMO	0.022
HOMO-5	→	LUMO	0.024
HOMO-7	→	LUMO	0.053
HOMO-3	→	LUMO	0.058

HOMO-2	→	LUMO	0.093
HOMO	→	LUMO	0.702
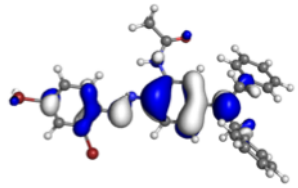		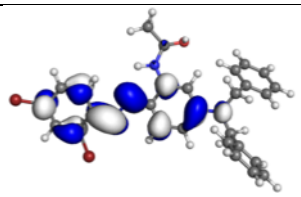	
BP86			
HOMO-1	→	LUMO	0.249
HOMO	→	LUMO	0.722
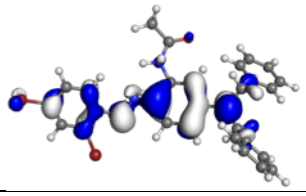		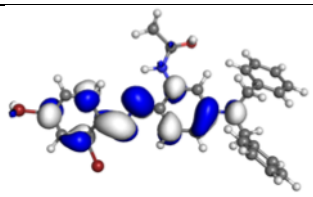	
PBE0			
HOMO-1	→	LUMO	0.142
HOMO-2	→	LUMO	0.155
HOMO	→	LUMO	0.653
		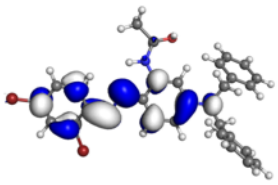	
BHandHLYP			
HOMO-4	→	LUMO	0.021
HOMO-8	→	LUMO	0.276
HOMO	→	LUMO	0.584
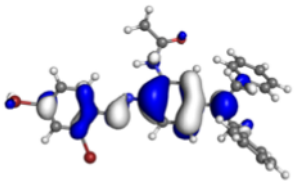		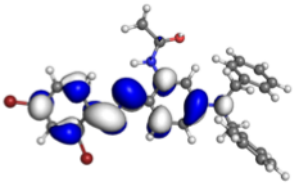	

Table S30. Dominant orbitals involved in excited state corresponding to λ_{max} for **A8**. High oscillator strength paradigm.

A8			
B3LYP+D2			
HOMO	→	LUMO	0.997

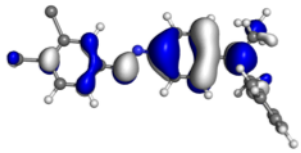		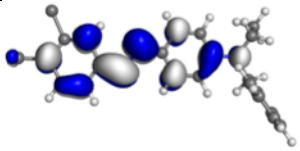	
M06			
HOMO		LUMO	0.989
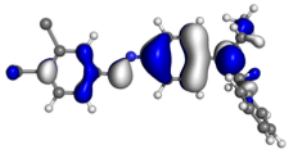	→	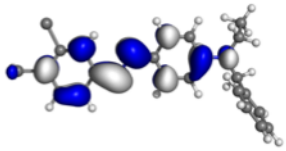	
CAM-B3LYP			
HOMO		LUMO	0.947
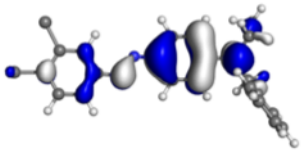	→	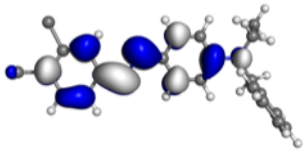	
BP86			
HOMO	←	LUMO	0.023
HOMO		LUMO	0.987
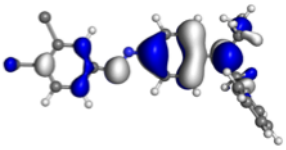	→	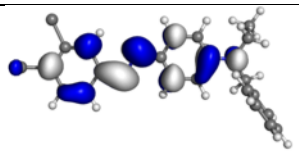	
PBE0			
HOMO		LUMO	0.995
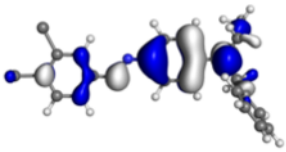	→	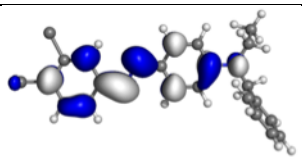	
BHandHLYP			
HOMO	→	LUMO	0.956
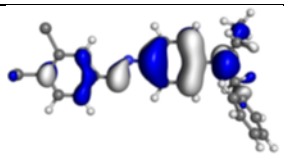		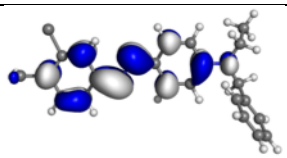	

Table S31. Dominant orbitals involved in excited state corresponding to λ_{max} for **A9**. High oscillator strength paradigm.

A9			
B3LYP+D2			
HOMO		LUMO	1.001
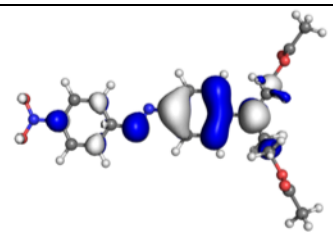	→	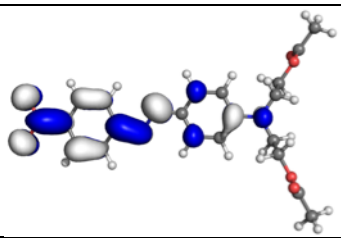	
M06			
HOMO		LUMO	0.990
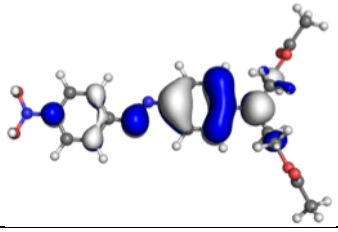	→	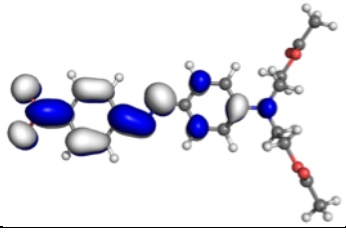	
CAM-B3LYP			
HOMO-3	→	LUMO	0.030
HOMO	→	LUMO+1	0.076
HOMO		LUMO	0.869
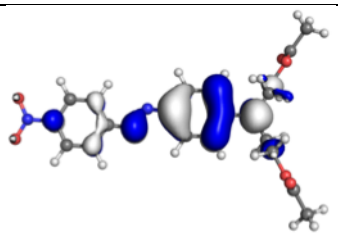	→	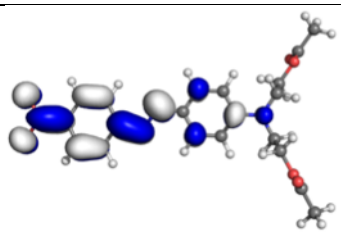	
BP86			
HOMO	→	LUMO+1	0.088
HOMO		LUMO	0.909
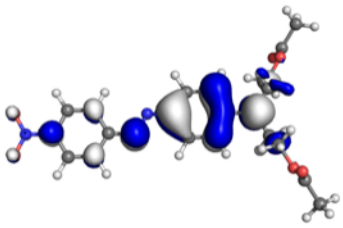	→	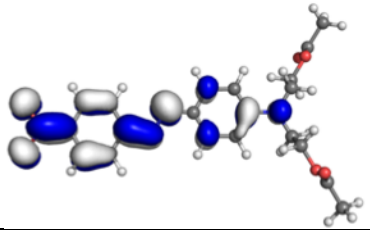	
PBE0			
HOMO	→	LUMO	0.998

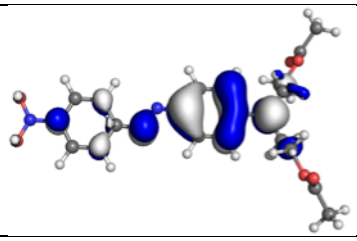		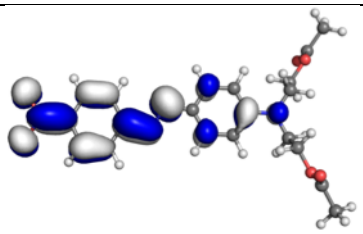	
BHandHLYP			
HOMO-3	→	LUMO	0.028
HOMO	→	LUMO+1	0.057
HOMO	→	LUMO	0.899
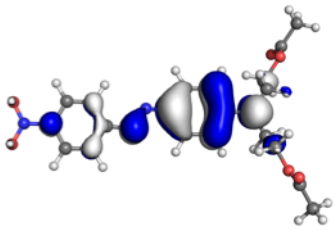		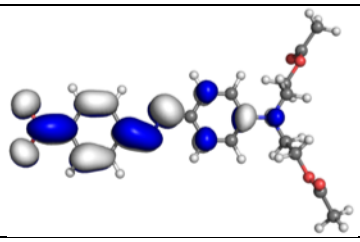	

Table S32. Dominant orbitals involved in excited state corresponding to λ_{max} for **A10**. High oscillator strength paradigm.

A10			
B3LYP+D2			
HOMO-1	→	LUMO	0.026
HOMO	→	LUMO	0.972
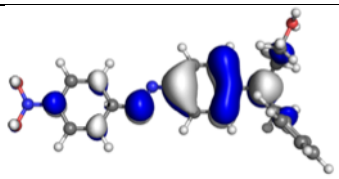		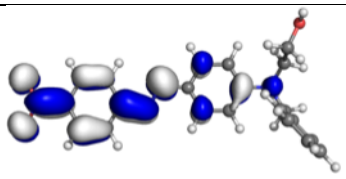	
M06			
HOMO	→	LUMO	0.990
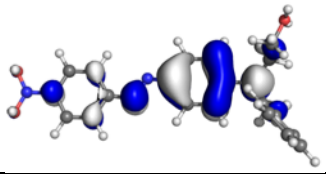		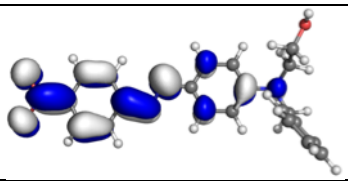	
CAM-B3LYP			
HOMO-4	→	LUMO	0.021
HOMO	→	LUMO+1	0.076
HOMO	→	LUMO	0.868

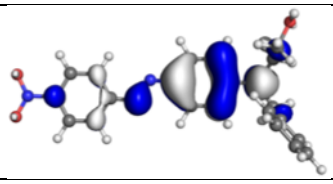		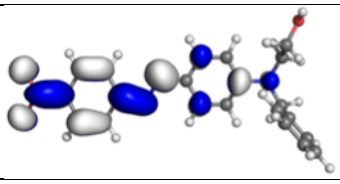	
BP86			
HOMO	→	LUMO+1	0.086
HOMO	→	LUMO	0.909
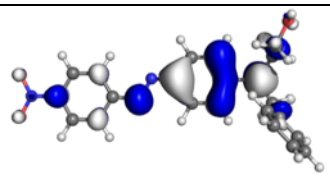		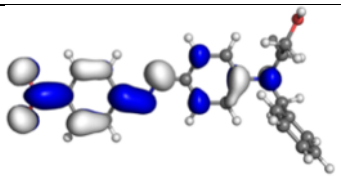	
PBE0			
HOMO	→	LUMO	0.996
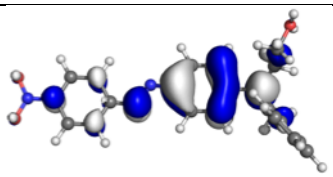		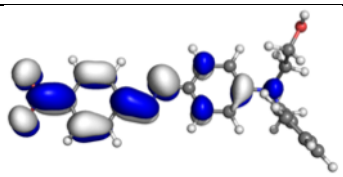	
BHandHLYP			
HOMO-5	→	LUMO	0.022
HOMO	→	LUMO+1	0.057
HOMO	→	LUMO	0.897
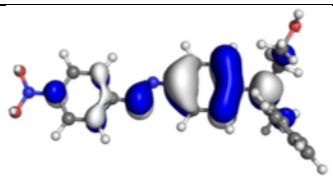		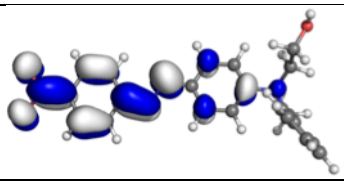	

Cyano excitation images: High oscillator strength selection paradigm

The following tables show the orbital pairs that contribute to each λ_{max} excitation for the cyano dyes. In this section, λ_{max} excitations were selected based on the highest oscillator strength paradigm when there was potential conflict. Images of the orbital pairs with the highest contribution values are provided. All orbital images in the SI were rendered with an isovalue of 0.03 (e/Å^3). The percent contribution of each excitation is indicated.

Table S33. Dominant orbitals involved in excited state corresponding to λ_{max} for **C1**. High oscillator strength paradigm.

C1			
B3LYP			
HOMO		LUMO	0.991
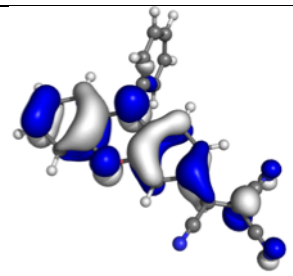	→	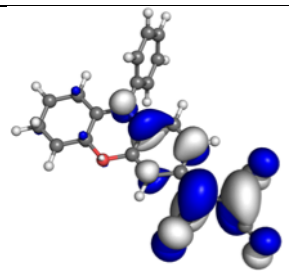	
M06			
HOMO		LUMO	0.990
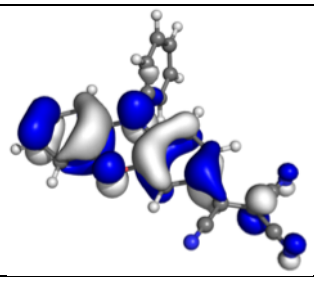	→	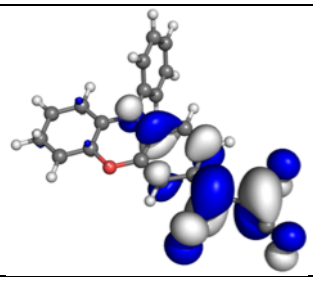	
CAM-B3LYP			
HOMO		LUMO	0.953
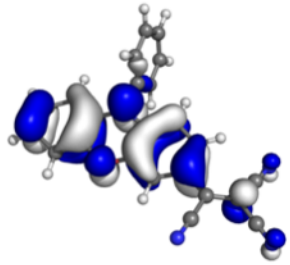	→	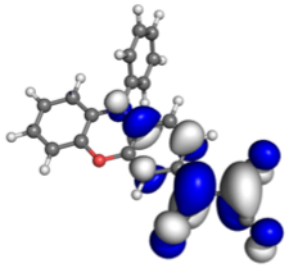	
BP86			
HOMO-1	→	LUMO	0.042
HOMO	←	LUMO	0.038

HOMO		LUMO	0.978
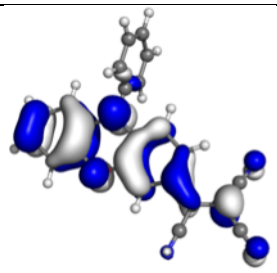	→	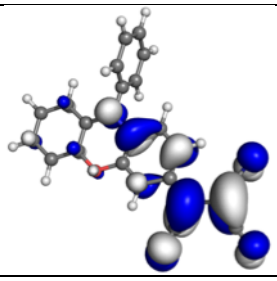	
PBE0			
HOMO		LUMO	0.992
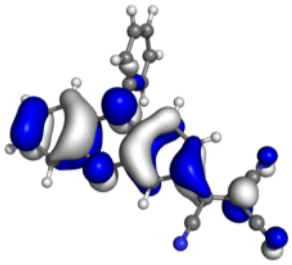	→	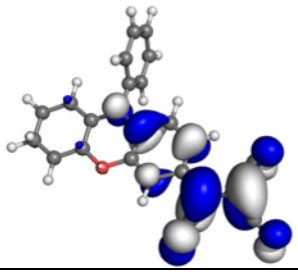	
BHandHLYP			
HOMO		LUMO	0.966
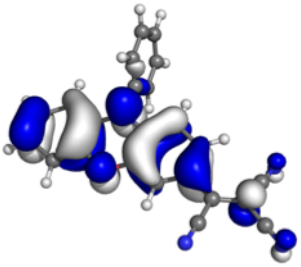	→	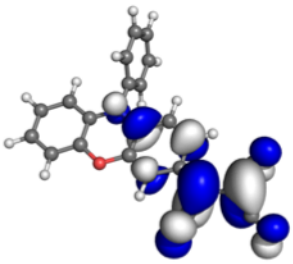	

Table S34. Dominant orbitals involved in excited state corresponding to λ_{max} for **C2**. High oscillator strength paradigm.

C2			
B3LYP			
HOMO		LUMO	0.985
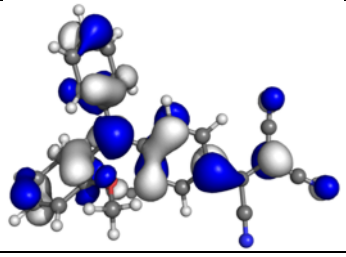	→	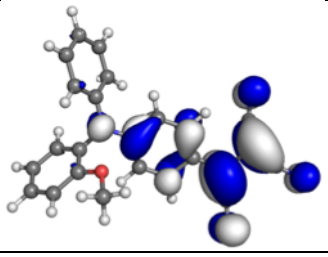	
M06			
HOMO	→	LUMO	0.997

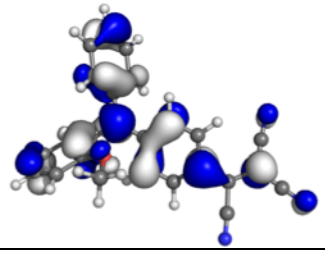		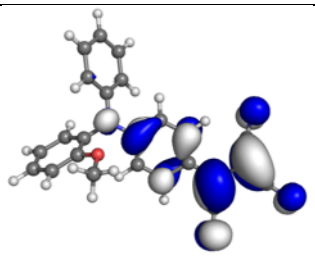	
CAM-B3LYP			
HOMO-2	→	LUMO	0.026
HOMO	→	LUMO	0.931
		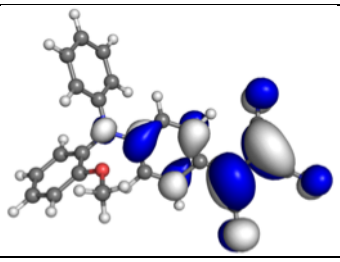	
BP86			
HOMO-1	→	LUMO	0.323
HOMO	→	LUMO	0.678
		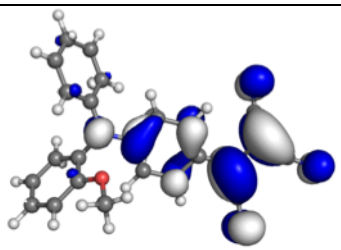	
PBE0			
HOMO	→	LUMO	0.996
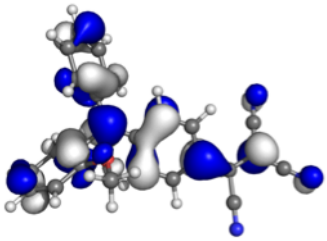		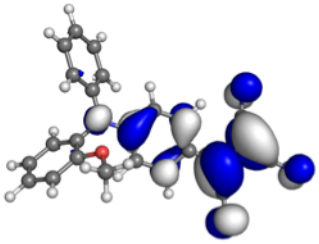	
BHandHLYP			
HOMO	→	LUMO	0.948
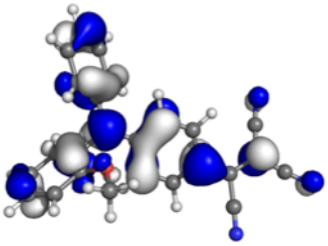		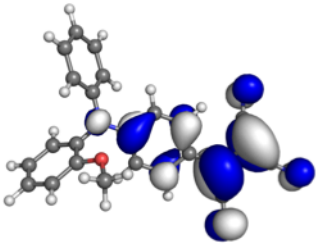	

Table S35. Dominant orbitals involved in excited state corresponding to λ_{max} for **C3**. High oscillator strength paradigm.

C3			
B3LYP+D2			
HOMO	→	LUMO	0.026
HOMO	→	LUMO+1	0.950
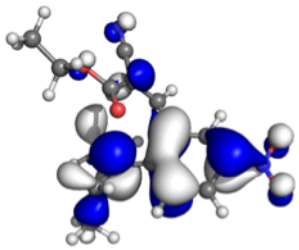		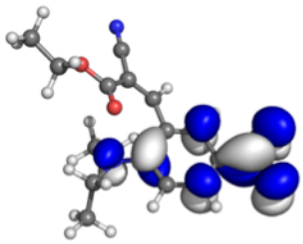	
M06			
HOMO	→	LUMO	0.129
HOMO	→	LUMO+1	0.836
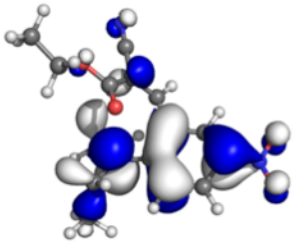		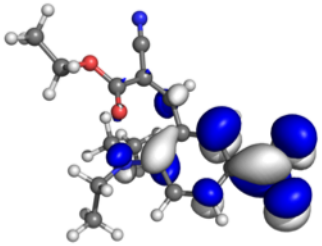	
CAM-B3LYP			
HOMO	→	LUMO+1	0.907
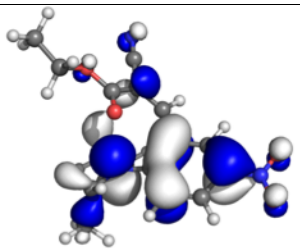		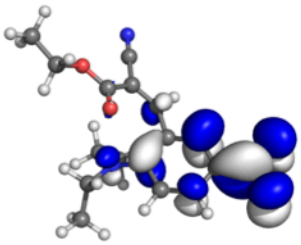	
BP86			
HOMO	→	LUMO	0.036
HOMO	→	LUMO+1	0.926
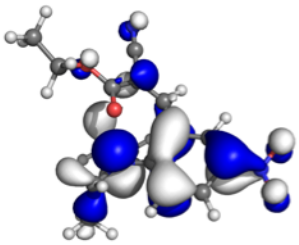		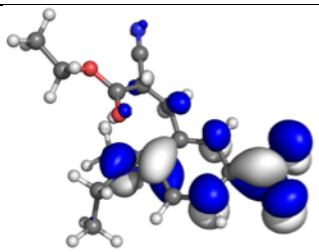	
PBE0			
HOMO	→	LUMO	0.034

HOMO		LUMO+1	0.937
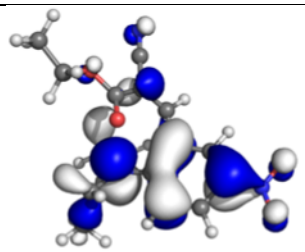	→	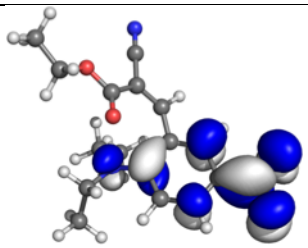	
BHandHLYP			
HOMO		LUMO+1	0.926
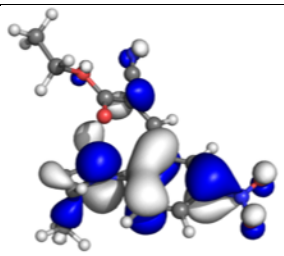	→	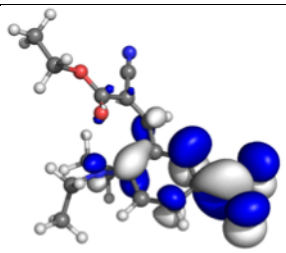	

Table S36. Dominant orbitals involved in excited state corresponding to λ_{max} for **C4**. High oscillator strength paradigm.

C4			
B3LYP+D2			
HOMO	→	LUMO	0.035
HOMO		LUMO+1	0.948
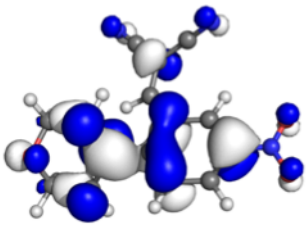	→	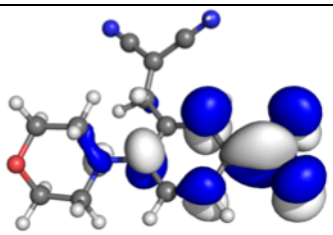	
M06			
HOMO	→	LUMO	0.031
HOMO		LUMO+1	0.941
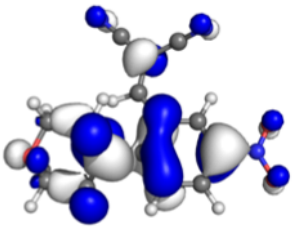	→	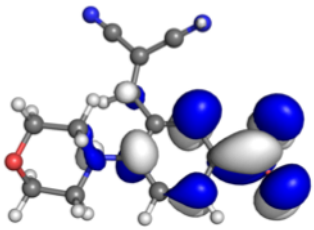	
CAM-B3LYP			
HOMO-4	→	LUMO+4	0.024
HOMO-4	→	LUMO+1	0.345
HOMO	→	LUMO+1	0.551

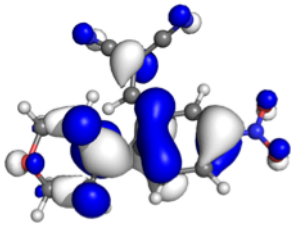		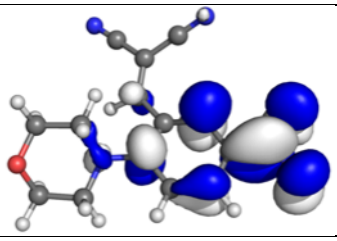	
BP86			
HOMO	→	LUMO	0.041
HOMO-1	→	LUMO	0.105
HOMO-1	→	LUMO+1	0.142
HOMO		LUMO+1	0.700
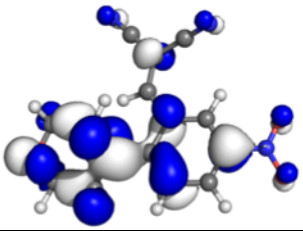	→	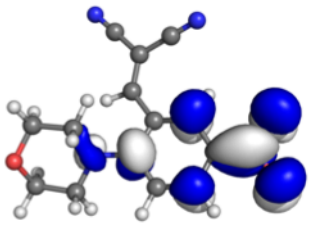	
PBE0			
HOMO		LUMO+1	0.960
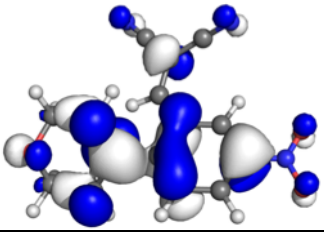	→	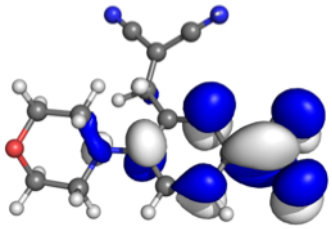	
BHandHLYP			
HOMO-7	→	LUMO+1	0.026
HOMO		LUMO+1	0.897
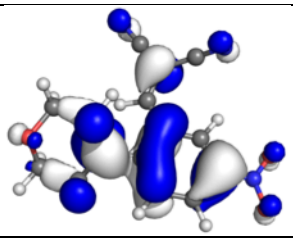	→	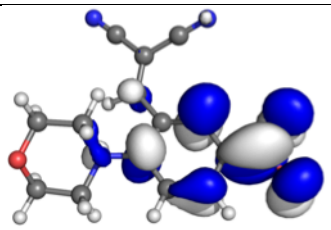	

Table S37. Dominant orbitals involved in excited state corresponding to λ_{max} for **C5**. High oscillator strength paradigm.

C5			
B3LYP+D2			
HOMO	→	LUMO	0.059
HOMO	→	LUMO+1	0.923
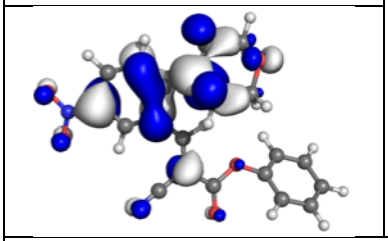		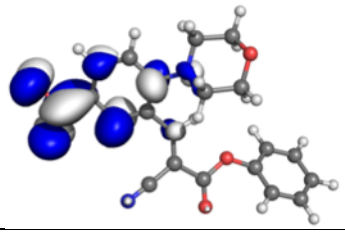	
M06			
HOMO	→	LUMO	0.066
HOMO	→	LUMO+1	0.907
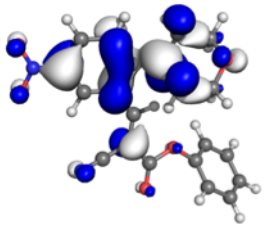		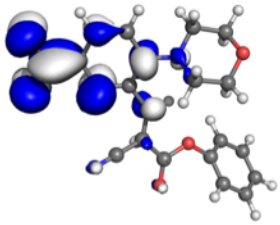	
CAM-B3LYP			
HOMO-7	→	LUMO+1	0.087
HOMO	→	LUMO+1	0.817
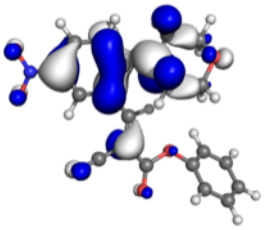		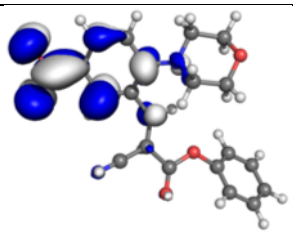	
BP86			
HOMO-2	→	LUMO	0.039
HOMO-1	→	LUMO+1	0.042
HOMO	→	LUMO	0.085
HOMO-2	→	LUMO+1	0.098
HOMO	→	LUMO+1	0.722
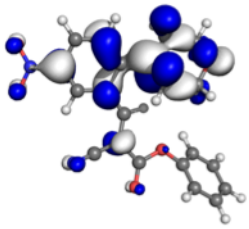		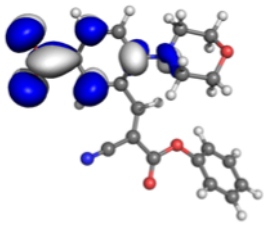	

PBE0			
HOMO	→	LUMO	0.030
HOMO	→	LUMO+1	0.949
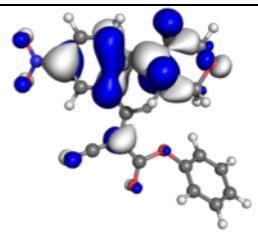		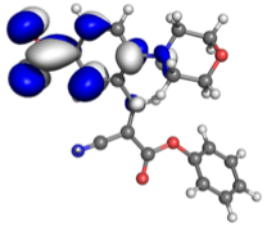	
BHandHLYP			
HOMO	→	LUMO+1	0.901
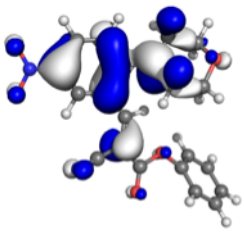		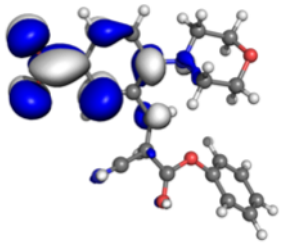	

Table S38. Dominant orbitals involved in excited state corresponding to λ_{max} for **C6**. High oscillator strength paradigm.

C6			
B3LYP+D2			
HOMO	→	LUMO	0.961
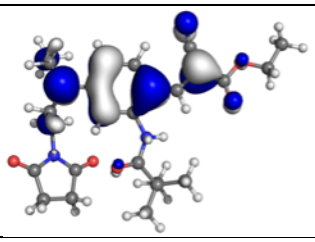		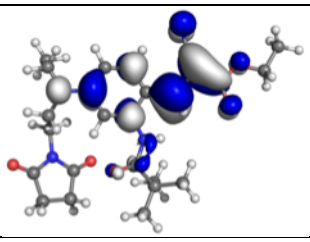	
M06			
HOMO	→	LUMO	0.985
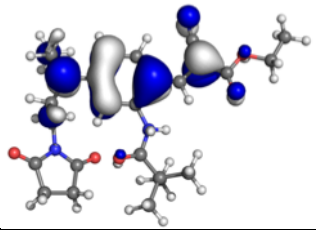		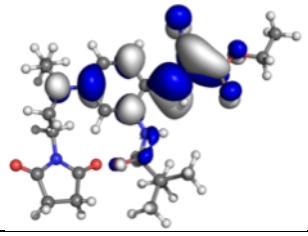	
CAM-B3LYP			
HOMO	→	LUMO	0.947

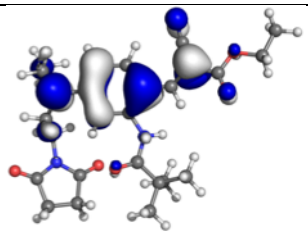		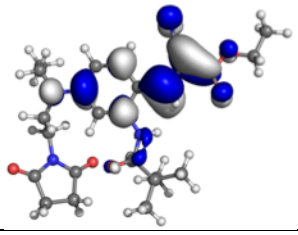	
BP86			
HOMO-1	→	LUMO	0.085
HOMO	→	LUMO	0.876
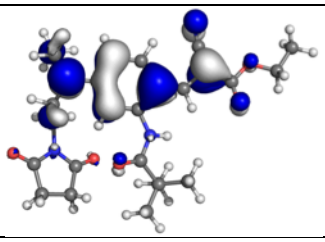		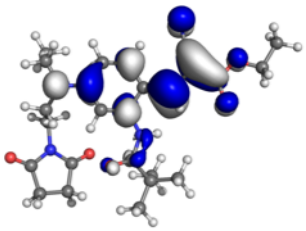	
PBE0			
HOMO	→	LUMO	0.991
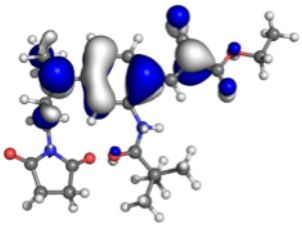		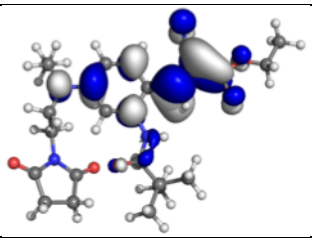	
BHandHLYP			
HOMO	→	LUMO	0.959
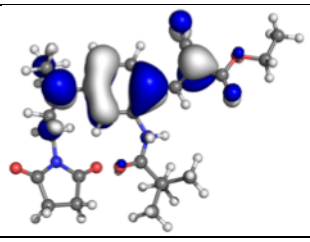		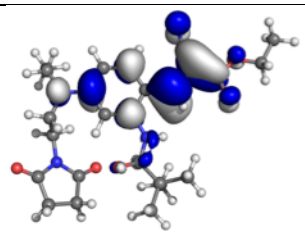	

Table S39. Dominant orbitals involved in excited state corresponding to λ_{max} for **C7**. High oscillator strength paradigm.

C7			
B3LYP+D2			
HOMO	→	LUMO	0.997

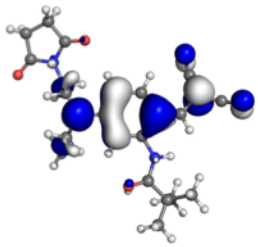		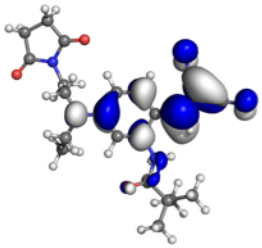	
M06			
HOMO		LUMO	0.987
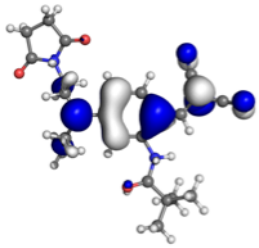	→	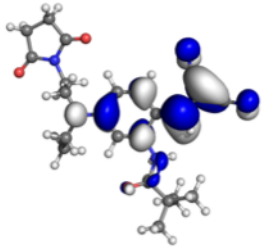	
CAM-B3LYP			
HOMO		LUMO	0.950
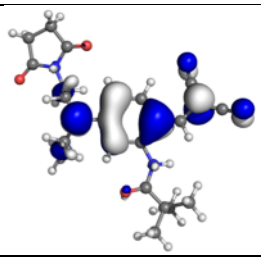	→	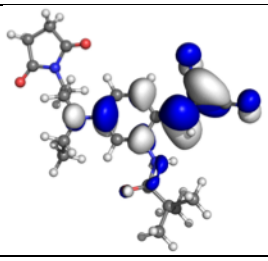	
BP86			
HOMO-2	→	LUMO	0.024
HOMO-1	→	LUMO	0.108
HOMO		LUMO	0.851
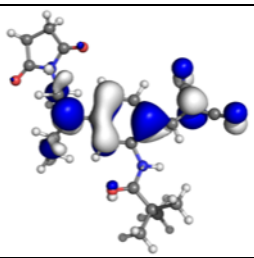	→	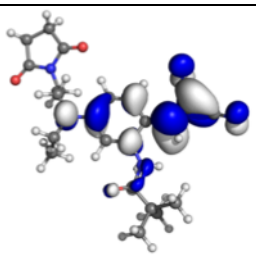	
PBE0			
HOMO		LUMO	0.994
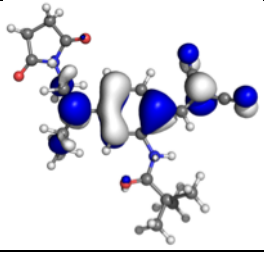	→	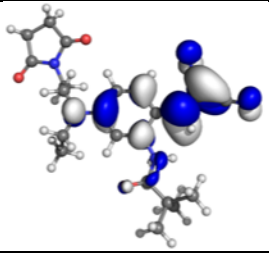	

BHandHLYP			
HOMO		LUMO	0.961
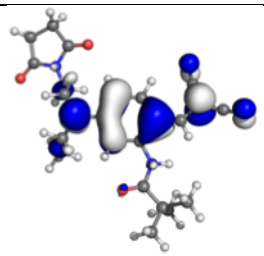	→	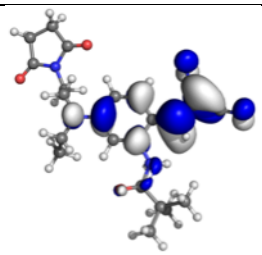	

Table S40. Dominant orbitals involved in excited state corresponding to λ_{max} for **C8**. High oscillator strength paradigm.

C8			
B3LYP+D2			
HOMO		LUMO	0.993
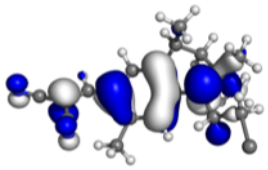	→	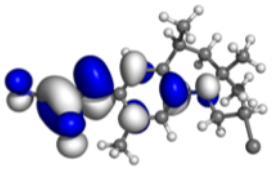	
M06			
HOMO		LUMO	0.987
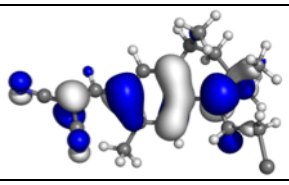	→		
CAM-B3LYP			
HOMO		LUMO	0.954
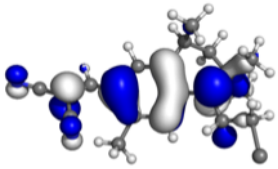	→	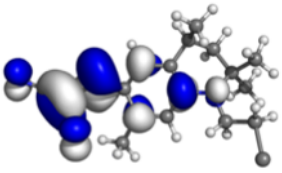	
BP86			
HOMO		LUMO	0.977
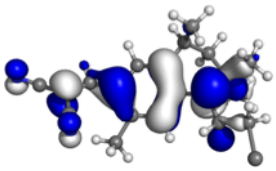	→	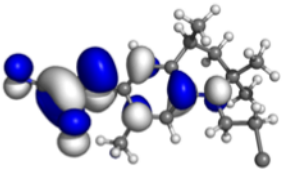	
PBE0			
HOMO	→	LUMO	0.992

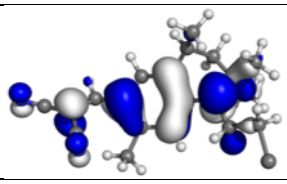		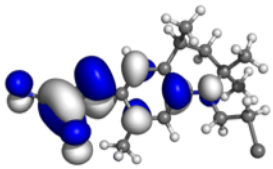	
BHandHLYP			
HOMO		LUMO	0.963
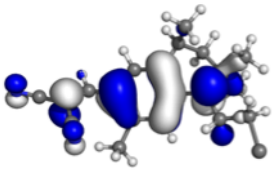	→		

Table S41. Dominant orbitals involved in excited state corresponding to λ_{max} for **C9**. High oscillator strength paradigm.

C9			
B3LYP+D2			
HOMO		LUMO	0.995
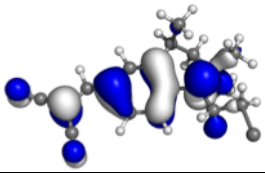	→	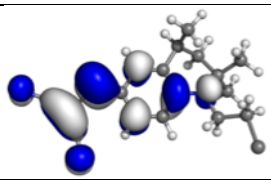	
M06			
HOMO		LUMO	0.992
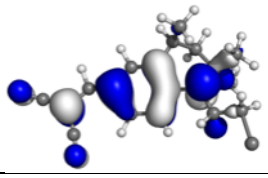	→	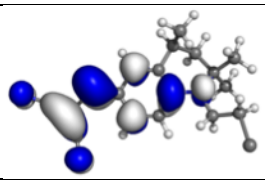	
CAM-B3LYP			
HOMO		LUMO	0.967
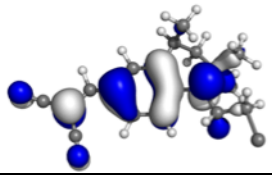	→	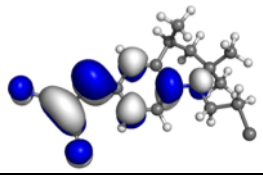	
BP86			
HOMO	←	LUMO	0.021
HOMO		LUMO	0.974
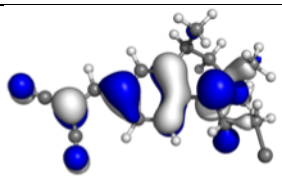	→	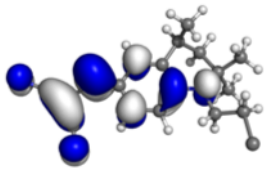	

PBE0			
HOMO	→	LUMO	0.995
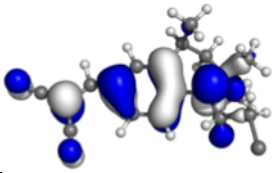		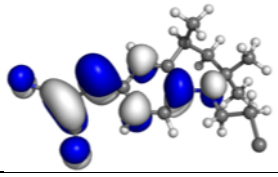	
BHandHLYP			
HOMO	→	LUMO	0.972
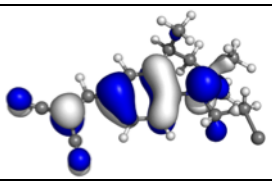		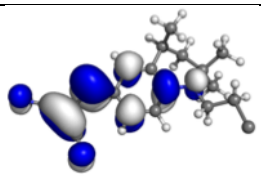	

Table S42. Dominant orbitals involved in excited state corresponding to λ_{max} for **C10**. High oscillator strength paradigm.

C10			
B3LYP+D2			
HOMO	→	LUMO	1.000
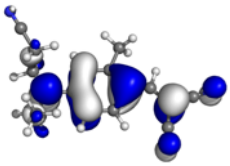		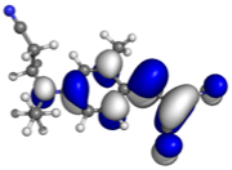	
M06			
HOMO	→	LUMO	0.993
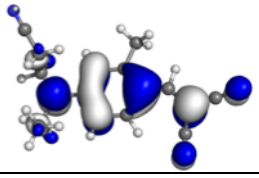		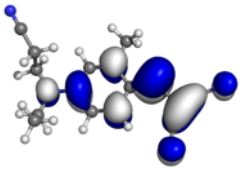	
CAM-B3LYP			
HOMO	→	LUMO	0.968
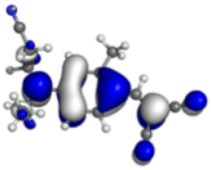		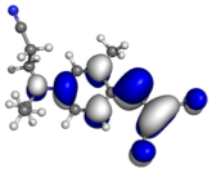	
BP86			
HOMO	←	LUMO	0.024
HOMO	→	LUMO	0.989

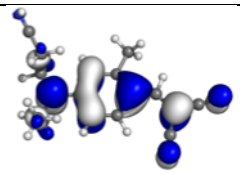		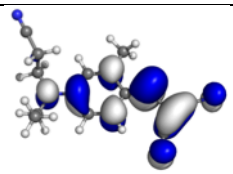	
PBE0			
HOMO	→	LUMO	0.998
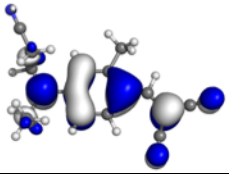		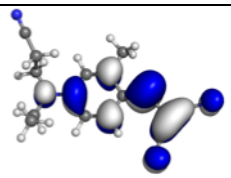	
BHandHLYP			
HOMO	→	LUMO	0.973
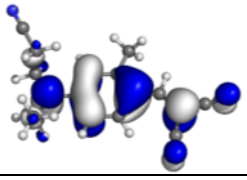		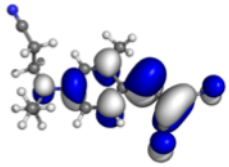	

MUE/MSE for alternate excitation assignments: Low energy selection paradigm

MUE/MSE (eV)	BP86	B3LYP+D2	PBE0	M06	BHandHLYP	CAM-B3LYP
Cyano	0.47/-0.46	0.26/-0.06	0.25/0.03	0.23/0.05	0.45/0.45	0.33/0.33
Azo	0.52/-0.52	0.16/-0.16	0.11/-0.09	0.17/-0.17	0.25/0.25	0.18/0.15

Table S43. MUEs and MSEs for calculation of λ_{max} for each dye family as determined with different functionals. All values are reported in eV. Unlike the similar table that appears in the paper, these λ_{max} values were selected because they were the lowest energy transitions reported.

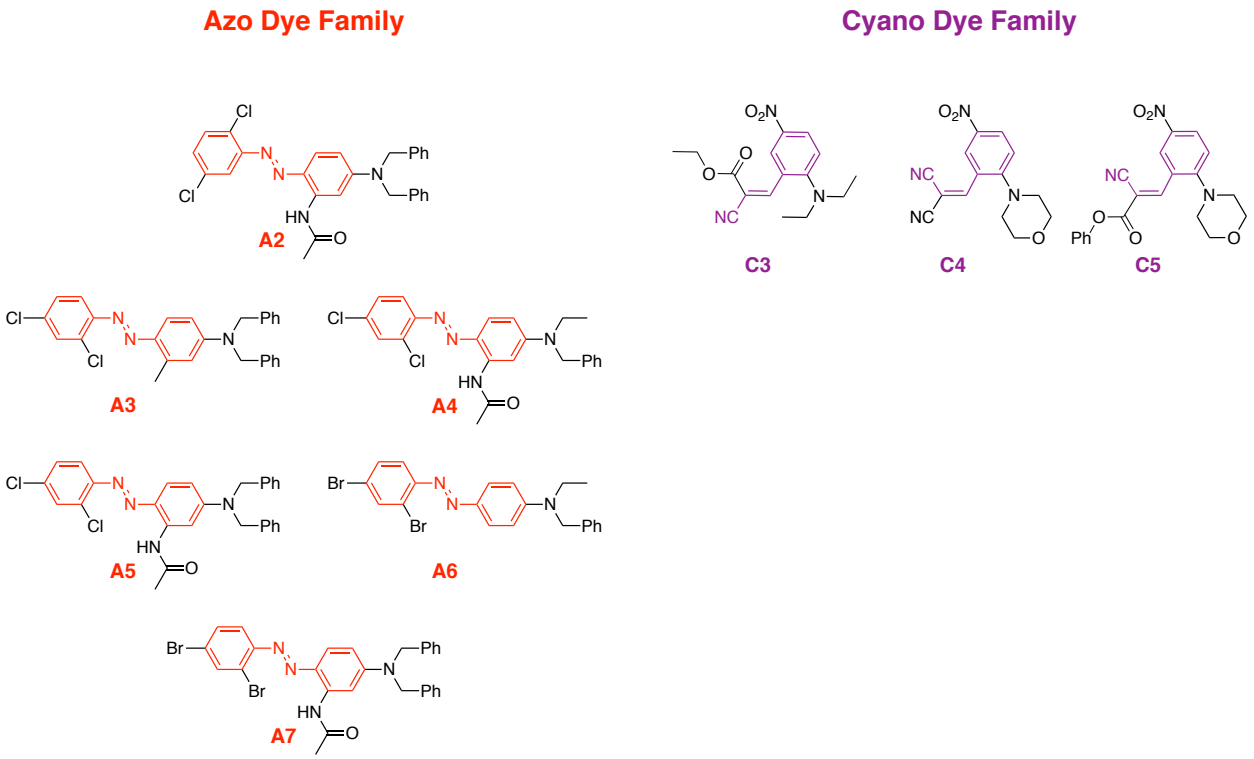

Figure S23. Dyes for which both selection paradigms did not agree.

Azo excitation data: Low energy selection paradigm

Note: Different excitation data is provided only for the dyes for which the selection has changed (**A2-A7**).

Table S44. Measured and calculated values of azo dyes using the low energy selection paradigm.

Number	Library Code	Experimental E_{max} (eV)	Functional	Calculated E_{max} (eV)	Osc. Strength	Transition Number	Λ	Δr (Å)	D_{CT} (Å)	S_C
A2	X-12683-21C	2.65	B3LYP+D2	2.62	0.30	1	0.623	1.032	0.077	0.924
			M06	2.53	0.12	1	0.608	1.334	0.292	0.905
			CAM-B3LYP	2.80	0.19	1	0.597	1.901	0.182	0.914
			BP86	2.29	0.09	1	0.601	0.685	0.081	0.882
			PBE0	2.66	0.24	1	0.620	0.961	0.149	0.912
			BHandHLYP	2.94	0.35	1	0.658	1.373	0.056	0.951
A3	X-12683-22A	2.84	B3LYP+D2	2.53	0.13	1	0.623	0.714	0.373	0.912
			M06	2.43	0.08	1	0.626	0.573	0.456	0.915
			CAM-B3LYP	2.71	0.08	1	0.644	0.872	0.431	0.910
			BP86	2.19	0.08	1	0.692	1.107	0.260	0.899
			PBE0	2.56	0.11	1	0.624	0.664	0.414	0.907
			BHandHLYP	2.86	0.10	1	0.574	2.698	0.461	0.921
A4	X-12683-22B	2.62	B3LYP+D2	2.62	0.44	1	0.656	1.688	0.153	0.950
			M06	2.53	0.20	1	0.643	0.794	0.211	0.922
			CAM-B3LYP	2.80	0.29	1	0.610	1.866	0.062	0.929
			BP86	2.30	0.15	1	0.612	0.713	0.058	0.894
			PBE0	2.66	0.37	1	0.639	1.313	0.062	0.935
			BHandHLYP	2.93	0.49	1	0.633	1.754	0.156	0.966
A5	X-12683-22C	2.65	B3LYP+D2	2.61	0.47	1	0.659	1.527	0.160	0.949
			M06	2.53	0.21	1	0.644	0.715	0.232	0.907
			CAM-B3LYP	2.79	0.29	1	0.572	2.716	0.087	0.919
			BP86	2.29	0.16	1	0.613	0.726	0.050	0.876
			PBE0	2.65	0.39	1	0.649	1.674	0.063	0.926
			BHandHLYP	2.93	0.49	1	0.640	1.559	0.122	0.965
A6	X-12683-23A	2.81	B3LYP+D2	2.61	0.17	1	0.641	1.021	0.505	0.952
			M06	2.52	0.10	1	0.643	0.844	0.575	0.951
			CAM-B3LYP	2.79	0.09	1	0.659	1.174	0.520	0.948
			BP86	2.28	0.12	1	0.673	1.210	0.481	0.939
			PBE0	2.64	0.14	1	0.642	0.963	0.529	0.949
			BHandHLYP	2.93	0.12	1	0.641	1.658	0.536	0.955
A7	X-12683-23C	2.66	B3LYP+D2	2.60	0.47	1	0.661	1.221	0.124	0.950
			M06	2.52	0.21	1	0.645	0.731	0.310	0.911
			CAM-B3LYP	2.78	0.29	1	0.572	2.430	0.152	0.920
			BP86	2.28	0.18	1	0.620	0.775	0.196	0.884
			PBE0	2.64	0.39	1	0.656	1.596	0.138	0.929
			BHandHLYP	2.92	0.48	1	0.606	2.119	0.073	0.963

Cyano excitation data: Low energy selection paradigm

Note: Different excitation data is provided only for the dyes for which the selection has changed (**C3**-**C5**).

Table S45. Measured and calculated values of cyano dyes using the low energy selection paradigm.

Number	Library Code	Experimental E_{max} (eV)	Functional	Calculated E_{max} (eV)	Osc. Strength	Transition Number	Λ	Δr (Å)	D_{CT} (Å)	S_C
C3	X-12833-83-1	3.20	B3LYP+D2	2.97	0.16	1	0.561	1.899	1.801	0.878
			M06	3.12	0.16	1	0.573	1.878	1.740	0.888
			CAM-B3LYP	3.39	0.19	1	0.576	1.641	1.656	0.901
			BP86	2.52	0.13	1	0.567	1.900	1.805	0.861
			PBE0	3.07	0.16	1	0.560	1.879	1.809	0.881
			BHandHLYP	3.56	0.20	1	0.586	1.569	1.571	0.909
C4	X-12833-88-1	3.36	B3LYP+D2	2.91	0.13	1	0.513	2.226	2.208	0.799
			M06	3.07	0.15	1	0.528	2.105	2.06	0.815
			CAM-B3LYP	3.44	0.23	1	0.550	1.927	1.958	0.824
			BP86	2.26	0.06	1	0.465	2.872	2.906	0.745
			PBE0	3.01	0.14	1	0.516	2.160	2.172	0.803
			BHandHLYP	3.66	0.27	1	0.573	1.740	1.823	0.839
C5	X-12833-89-1	3.37	B3LYP+D2	2.93	0.14	1	0.519	2.232	2.151	0.859
			M06	3.10	0.16	1	0.540	2.081	2.008	0.874
			CAM-B3LYP	3.47	0.23	1	0.553	1.912	1.923	0.881
			BP86	2.28	0.07	1	0.470	2.818	2.684	0.796
			PBE0	3.03	0.15	1	0.517	2.197	2.122	0.862
			BHandHLYP	3.68	0.26	1	0.577	1.679	1.788	0.893

Comments on alternate tautomer of A1

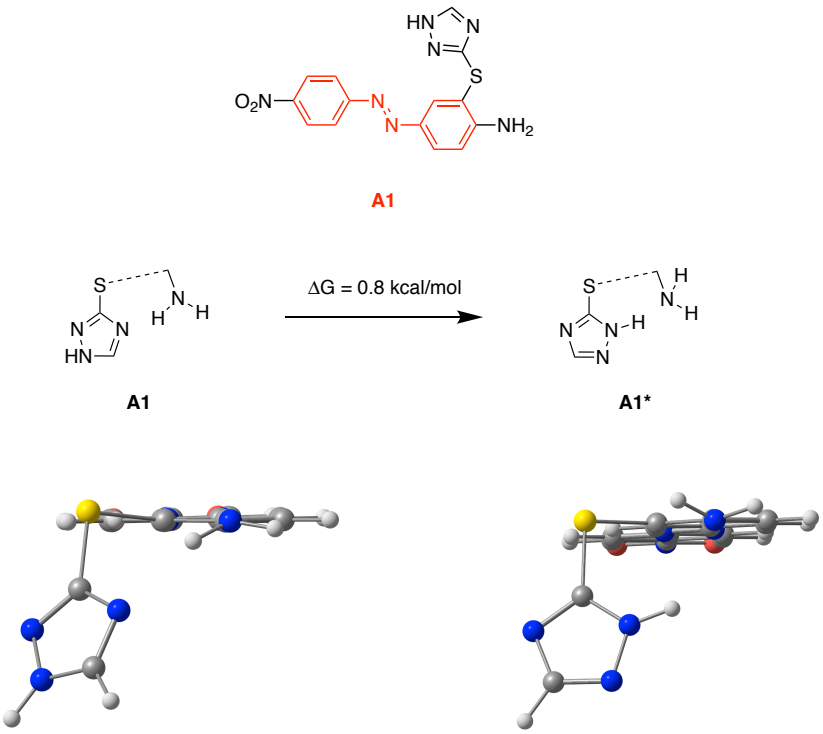

Figure S24. Schematic showing the alternative tautomer of **A1** considered.

As mentioned in the text, **A1** seemed to be a moderate outlier in terms of the functional dependence of ΔE_{max}. Specifically, in Figure 5a the ΔE_{max} values for **A1** appear to be red-shifted (more negative) than the other azo dyes. One potential explanation for this is that the dominant form in solution of **A1** is an alternate tautomer to the one that was indicated on the sample vial in the MWDL (shown in Figure 1 and Figure S22). Figure S22 shows an alternate tautomer to **A1** referred to as **A1***. It has been shown that such proton tautomerization can occur for triazole compounds (see references provided in the main text). In this case **A1*** is calculated as being only 0.8 kcal/mol higher in solvated free energy than **A1**, supporting this possibility. Performing TD-DFT on **A1*** does result in modest blue-shifts of ΔE_{max} (more positive) with each functional (Figure S23), making it less of an outlier. It may be that a more accurate way of calculating λ_{max} for this dye is to perform a weighted average of the two spectra to simulate an equilibrium mixture in solution. This was not performed here, however, for the sake of simplicity as the corrections would be minor and not significantly alter any of the main conclusions in the paper.

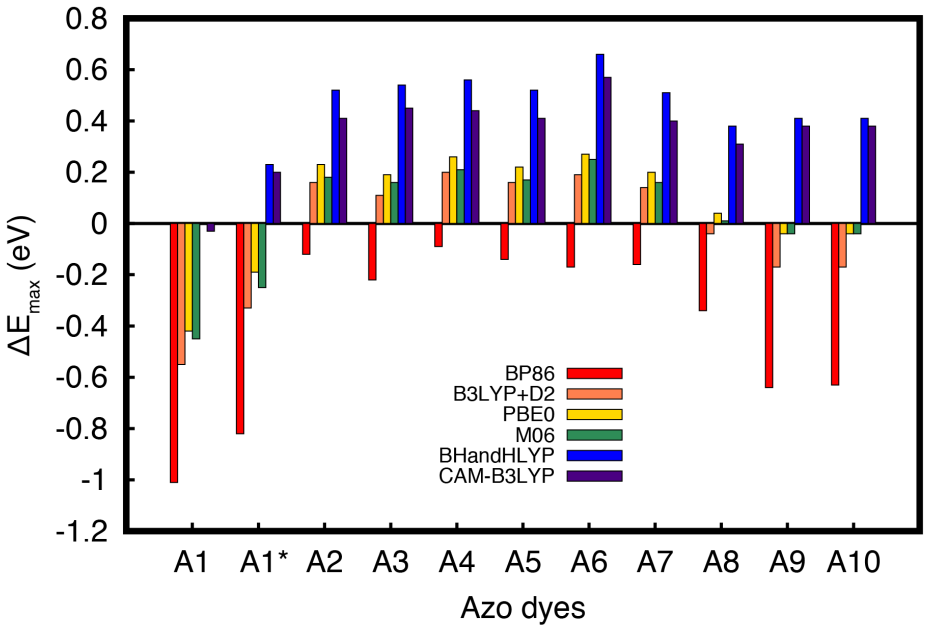

Figure S25. ΔE_{max} determined for all six functionals for the azo dyes including the additional tautomer **A1***.

Dependence of ΔE_{max} on CT parameters

The following plots are analogous to Figure 10 and Figure 11 in the main manuscript. Note that all the below plots are made using the using the highest oscillator strength selection paradigm.

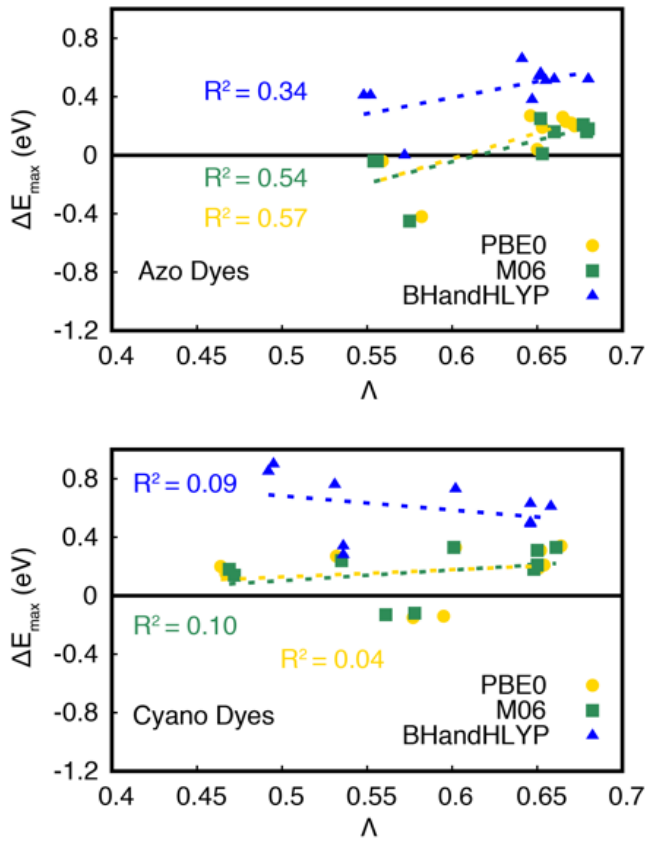

Figure S26. Relationship between Λ and ΔE_{max} for PBE0, M06, and BHandHLYP.

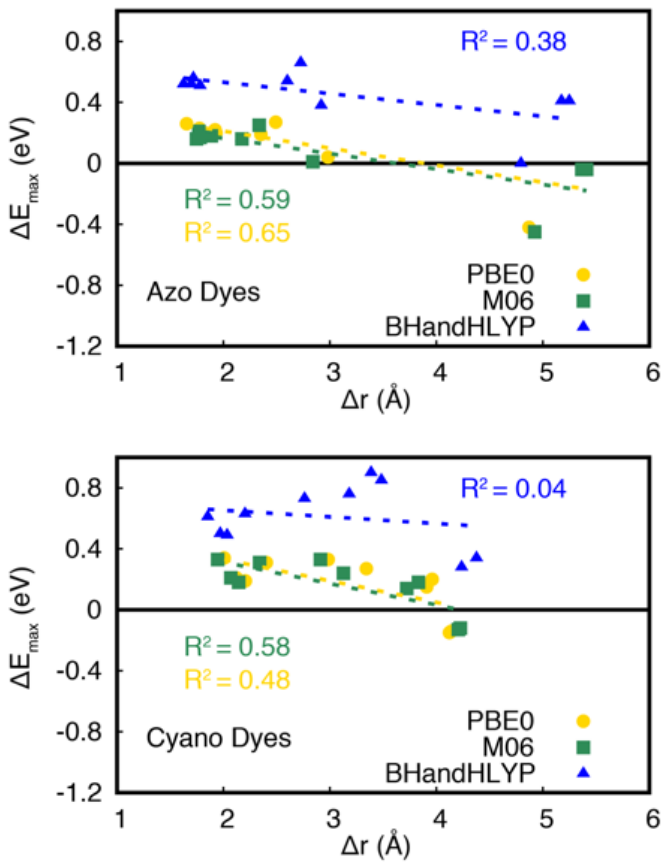

Figure S27. Relationship between Δr and ΔE_{max} for PBE0, M06, and BHandHLYP.

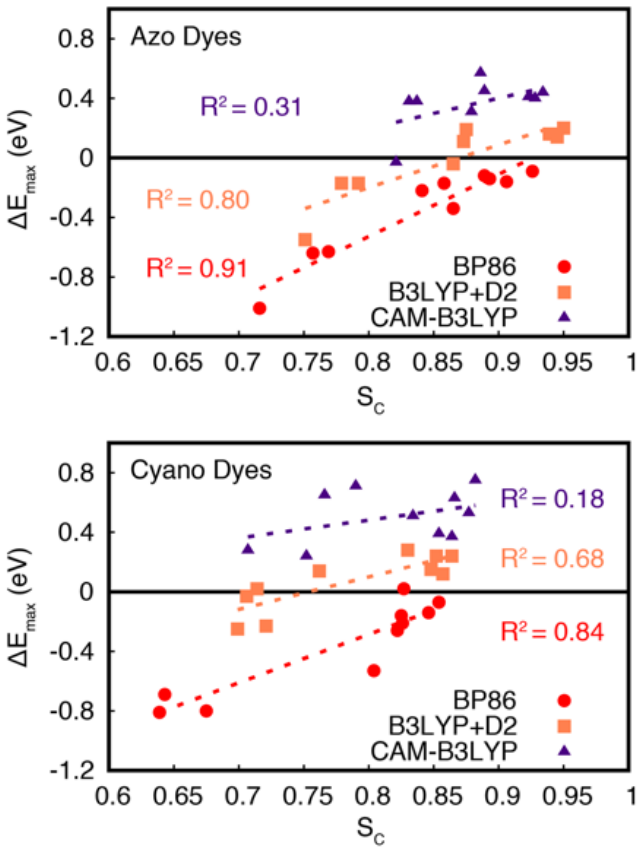

Figure S28. Relationship between S_C and ΔE_{max} for BP86, B3LYP+D2, and CAM-B3LYP.

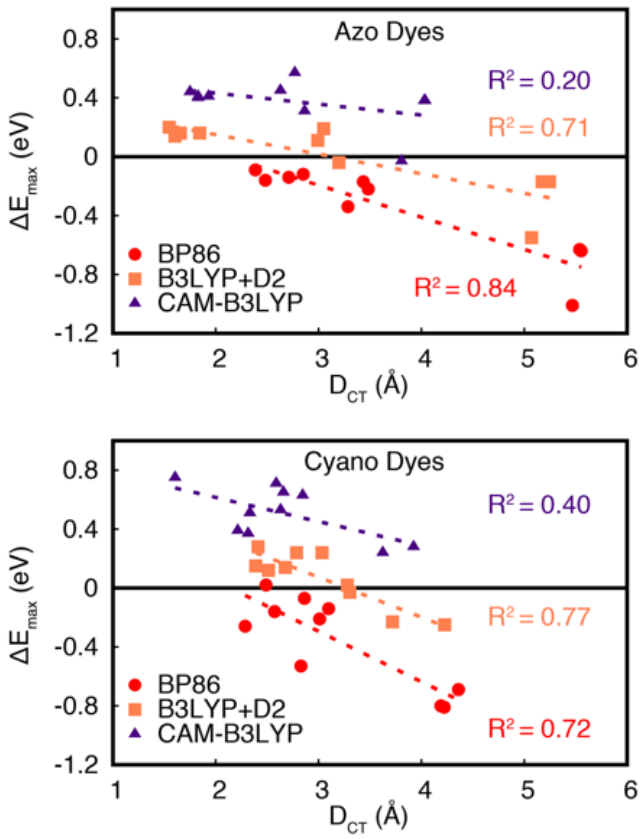

Figure S29. Relationship between D_{CT} and ΔE_{max} for BP86, B3LYP+D2, and CAM-B3LYP.

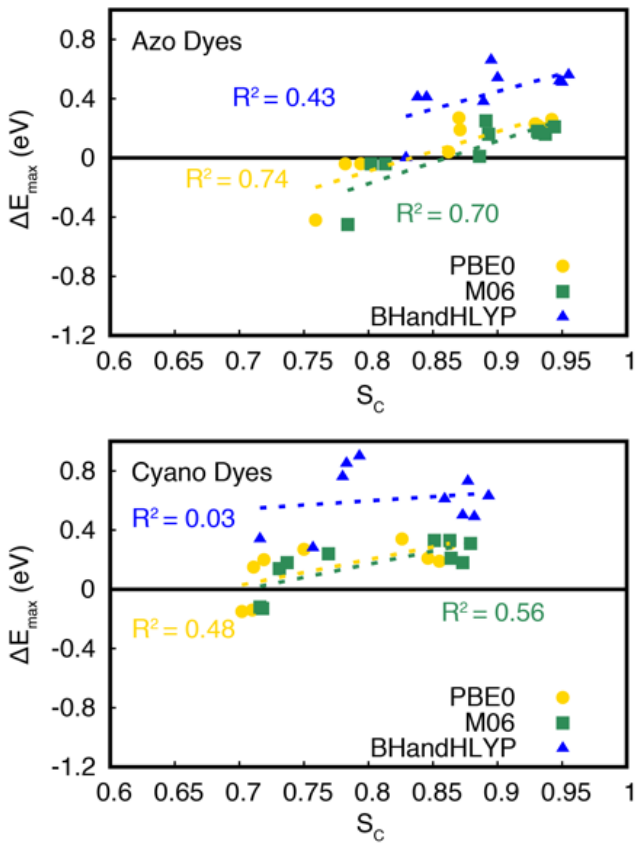

Figure S30. Relationship between S_C and ΔE_{max} for PBE0, M06, and BHandHLYP.

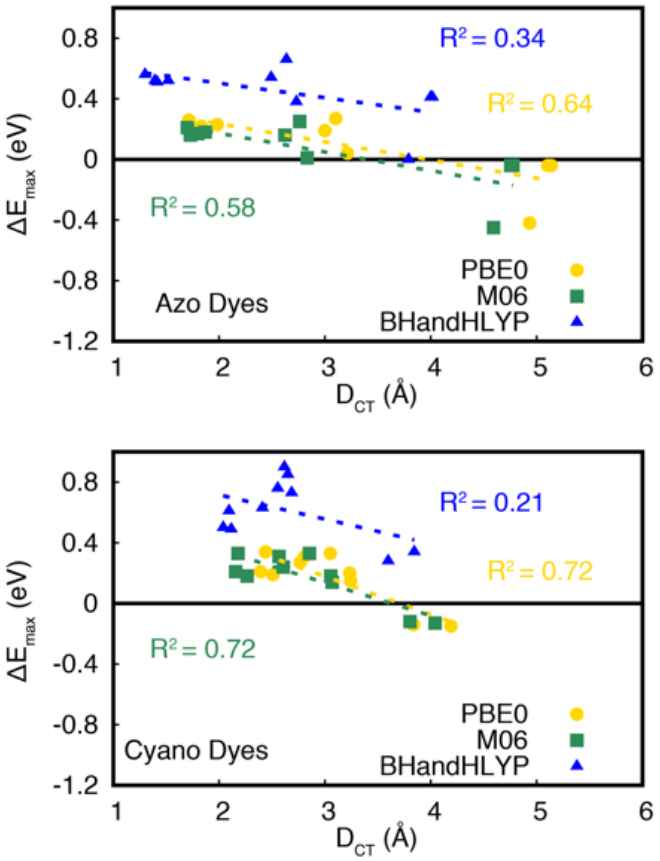

Figure S31. Relationship between D_{CT} and ΔE_{max} for PBE0, M06, and BHandHLYP.

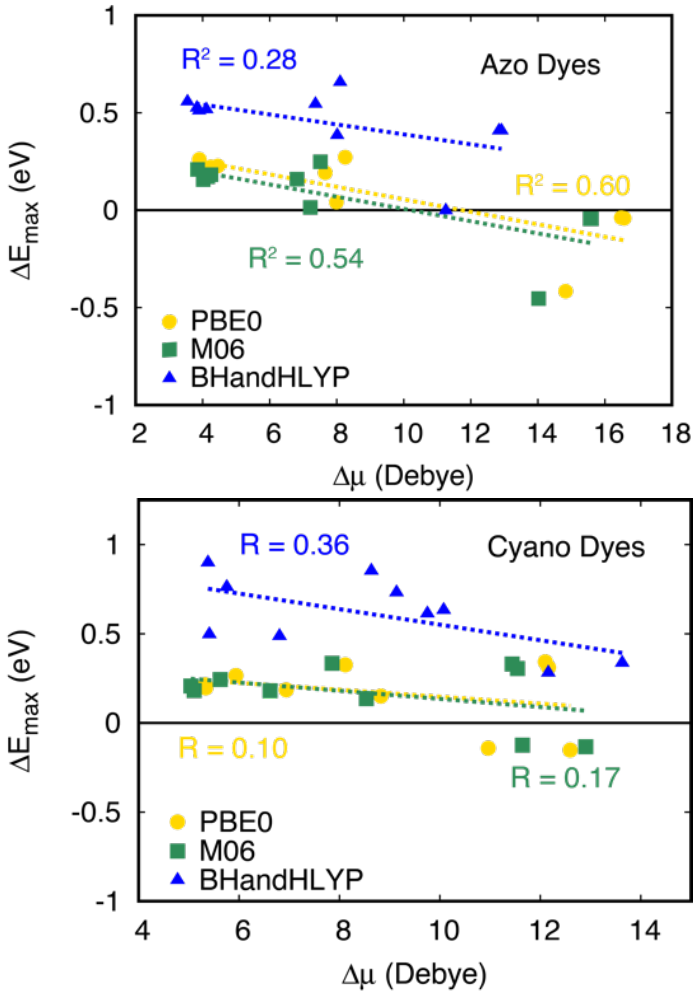

Figure S32: Relationship between Δμ and ΔE_{max} for PBE0, M06, and BHandHLYP.

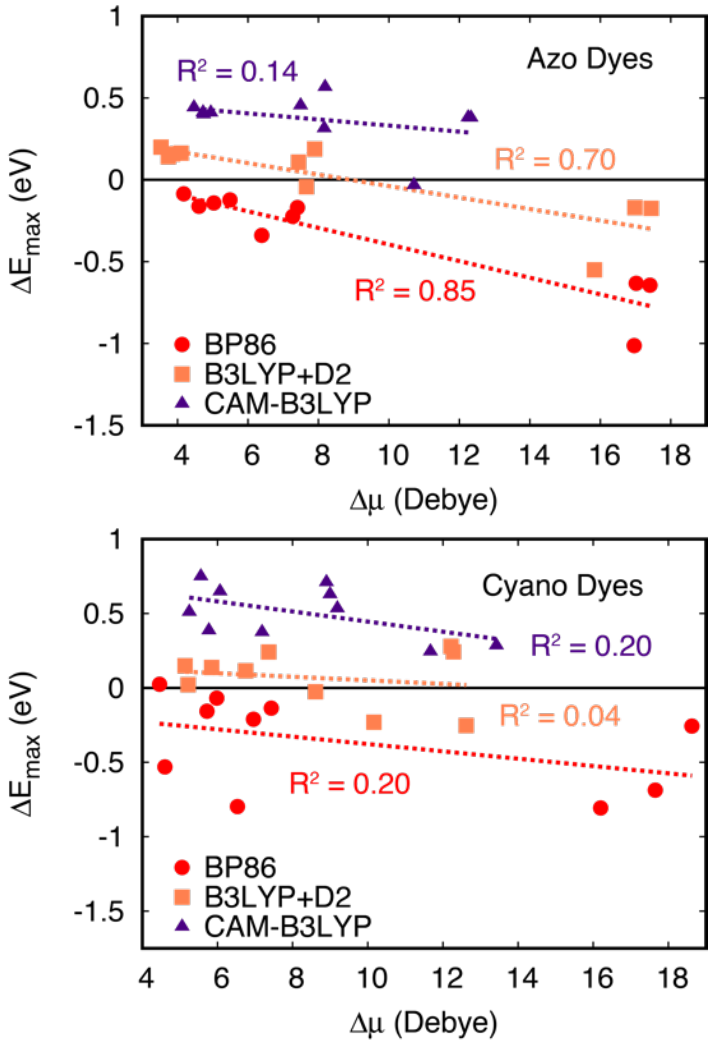

Figure S33: Relationship between $\Delta\mu$ and ΔE_{max} for BP86, B3LYP+D2, CAM-B3LYP.

LASSO analysis

We used LASSO analysis to determine whether multivariate regression could capture the relationship between methodological performance and density parameters better than simple linear regression. The target value of the analysis was the error in λ_{max}, referred to as ΔE_{max} which is taken as E_{max}(calc) - E_{max}(expt). All error values were then normalized by dividing by the standard deviation of the column of errors. Thus, the target of the analysis was ΔE_{max} divided by $\sigma(\Delta E_{max})$ for all dye values. The following table presents the R^2 values of each multivariate regression for each of the functionals. Beside this, you can see the ranking of each of the CT parameters given in order of importance with 1 being the most important. (For example, Δr dropped out first for B3LYP+D2.) All LASSO plots are provided after the table.

Table S44. Order of importance for CT parameters as determined with LASSO analysis. Importance is denoted with rank; one is the highest rank.

Functional	R^2	Λ	Δr	D_{CT}	S_C
B3LYP+D2	0.67		1	2	
M06	0.56			1	
CAM-B3LYP	0.56	2	3	1	
BP86	0.85		2	3	1
PBE0	0.59			1	
BHandHLYP	0.61	2	3	1	

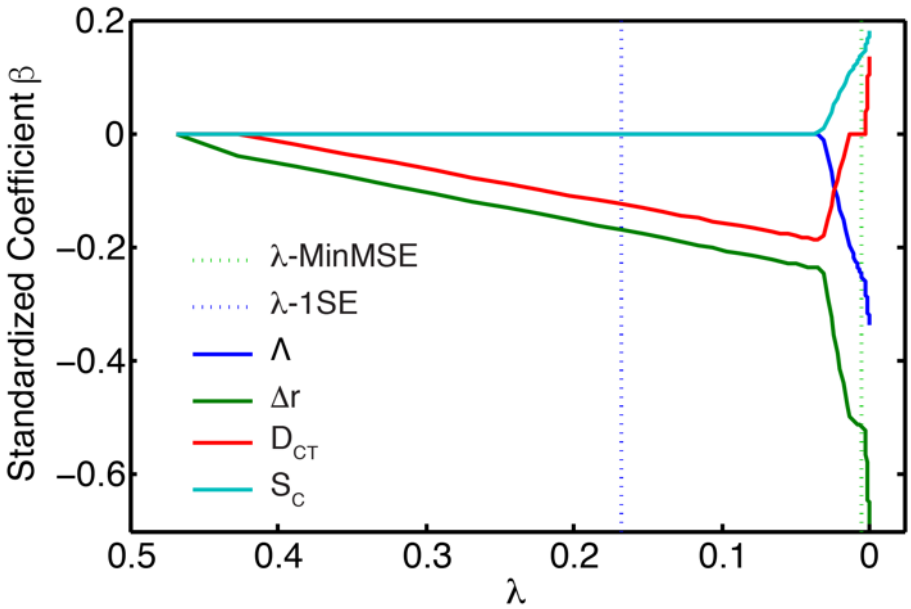

Figure S34. LASSO analysis plot for B3LYP+D2 methodology with target of ΔE_{max}.

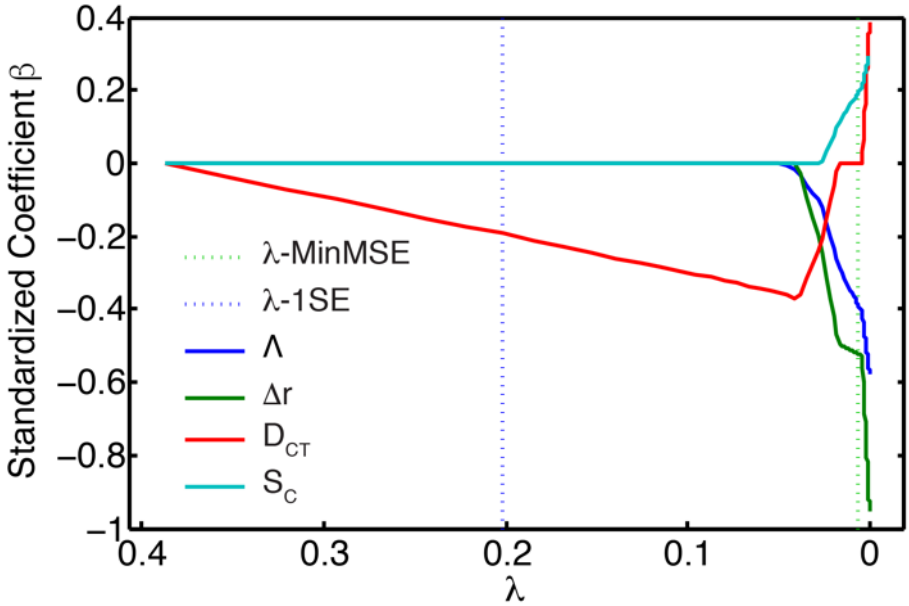

Figure S35. LASSO analysis plot for M06 methodology with target of ΔE_{max}.

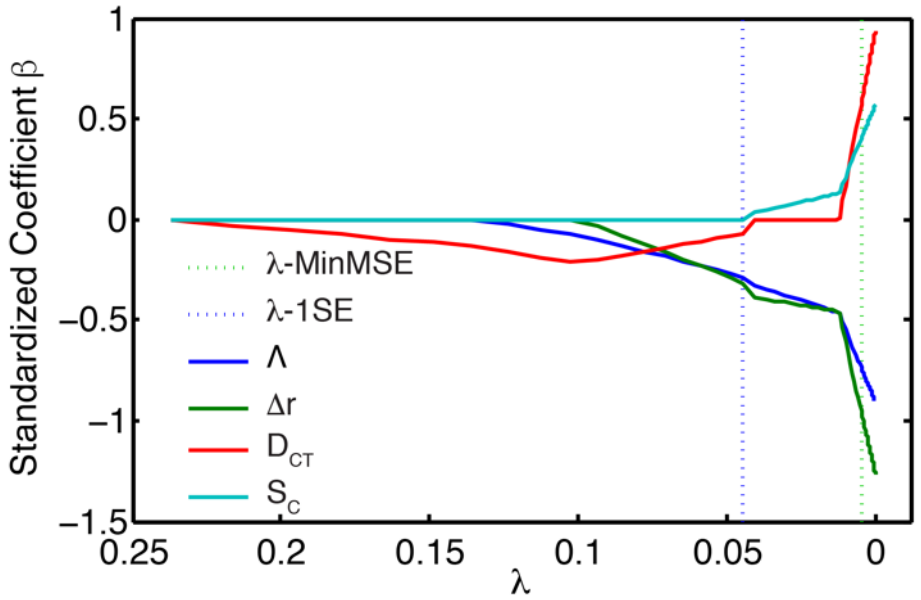

Figure S36. LASSO analysis plot for CAM-B3LYP methodology with target of ΔE_{max}.

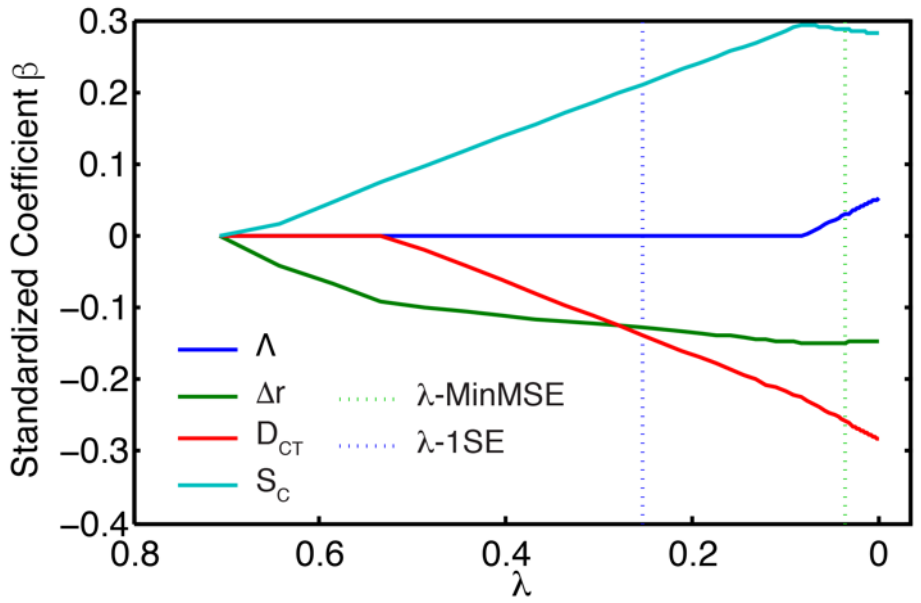

Figure S37. LASSO analysis plot for BP86 methodology with target of ΔE_{max}.

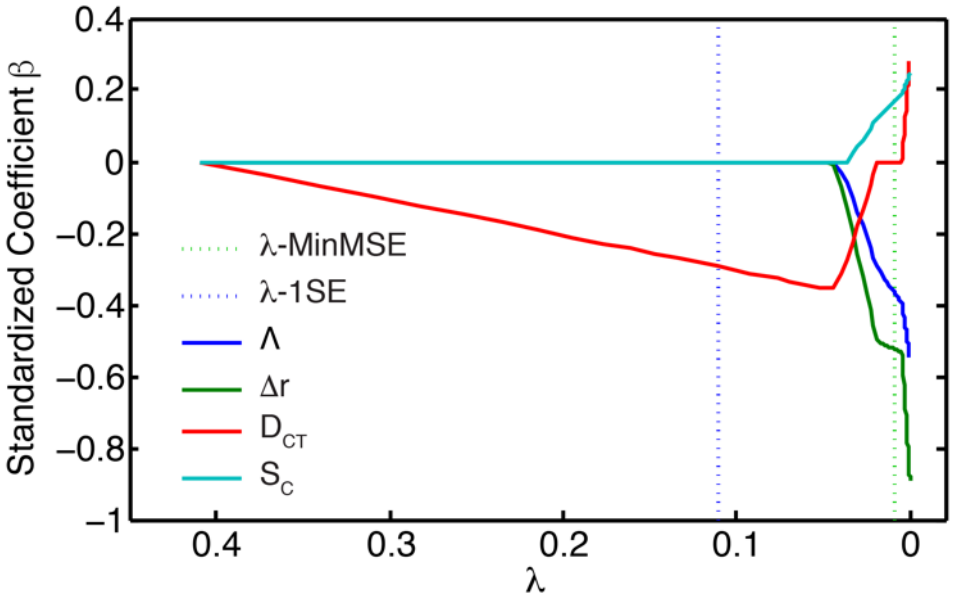

Figure S38. LASSO analysis plot for PBE0 methodology with target of ΔE_{max}.

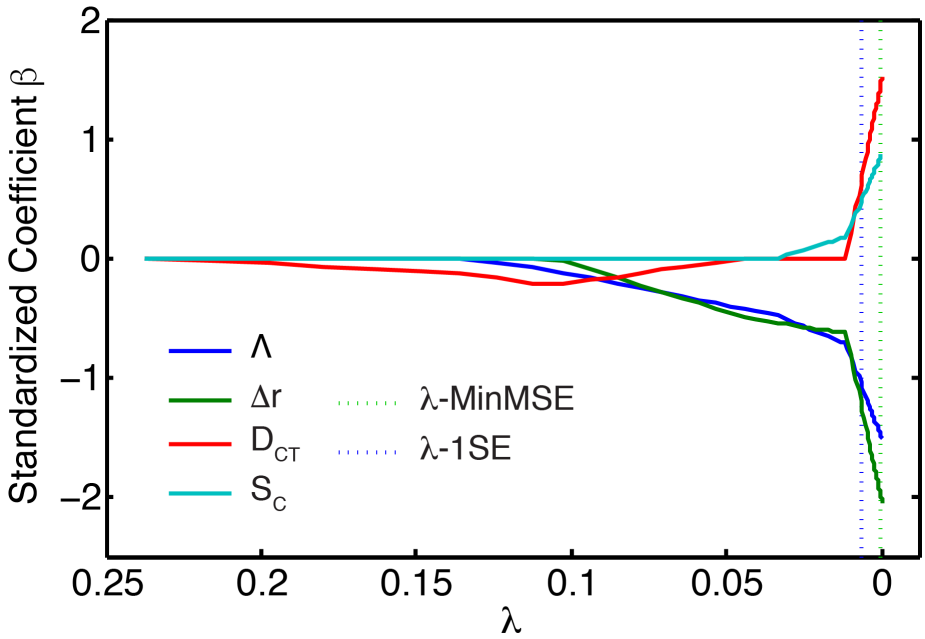

Figure S39. LASSO analysis plot for BHandHLYP methodology with target of ΔE_{max}.

State-specific solvation root flipping

For some compounds in this study, usage of the IBSF SS polarization scheme caused root flipping, thereby preventing us from comparing transitions properly for affected compounds. As an example of root flipping, consider Table S47 which shows transitions and contributions for a B3LYP+D2 calculation done on dye C3. Results with IBSF solvation show that transition 1 is dominated by the transition between HOMO and LUMO+1 while transition 2 is dominated by the transition between HOMO and LUMO. Within the LR scheme, transition 1 is dominated by the HOMO to LUMO transition and transition 2 is dominated by the transition between HOMO and LUMO+1. Due to the different orbital compositions reported by the two solvation methods, the CT parameters can vary dramatically across them. This ambiguity in determining a comparable state across the LR and IBSF methods affected BP86 calculations and calculations on dyes C3, C4, and C5. As such, these results were omitted from Table 2 reported in the manuscript.

Table S45. Excitation orbital pairs and contribution values for the IBSF and LR methods for dye C3.

State	Solvation scheme	Orbitals	Weight	Orbitals	Weight
1	IBSF	84 → 86	0.582	84 → 85	0.391
	LR	84 → 85	0.695	84 → 86	0.11
2	IBSF	84 → 85	0.575	84 → 86	-0.394
	LR	84 → 86	0.689	84 → 85	-0.113

NMR Characterization Details

^{1}H, and ^{13}C NMR spectra were obtained on a Brüker 500 MHz spectrometer at room temperature. Chemical shifts are listed in parts per million (ppm) and referenced to the residual protons or carbons of the deuterated solvents respectively.

A1. Not soluble in Chloroform

A2. ^{1}H NMR (500 MHz, Chloroform-*d*) δ 12.16 (s, 1H), 8.51 (d, *J* = 2.8 Hz, 1H), 7.79 (d, *J* = 9.1 Hz, 1H), 7.77 (d, *J* = 2.5 Hz, 1H), 7.45 (d, *J* = 8.6 Hz, 1H), 7.38 (dd, *J* = 7.9, 6.6 Hz, 4H), 7.34 – 7.29 (m, 5H), 7.26 (dd, *J* = 8.6, 2.5 Hz, 1H), 6.63 (dd, *J* = 9.2, 2.8 Hz, 1H), 4.81 (s, 4H), 2.28 (s, 3H). ^{13}C NMR (151 MHz, $CDCl_3$) δ 170.51, 153.46, 148.92, 136.71, 133.73, 131.43, 131.07, 130.60, 129.11, 128.89, 128.44, 127.51, 126.80, 117.30, 107.86, 101.92, 54.22, 25.93.

A3. ^{1}H NMR (500 MHz, Chloroform-*d*) δ 7.88 (d, *J* = 8.8 Hz, 1H), 7.67 (d, *J* = 8.7 Hz, 1H), 7.62 (d, *J* = 8.6 Hz, 1H), 7.62 – 7.55 (m, 1H), 7.54 (d, *J* = 2.2 Hz, 1H), 7.41 – 7.28 (m, 14H), 7.25 (dd, *J* = 13.3, 6.6 Hz, 2H), 6.91 – 6.86 (m, 1H), 6.82 (d, *J* = 8.6 Hz, 1H), 4.77 (s, 4H), 2.80 (s, 2H), 2.63 (s, 3H). ^{13}C NMR (151 MHz, $CDCl_3$) δ 170.51, 153.45, 148.91, 136.71, 133.73, 131.43, 131.07, 130.59, 129.11, 128.90, 128.49, 128.44, 127.51, 126.81, 117.30, 107.87, 101.92, 77.26, 77.05, 76.84, 54.22, 25.94.

A4. ^{1}H NMR (500 MHz, Chloroform-*d*) δ 12.15 (s, 1H), 8.44 (s, 1H), 7.78 (d, *J* = 9.1 Hz, 1H), 7.75 (d, *J* = 8.8 Hz, 1H), 7.55 (d, *J* = 2.3 Hz, 1H), 7.39 – 7.29 (m, 7H), 7.28 (s, 1H), 6.63 (d, *J* = 8.0 Hz, 1H), 4.70 (s, 2H), 3.64 (q, *J* = 7.1 Hz, 2H), 2.31 (s, 3H), 1.34 (t, *J* = 7.1 Hz, 3H).

A5. ^{1}H NMR (500 MHz, Chloroform-*d*) δ 12.17 (s, 1H), 8.51 (d, *J* = 2.8 Hz, 1H), 7.79 (d, *J* = 9.1 Hz, 1H), 7.77 (d, *J* = 2.5 Hz, 1H), 7.44 (d, *J* = 8.5 Hz, 1H), 7.38 (dd, *J* = 8.0, 6.7 Hz, 4H), 7.34 – 7.30 (m, 4H), 7.26 (dd, *J* = 8.5, 2.6 Hz, 1H), 6.63 (dd, *J* = 9.1, 2.8 Hz, 1H), 4.81 (s, 4H), 2.28 (s, 3H).

A6.

A7. ^{1}H NMR (500 MHz, Chloroform-*d*) δ 11.82 (s, 1H), 11.10 (s, 0H), 8.62 (s, 0H), 8.50 (d, *J* = 2.7 Hz, 1H), 8.01 (s, 0H), 7.97 (s, 0H), 7.93 (s, 1H), 7.93 (d, *J* = 2.3 Hz, 0H), 7.87 (d, *J* = 2.1 Hz, 1H), 7.82 (d, *J* = 9.1 Hz, 1H), 7.69 – 7.42 (m, 5H), 7.41 – 7.29 (m, 16H), 7.25 (d, *J* = 7.4 Hz, 1H), 4.81 (s, 4H), 4.47 (s, 2H), 2.30 (s, 3H).

A8. ^{1}H NMR (500 MHz, Chloroform-*d*) δ 7.98 (d, *J* = 2.3 Hz, 1H), 7.92 (d, *J* = 8.6 Hz, 2H), 7.76 (dd, *J* = 8.5, 2.3 Hz, 1H), 7.55 (d, *J* = 8.5 Hz, 1H), 7.36 (dd, *J* = 8.0, 6.6 Hz, 2H), 7.33 – 7.29 (m,

1H), 7.27 – 7.24 (m, 2H), 6.86 (d, *J* = 8.7 Hz, 2H), 4.69 (s, 2H), 3.63 (q, *J* = 7.1 Hz, 2H), 1.33 (t, *J* = 7.1 Hz, 3H).

A9. ^{1}H NMR (500 MHz, Chloroform-*d*) δ 8.38 – 8.33 (m, 2H), 8.00 – 7.93 (m, 4H), 6.94 – 6.87 (m, 2H), 4.34 (t, *J* = 6.2 Hz, 4H), 3.78 (t, *J* = 6.2 Hz, 4H), 2.09 (s, 6H). ^{13}C NMR (151 MHz, $CDCl_3$) δ 170.85, 156.33, 151.16, 147.63, 144.18, 126.35, 124.76, 124.70, 122.72, 111.80, 61.06, 49.76, 20.86.

A10. ^{1}H NMR (500 MHz, Chloroform-*d*) δ 8.36 – 8.32 (m, 2H), 7.96 – 7.92 (m, 2H), 7.91 – 7.87 (m, 2H), 7.39 – 7.34 (m, 2H), 7.32 – 7.29 (m, 1H), 7.25 – 7.21 (m, 2H), 6.90 – 6.85 (m, 2H), 4.81 (s, 2H), 3.98 (t, *J* = 5.8 Hz, 2H), 3.79 (t, *J* = 5.8 Hz, 2H), 1.62 (s, 3H). ^{13}C NMR (151 MHz, $CDCl_3$) δ 147.48, 144.05, 137.04, 128.95, 127.41, 126.29, 124.71, 122.60, 112.27, 60.39, 55.01, 53.34.

C1. ^{1}H NMR (500 MHz, Chloroform-*d*) δ 7.72 – 7.67 (m, 2H), 7.64 – 7.59 (m, 1H), 7.54 (d, *J* = 2.4 Hz, 1H), 7.45 (dd, *J* = 8.8, 2.4 Hz, 1H), 7.37 – 7.32 (m, 2H), 6.86 (td, *J* = 7.7, 1.4 Hz, 1H), 6.79 (dd, *J* = 8.0, 1.5 Hz, 1H), 6.70 (ddd, *J* = 8.1, 7.4, 1.5 Hz, 1H), 6.05 – 5.98 (m, 2H). ^{13}C NMR (176 MHz, $CDCl_3$) δ 144.23, 143.61, 141.80, 136.88, 136.08, 131.65, 131.04, 130.03, 129.89, 129.42, 124.76, 124.13, 122.42, 116.11, 115.04, 114.44, 113.98, 113.20, 112.92, 112.89.

C2. ^{1}H NMR (500 MHz, Chloroform-*d*) δ 7.98 (d, *J* = 9.3 Hz, 2H), 7.46 – 7.40 (m, 2H), 7.40 – 7.37 (m, 1H), 7.34 – 7.30 (m, 3H), 7.24 (dd, *J* = 7.7, 1.7 Hz, 1H), 7.09 – 7.02 (m, 2H), 6.77 – 6.71 (m, 2H), 3.79 (s, 3H). ^{13}C NMR (151 MHz, $CDCl_3$) δ 155.41, 154.96, 143.65, 138.03, 132.36, 131.74, 129.92, 129.67, 127.12, 126.68, 121.85, 119.50, 116.07, 114.30, 113.50, 113.30, 112.83, 80.18, 55.72.

C3. ^{1}H NMR (500 MHz, Chloroform-*d*) δ 8.91 (dd, *J* = 2.6, 0.6 Hz, 1H), 8.34 (s, 1H), 8.27 (dd, *J* = 9.2, 2.7 Hz, 1H), 7.11 (d, *J* = 9.2 Hz, 1H), 4.43 (q, *J* = 7.1 Hz, 2H), 3.32 (q, *J* = 7.1 Hz, 4H), 1.44 (t, *J* = 7.1 Hz, 3H), 1.23 (t, *J* = 7.1 Hz, 6H). ^{13}C NMR (151 MHz, $CDCl_3$) δ 162.25, 157.46, 153.69, 152.30, 140.30, 128.08, 127.48, 126.67, 126.36, 124.39, 123.04, 118.60, 118.28, 114.65, 103.93, 62.87, 62.76, 47.84, 47.62, 14.17, 13.95, 12.90, 12.82.

C4. ^{1}H NMR (500 MHz, Chloroform-*d*) δ 8.88 (d, *J* = 2.6 Hz, 1H), 8.41 (dd, *J* = 9.0, 2.6 Hz, 1H), 7.96 (s, 1H), 7.23 (d, *J* = 9.1 Hz, 1H), 4.00 – 3.85 (m, 4H), 3.26 – 3.09 (m, 4H). ^{13}C NMR (151 MHz, $CDCl_3$) δ 157.97, 155.36, 142.24, 129.30, 125.59, 123.46, 119.26, 113.05, 111.51, 85.28, 66.55, 53.38.

C5. ^{1}H NMR (500 MHz, Chloroform-*d*) δ 8.78 (d, *J* = 2.6 Hz, 1H), 8.43 (s, 1H), 8.36 (dd, *J* = 9.1, 2.6 Hz, 1H), 8.04 (dd, *J* = 8.5, 1.3 Hz, 2H), 7.81 – 7.77 (m, 1H), 7.68 (dd, *J* = 8.4, 7.4 Hz, 2H),

7.18 (d, J = 9.0 Hz, 1H), 4.02 – 3.94 (m, 4H), 3.19 – 3.13 (m, 4H). ^{13}C NMR (151 MHz, $CDCl_3$) δ 158.20, 157.06, 149.73, 147.20, 142.05, 141.44, 138.22, 137.58, 135.37, 135.09, 130.02, 129.97, 128.83, 128.76, 128.62, 128.43, 127.95, 125.45, 123.70, 122.59, 119.92, 118.80, 118.03, 117.23, 114.33, 112.04, 66.67, 66.54, 53.25, 52.80.

C6. ^{1}H NMR (500 MHz, Chloroform-*d*) δ 8.40 (d, J = 9.1 Hz, 1H), 8.18 (s, 1H), 7.40 (s, 1H), 7.02 (d, J = 2.7 Hz, 1H), 6.73 (dd, J = 9.2, 2.7 Hz, 1H), 4.34 (q, J = 7.1 Hz, 2H), 3.75 (t, J = 6.9 Hz, 2H), 3.59 (t, J = 6.8 Hz, 2H), 3.49 (q, J = 7.1 Hz, 2H), 2.66 (s, 4H), 1.41 (s, 9H), 1.38 (t, J = 7.1 Hz, 3H), 1.25 (t, J = 7.1 Hz, 3H). ^{13}C NMR (151 MHz, $CDCl_3$) δ 177.53, 177.26, 163.82, 151.47, 148.03, 140.61, 130.93, 116.91, 114.99, 110.35, 108.82, 96.54, 62.11, 47.12, 45.55, 39.78, 35.65, 29.72, 28.20, 28.10, 27.67, 27.57, 14.26, 12.14.

C7. ^{1}H NMR (500 MHz, Chloroform-*d*) δ 8.27 (d, J = 9.2 Hz, 1H), 7.50 (s, 1H), 7.33 (s, 1H), 6.86 (d, J = 2.7 Hz, 1H), 6.71 (dd, J = 9.3, 2.7 Hz, 1H), 3.75 (dd, J = 7.8, 6.3 Hz, 2H), 3.57 (t, J = 7.1 Hz, 2H), 3.51 (q, J = 7.1 Hz, 2H), 2.67 (s, 4H), 1.40 (s, 9H), 1.25 (t, J = 7.1 Hz, 3H). ^{13}C NMR (151 MHz, $CDCl_3$) δ 177.91, 177.18, 152.82, 152.80, 140.63, 130.68, 115.74, 115.09, 114.38, 110.27, 108.58, 74.27, 46.88, 45.27, 39.75, 35.55, 28.19, 27.62, 27.53, 12.27.

C8. ^{1}H NMR (500 MHz, Chloroform-*d*) δ 8.30 (d, J = 1.4 Hz, 1H), 7.81 (s, 1H), 6.38 (s, 1H), 3.86 – 3.75 (m, 1H), 3.66 – 3.54 (m, 3H), 2.90 (tq, J = 12.3, 6.3 Hz, 1H), 2.42 (s, 3H), 1.84 (dd, J = 13.4, 4.6 Hz, 1H), 1.58 (t, J = 13.2 Hz, 1H), 1.42 (s, 3H), 1.40 (d, J = 6.6 Hz, 3H), 1.29 (s, 3H). ^{13}C NMR (151 MHz, $CDCl_3$) δ 154.46, 149.84, 142.06, 127.16, 126.87, 118.92, 116.36, 115.28, 112.59, 72.14, 56.15, 46.81, 45.49, 40.12, 29.55, 26.86, 25.74, 20.08, 19.57.

C9. ^{1}H NMR (500 MHz, Chloroform-*d*) δ 7.87 (s, 1H), 7.64 (dd, J = 8.9, 2.3 Hz, 1H), 7.50 (s, 1H), 6.61 (d, J = 8.9 Hz, 1H), 3.82 (tt, J = 11.4, 5.9 Hz, 1H), 3.65 – 3.53 (m, 3H), 2.92 (dt, J = 12.5, 6.1 Hz, 1H), 1.86 (dd, J = 13.3, 4.6 Hz, 1H), 1.61 (d, J = 13.2 Hz, 1H), 1.43 (s, 4H), 1.40 (d, J = 6.5 Hz, 4H), 1.30 (s, 3H). ^{13}C NMR (151 MHz, $CDCl_3$) δ 158.17, 149.89, 132.85, 129.38, 128.57, 120.04, 115.80, 114.85, 111.20, 72.75, 56.10, 46.91, 45.35, 39.98, 29.48, 26.95, 25.87, 19.45.

C10. ^{1}H NMR (500 MHz, Chloroform-*d*) δ 8.34 (d, J = 9.1 Hz, 1H), 7.85 (s, 1H), 6.63 (dd, J = 9.2, 2.8 Hz, 1H), 6.55 (d, J = 2.7 Hz, 1H), 3.78 (t, J = 6.8 Hz, 2H), 3.60 (q, J = 7.1 Hz, 2H), 2.70 (t, J = 6.8 Hz, 2H), 2.45 (s, 3H), 1.29 (t, J = 7.1 Hz, 3H). ^{13}C NMR (151 MHz, $CDCl_3$) δ 154.63, 151.11, 143.85, 131.11, 119.37, 117.38, 115.85, 114.63, 113.05, 110.16, 77.24, 77.03, 76.81, 74.07, 46.14, 45.83, 20.59, 16.36, 12.44.

Liquid Chromatography-Mass Spectrometry (LC-MS)

Samples were analyzed using a liquid chromatography-quadrupole time-of-flight mass spectrometry (LC-QTOF-MS) instrument which consisted of a 1200 Infinity LC (Agilent Technologies) connected to a 6520 Accurate Mass QTOF-MS (Agilent Technologies). The QTOF was operated in positive electrospray ionization (ESI) mode at high resolution (4 GHz) with a resolving power ranging from 9700 to 18000 for the m/z 100 and 1600 respectively. The parameters of the MS were optimized for the highest intensity of the ions as follows: drying gas flow rate 12 L/min at 355 °C, nebulizer pressure 35 psi, fragmentor voltage 110 V with the V cap voltage 3500 V.

All samples were collected from the NC State MWDL. Stock solutions were prepared by dissolving 1 mg of each dye in 1 mL of acetonitrile (LC-MS grade, 99.9%) to obtain a concentration of 1000 µg/mL. The stock solutions were then diluted to a concentration of 30 µg/mL with the same solvent. Purified water (18.2Ω) was generated in-house using Milli-Q System (PURELAB Ultra from VWR). Before analysis, all samples were filtered using a 0.2 µm PVDF filter (Sigma-Aldrich). The chromatographic separation was achieved by using a Zorbax Eclipse Plus C18 (2.1×50 mm, 3.5 µm) column with a Zorbax Eclipse Plus C18 narrow bore guard column (2.1×12.5 µm, 5 µm) at 40 ºC. The mobile phases A and B consisted of water and acetonitrile respectively with 0.1% formic acid (HPLC grade, Sigma-Aldrich) in both. The eluent flow was 0.5 mL/min and an injection volume of the dye solution of 2 µL. The acetonitrile concentration started at 40% and was ramped to 90% over 3.5 minutes and held constant for 3.5 minutes. In the next 7 minutes, the acetonitrile concentration was ramped down to 40%, resulting in a total sample run time of 14 min. Diode array detector (DAD) was used for the wavelength analysis. Wavelengths commonly monitored included 254 410, 460, 540 and 610 nm.